# Role of modulators of small GTPases in chemotaxis, cytokinesis and development in *Dictyostelium discoideum*

INAUGURAL-DISSERTATION

zur

Erlangung des Doktorgrades

der Mathematisch-Naturwissenschaftlichen Fakultät

der Universität zu Köln

vorgelegt von

**Subhanjan Mondal**

aus Kulti, Indien

2007

| | |
|---|---|
| Referees/Berischterstatter | Prof. Dr. Angelika A. Noegel<br>Prof. Dr. Martin Hülskamp |

| | |
|---|---|
| Date of oral examination/<br>Tag der mündlichen Prüfung | 14.02.2008 |

The present research work was carried out under the supervision and direction of Prof. Dr. Angelika A. Noegel in the Institute of Biochemistry, Medical Faculty, University of Cologne, Germany, from November 2004 to November 2007.

Diese Arbeit wurde von November 2004 bis November 2007 am Biochemischen Institut I der Medizinischen Fakultät der Universität zu Köln unter Leitung und Betreuung von Prof. Dr. Angelika A. Noegel durchgeführt.

# Acknowledgement

First and foremost, I express my heartiest gratitude to my advisor Prof. Angelika Noegel for giving me the opportunity to work in her lab. Her valuable guidance, creative suggestions, constructive criticism, constant encouragement, immense support, optimism and promptness and sustained interest in the projects proved valuable for the successful completion of my PhD work.

I acknowledge Dr. Francisco Rivero for his support, guidance throughout the course of my Ph.D. He had been extremely patient and prompt in helping with microscopes and *Dictyostelium* work, sharing reagents, creative suggestions.

I take this opportunity to thank all investigators who extended their support in form of collaborative work and sharing reagents. I thank Prof. Micheal Schleicher, Dr. Jan Faix, Dr. Paul Steimle for successful collaborative efforts. I also thank Prof. Gerry Weeks, Prof Tom Egelhoff, Dr. C. H. Siu, Dr. Carole Parent, Prof. Robert Insall, Prof. Kees Weijer, Dr Reza Ahmedian, Dr. Gerrit Praefcke and the Dicty Stock Center for sharing reagents with us, which proved indispensable for the work.

I thank Rolf Müller and Berthold Gaßen for their excellent technical support with generation of monoclonal antibodies, two-dimensional gel electrophoresis, clonings and actin polymerization assays.

I thank Neelamegan Dhamodaran, Yogikala Prabhu and Deenadayalan Bakthavatsalam with whom I not only shared work but also spend nice time together in the initial days of my time here. I also thank Charles and Vivek for their company and friendship. I also thank all members of the lab Rosi, Maria, Hua, Tanya, Anne, Mary, Kristina, Georgia, Kartik, Surayya, Rashmi, Jianbo for their wonderful company, help and support. I also thank Dörte Püsche for her help and co-operation with the administrative work that made my life easy.

I express my heartfelt gratitude to my parents and my brother for their patience, tolerance, sacrifice and encouragement throughout my life. I also thank my uncle whom I consider as a role model.

I also thank my alma mater The All India Institute of Medical Sciences, New Delhi and Madurai Kamaraj University for the excellent undergraduate education and the Government of India for supporting me through my undergraduate education. I also thank the Deutsche Forschungsgemeinschaft for financial assistance during my Ph.D.

Cologne
10.11.2007

Subhanjan Mondal

Table of Contents

| Chapter | Description | Page |
|---|---|---|

# Prologue

*In this thesis I summarize the results of my investigations performed in the lab of Angelika Noegel since November 2004. The genesis of the projects I pursued was rather individual than sequential. The Dictyostelium genome (Eichinger et al., 2005) was published shortly after I started my Ph.D. and held an immense potential to use the system to study molecular details of actin cytoskeleton based processes like chemotaxis and cytokinesis, for which Dictyostelium has been widely accepted as a model system. I describe my work on three projects, which do not have any immediate interrelation but can be linked as involving proteins that regulate small GTPases.*

Here I introduce for an easier understanding, the scheme I followed in preparing the manuscript for the thesis. First I introduce the **actin cytoskeleton** and then briefly describe the processes it regulates like cell migration and cytokinesis. I also introduce the **model organism** used in the study, *Dictyostelium discoideum*. Then I divide my thesis into **three chapters**, which includes an independent **Introduction, Material and Methods**, **Results** and **Discussion** section each.

Chapter 1: "**Linking Ras to Myosin II functions. RasGEF Q, a *Dictyostelium* exchange factor for RasB, affects myosin II functions"** describes the role of a *Dictyostelium* exchange factor for RasGTPases, RasGEF Q in regulating myosin II functions by regulation myosin heavy chain kinase.

Chapter 2: "**GxcDD, a putative RacGEF, is involved in *Dictyostelium* development"** describes a multidomain protein GxcDD and its role in proper streaming during *Dictyostelium* development.

Chapter 3: "**Association of Filamin and Cortexillin with the IQGAP related protein GAPA in regulation of cytoskeletal organization"** describes localization and properties of GAPA and also examines the association of GAPA with Filamin and cortexillin, two actin crosslinking proteins, in regulating the actin cytoskeleton.

Finally, I end by briefly summarizing my results and emphasising the diversity of processes regulated by small GTPases and their regulators.

I wish all readers a pleasant reading of my thesis.

# Introduction

*The actin cytoskeleton is one of the major structural components of the cell. It often undergoes rapid reorganization and plays crucial roles in a number of dynamic cellular processes, including cell migration, cytokinesis, membrane trafficking, and morphogenesis (Pollard and Borisy, 2003). The actin cytoskeleton is comprised largely of actin and myosin and results from studies performed with Saccharomyes cerevisiae, Acanthamoeba castellanii, several cultured metazoan cell types such as neutrophils, fibroblasts, melanocytes and neuroblasts and the social amoeba Dictyostelium discoideum have contributed to its understanding.*

## 1.1. The model system: *Dictyostelium discoideum*

*Dictyostelium discoideum* is a soil amoeba capable of extraordinary feats of survival, motility, chemotaxis and development. Known as the "social amoeba" or the "cellular slime mould", this organism has been subject of serious study since the 1930s. Research on *Dictyostelium* has been instrumental in shaping general views of differentiation, morphogenesis and signal transduction events. *Dictyostelium* live as single cell in the soil where they feed on bacteria. Their prey is traced by chemotaxis towards secretion products of bacteria such as folic acid and pterin. Upon food depletion, the cells enter a developmental cycle that is regulated by cAMP. The pulsatile secretion of this compound serves as a chemoattractant that leads to the aggregation of the cells into clumps of about 100,000 cells. The aggregates subsequently develop into fruiting bodies that are composed of dead stalk cells and viable spores. When food becomes available again, the spores hatch into amoeba that are capable of mitotic reproduction (Figure 1, (Chisholm and Firtel, 2004). Several cellular features of *Dictyostelium* can be attributed to its elaborate cytoskeleton.

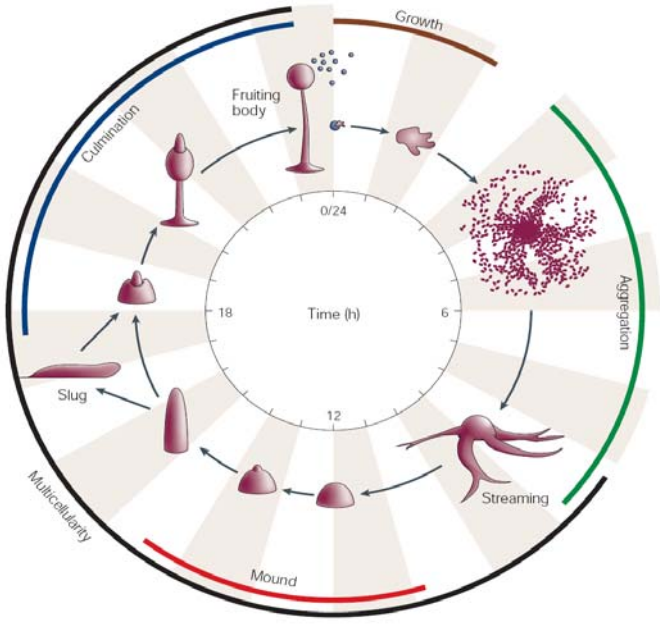


**Figure 1. Schematic representation of developmental cycle in Dictyostelium. Taken from (Chisholm and Firtel, 2004)**

## 1.2. Chemotaxis

Chemotaxis, cell movement up a chemical gradient, is vital to many biological processes in eukaryotic organisms. Examples are the migration of neutrophils to sites of inflammation, the organization of embryonic cells during morphogenesis, metastasis of tumor cells that all result from the capacity to detect and move to the source of a signal. The basic migratory systems are conserved from protozoa to vertebrates and can be dissected into two types of processes: (1) an amoeboid type crawling system, driven by filamentous actin assembly induced force; (2) an adhesion receptor-mediated cell movement, driven by remodelling of the extracellular matrix, such as adhesion receptor and integrin mediated attachments seen in fibroblast, myoblasts and neural crest cells. On the other hand, amoeboid movement depends on cytoskeleton-mediated cell movement, in which the assembly of a branched network of actin filament provides the mechanical propulsion. Cell migration in neutrophils and *Dictyostelium* are amoeboid in nature.

Chemoattractants are sensed by membrane receptors coupled to heterotrimeric G-proteins (GPCRs). Receptors convert the extracellular cues into intracellular signalling; signalling molecules undergo dynamic changes of their location and activated state which causes asymmetric localization of cellular components; polarized signalling molecules induce coordinated remodelling of the actin cytoskeleton and cell adhesion to the substratum, which produce new pseudopods in the direction of the chemoattractant gradient, resulting in cellular movement.

### 1.2.1. Asymmetry of the actin cytoskeleton

F-actin localizes to the leading edge, where it assembles to induce protrusions of pseudopodia, and to a lesser extent to the posterior (Ridley et al., 2003). Leading edges are enriched in actin-modifying proteins such as Arp2/3 complex, WAVE/Scar, WASP,

ADF/cofilin (Mullins et al., 1997; Svitkina and Borisy, 1999; Welch et al., 1997). Myosin II is assembled at the cell's posterior and the lateral sides where it provides rigidity to the polarized cells through cortical tension. Contraction of myosin II in the uropod enables the uropod to lift off the substratum and retract towards the fast moving pseudopod. Cells lacking myosin II or components that regulate its contraction cannot retract the uropod properly (Devreotes and Janetopoulos, 2003; Worthylake and Burridge, 2003). The remodelling of the actin cytoskeleton is essential for cell motility. Treatment with an F-actin polymerization inhibitor, Latrunculin A (LatA) induces cells to become rounded in shape and completely abrogates cell migration.

### 1.2.2. Brief overview of signal transduction events during *Dictyostelium* chemotaxis

In *Dictyostelium* as in neutrophils chemoattractants are sensed by GPCRs. This induces dissociation of a heterotrimetic G-protein, G2, into $\alpha$ and $\beta\gamma$ subunits. The chemoattractant also locally activates Ras at the presumptive leading edge. Upon gradient sensing, PI3K is recruited at the plasma membrane in the leading edge. Activated Ras and $\beta\gamma$ subunits activatePI3K, leading to a localized production of PtdIns(3,4,5)$P_3$ and PtdIns(3,4)$P_2$. In contrast, PTEN (phosphatase and tension homologue deleted on chromosome ten), which degrades PtdIns(3,4,5)$P_3$ and PtdIns(3,4)$P_2$ is associated with the membrane at the lateral sides and posterior of the cell, thus generating a gradient of PtdIns inside the cell, which acts as a compass in detecting the chemotactic gradient. Localized accumulation of PtdIns leads to recruitment of several PH domain containing proteins like RacGEFs, Akt/PKB, CRAC, PhdA and also other Rac effectors like Scar/WAVE and WASP to the leading edge. Rac is activated by recruitment to RacGEFs, which then activate Scar/WAVE and WASP family proteins. This leads to activation of the Arp2/3 complex to produce a robust F-actin polymerization at the leading edge. Myosin heavy chain kinase A (MHCK A), a kinase that phosphorylates myosin is also recruited to the leading edge where it phosphorylates myosin. Phosphorylated

myosin is unable to assemble into bipolar filaments and thus generates a polarity in localization of filamentous myosin II distribution, which is important for directed cell migration (Figure2, (Chisholm and Firtel, 2004; Franca-Koh et al., 2006; Sasaki and Firtel, 2006; Van Haastert and Devreotes, 2004).

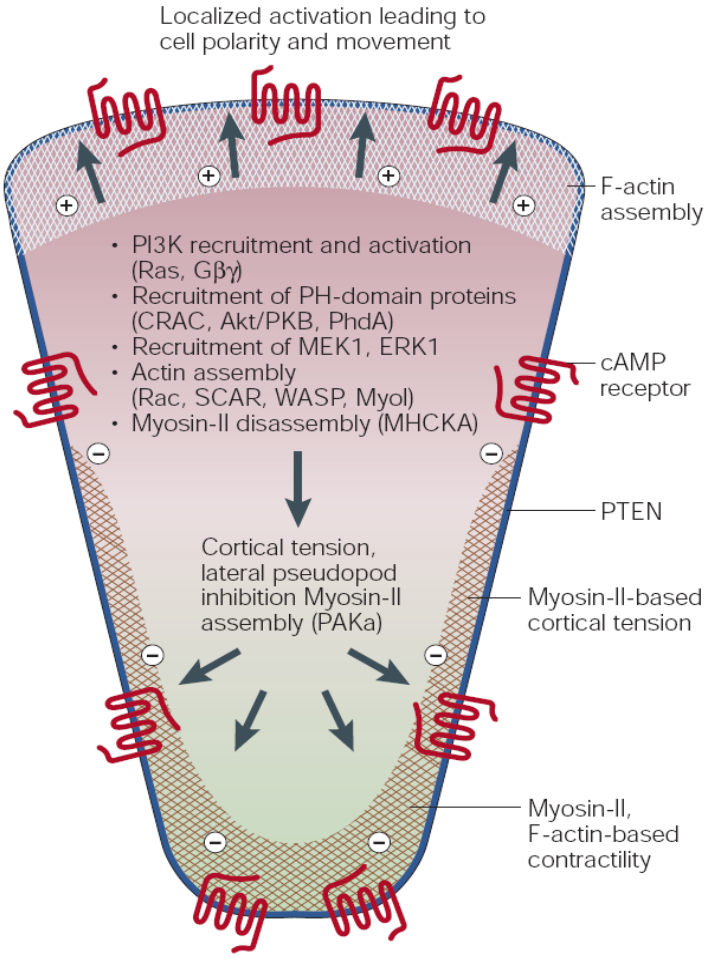


**Figure 2. A Schematic representation of signal transduction events during *Dictyostelium* chemotaxis. Taken from (Chisholm and Firtel, 2004)**

Aggregating *Dictyostelium* cells migrate towards a cAMP source by forming streams. Cells can sense cAMP and relay cAMP to the following cell generating a streaming pattern. Adenylyl cyclase (ACA) are 12 transmembrane proteins that mediate cell-cell signalling via cAMP induced cAMP production. Cells lacking ACA are able to sense cAMP, but fail to

form streams during migration. During chemotaxis CRAC (cytosolic regulator of adenylyl cyclase) is recruited to the plasma membrane of the leading edge by its PH (Pleckstrin homology) domain and is required for ACA activation. A set of proteins including MAP kinase, ERK2, the small GTPase RasC, exchange factor RasGEF A (*aimless*), Ras interacting protein Rip3 (a homolog of AVO1/hSIN1 involved in TOR signalling complex, TORC2), and a protein pianissimo (Pia, a homolog of Rictor/mAVO3 involved in the TOR signalling complex, TORC2) are also required for ACA activation (Sasaki and Firtel, 2006). cAMP produced by ACA is rapidly secreted to further ACA in a positive feedback loop. cAMP is degraded by extracellular and intracellular phosphodiesterases (Figure 3A, (Saran et al., 2002). ACA localizes to the rear of a migrating cell mediated presumably by a vesicle dependent mechanism and is reqired for generating a streaming behaviour during aggregation (Figure 3B, (Kriebel et al., 2003).

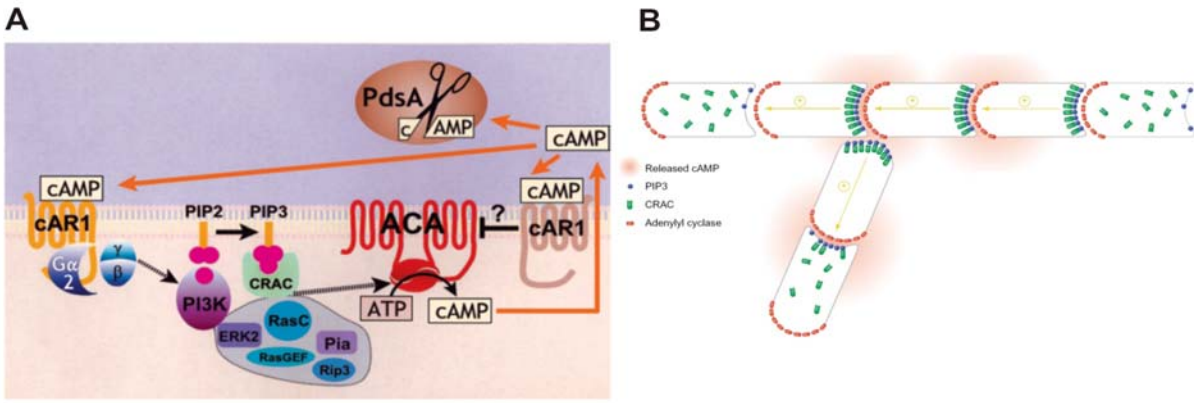


**Figure 3. Regulation of Adenylyl cyclase and generation of streaming behaviour in *Dictyostelium* chemotaxis. Figure A taken from (Saran et al., 2002) and Figure B taken from (Dormann and Weijer, 2006)**

## 1.3. Cytokinesis

Cytokinesis is the critical final step of cell division. It is responsible for equal partitioning and separation of the cytoplasm between daughter cells to complete mitosis. In

order to generate two identical cells from mitosis, the fidelity of cytokinesis must be precisely controlled establishing the spatial organization of the cleavage plane and the actual timing of the cleavage onset. Actin and myosin are major components of the contractile ring, a structure at the equator between the dividing cells, which provides the force necessary to constrict the cytoplasm. *Dictyostelium* is particularly useful to study cytokinesis. Mutants that fail to perform cytokinesis become multinucleated and many such mutants like cells lacking myosin II can divide by attachment mediated cytofission. Genetic screens in *Dictyostelium* have revealed several proteins crucial for cytokinesis, like components of the cytoskeleton or small GTPases or their regulators. Cytokinesis has four phases. First, position of the cleavage furrow, which depends on the orientation of the spindle such that the plane is orthogonal to the spindle and placed at its centre. Second, assembly of actin at the plasma membrane where the furrow will form, followed by myosin II, which generates the force of contraction. Contraction of the contractile ring, which generates the cleavage furrow, is the third step followed by the fourth phase, which involves membrane fusion to separate the two daughter cells (Figure 4, (Chisholm, 1997)

A number of Ras family signalling molecules play a role in cytokinesis. Cells lacking RacE expression fail to grow in suspension and become multinucleate, they successfully complete the normal *Dictyostelium* developmental program and are able to cap receptors normally, both processes known to be dependent on acto-myosin function(Larochelle et al., 1997). RacE does not localize to the contractile ring, which is formed normally in its absence but regulates cytokinesis by indirectly controlling cortical tension. Deletion of RasG also causes a cytokinesis defect, which is thought to be due to its influence on the actin-cytoskeleton (Tuxworth et al., 1997). Two IQ-GAP related proteins DGAP1 and GAPA are also required for cytokinesis (Adachi et al., 1997; Faix and Dittrich, 1996; Lee et al., 1997). In addition to myosin II heavy chain, the regulatory and the essential myosin light chains and myosin heavy chain kinase A are also required for proper cytokinesis (Bosgraaf and van

Haastert, 2006). In addition, the actin binding proteins coronin and cortexillins are also required for cytokinesis (de Hostos et al., 1993; Faix et al., 1996). Disruption of clathrin also revealed its unexpected role in cytokinesis (Niswonger and O'Halloran, 1997).

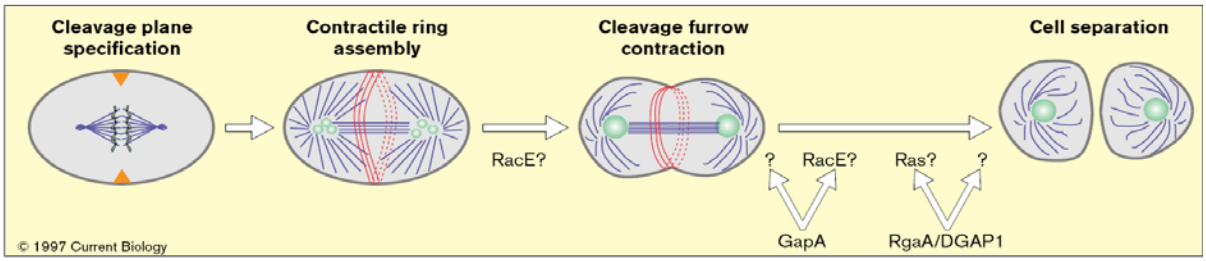


**Figure 4. Steps in cytokinesis indicating involvement of small GTPases**

# Chapter 1

## Linking Ras to myosin function: RasGEF Q, a *Dictyostelium* exchange factor for RasB, affects myosin II functions

*RasGEF Q, a nucleotide exchange factor from D. discoideum, is a 143 kDa protein containing RasGEF domains and a DEP domain. We show that RasGEF Q is the predominant exchange factor for RasB and that RasB is activated by cAMP. Overexpression of the GEF domain constitutively activates RasB and leads to a cytokinesis defect in suspension phenocopying cells expressing a constitutively active RasB and myosin null mutants. Furthermore, RasGEF Q$^-$ mutants show myosin II overassembly having higher levels of unphosphorylated myosin II, and overexpression of the GEF domain causes enhanced recruitment of MHCK A to the cortex. RasGEF Q can bind to F-actin and has the potential to form complexes with MHCK A that contain active RasB. Together our results suggest that starvation signals through RasGEF Q to activate RasB, which then regulates processes requiring myosin II. In addition to cell polarity defects RasGEF Q$^-$ mutants also have defects in cell sorting and slug migration during later stages of development.*

## 2.1. Introduction

The actin cytoskeleton is composed of actin and myosin and several proteins that bind to them and play crucial roles in cell motility, cytokinesis, phagocytosis and intracellular transport processes (Cooper, 1991; Matsumura, 2005). Coordinated cell movement requires protrusive forces generated by polymerization of actin filaments at the leading edge and contractile forces via myosin motors at the rear of a cell. Myosin II, the conventional two-headed myosin, is also the primary motor protein required for cytokinesis in eukaryotes. *Dictyostelium* cells lacking myosin II heavy chain (*mhcA*$^{-}$) show a plethora of defects which includes a cytokinesis defect in suspension, but they undergo cytokinesis when grown on a solid support by an abnormal "traction-mediated" mechanism (De Lozanne and Spudich, 1987). This correspond to the localization of myosin at the contractile ring (cleavage furrow) during cytokinesis. *MhcA*$^{-}$ cells have a decreased chemotactic efficiency due to reduction in cell polarity and an inability to suppress lateral pseudopods and retract the uropod (Wessels and Soll, 1990; Wessels et al., 1988). They also have a developmental defect, halting the developmental process shortly after cells have aggregated.

The regulation of myosin II appears to differ between higher and lower eukaryotes. In *D. discoideum* phosphorylation of myosin takes place at three threonine residues in the tail region by myosin II heavy chain kinases (MHCKs) (Luck-Vielmetter et al., 1990; Vaillancourt et al., 1988). Phosphorylated myosin is inactive and does not assemble into filaments, whereas unphosphorylated myosin II can spontaneously assemble into bipolar filaments (Figure 5). It is only these filaments that perform cellular myosin II functions (Egelhoff et al., 1993). Significant knowledge about the function of myosin II regulation has been derived from mutant myosin IIs: 3XALA myosin, where the three phosphorylatable threonines have been mutated to alanine rendering it a poor substrate for MHCKs, and 3XASP myosin, where the three threonines were replaced by aspartate, mimicking the

phosphorylated state. 3XALA myosin mutants show significant myosin overassembly in cytoskeletal fractions and they form very stable myosin II filaments which accumulate in the rear cortex. Cells expressing 3XALA myosin are drastically impaired in cell migration and chemotaxis, making frequent turns and extending lateral pseudopods, which is due to the inability to disassemble myosin filaments, and have severely affected motility (Egelhoff et al., 1996; Heid et al., 2004; Stites et al., 1998). On the other hand 3XASP myosin does not assemble into bipolar filaments, is non-functional in vivo and fails to complement cytokinesis and development defects of myosin II null cells (Egelhoff et al., 1993).

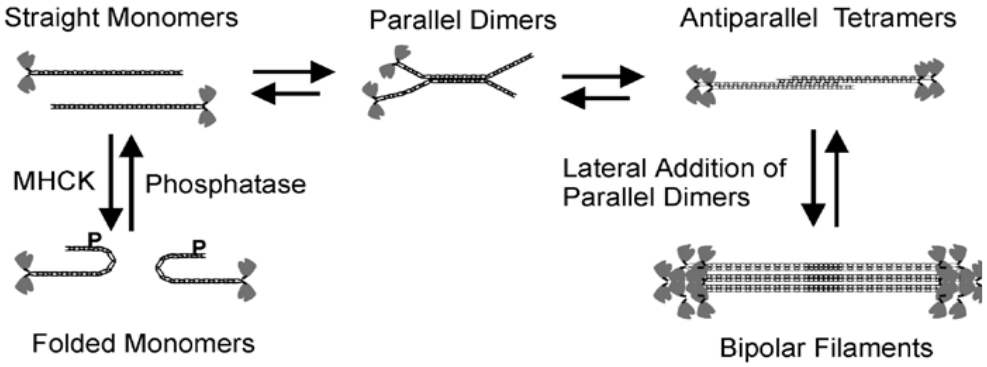


**Figure 5. Regulation of myosin II assembly in *D. discoideum*. The phosphorylation status of myosin II is critical for myosin II filament assembly. In its unphosphorylated state myosin can spontaneously assemble into bipolar filaments, which is the functional form of myosin. Myosin II can also be phosphorylated by myosin II heavy chain kinases (MHCK). The phosphorylated form is unavailable for filament assembly.**

Signalling pathways based on small GTPases of the Ras family regulate a myriad of cellular processes in eukaryotic cells. The *D. discoideum* genome encodes a large and varied family of Ras GTPases consisting of 15 Ras proteins. *D. discoideum* uses its Ras proteins to regulate several pathways controlling cell motility and polarity, cytokinesis, phagocytosis, pinocytosis and multicellular development (Charest and Firtel, 2007).

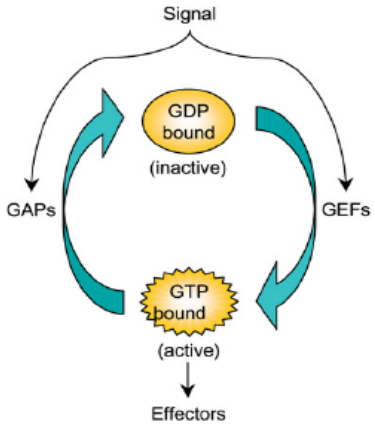


**Figure 6. The GTPase cycle. Inactive GDP bound small GTPases are activated by exchange factors, GEFs, which promote the release of GDP and allow its replacement by GTP. Active GTP-bound small GTPases can then promote the activation of different effectors until they return to their GDP-bound inactive state upon hydrolysis of the GTP to GDP, which is catalysed by GTPase activating proteins, GAPs. Extracellular or intracellular signals regulate the small GTPases by acting on either GEFs or GAPs.**

*D. discoideum* expresses at least 25 RasGEFs (Wilkins et al., 2005). However, it does not code for conventional receptor tyrosine kinases (RTKs), which are the major inputs for Ras signaling in higher eukaryotes (Eichinger et al., 2005). Functions of some of the RasGEFs are slowly being understood through mutant analysis. The *RasGEF A*$^{-}$ cells (*aimless*) fail to aggregate upon starvation and are unable to synthesize and respond to cAMP (Insall et al., 1996; Kae et al., 2007), showing phenotypic similarities to *RasC*$^{-}$ cells indicating they may act to regulate activation of adenylyl cyclase. The cGMP binding proteins GbpC and D, which have RasGEF domains, show altered myosin II localization during chemotaxis (Bosgraaf et al., 2005). cGMP and GbpC induce myosin II filament formation, but its corresponding Ras GTPase has not been identified. GbpD is thought to activate Rap1 and regulate cell-surface adhesion and motility (Kortholt *et al.*, 2006). RasG, the most abundant Ras in vegetative cells and the closest relative to mammalian Ras, is thought to regulate several actin cytoskeleton based processes like cell polarity and cytokinesis (Tuxworth et al., 1997). RasGEF R appears to be required for maximal activation of RasG upon response to cAMP (Kae et al., 2007). RasGEF M also appears to be required for the cAMP relay system (Arigoni et al., 2005).

Here we have focused on RasGEF Q. Our experiments identify RasB as a substrate for RasGEF Q. They further indicate that RasGEF Q acts upstream of RasB and regulates processes requiring myosin II like cytokinesis and cell motility and suppression of lateral pseudopods. *RasGEF Q*$^{-}$ cells show myosin overassembly due to high levels of unphosphorylated myosin II and produce many random pseudopodia. Cells that overexpress the GEF domain of RasGEF Q have constitutively activated RasB, which is normally activated during aggregation upon a cAMP stimulus, and have defects in cytokinesis in suspension as do *mhcA*$^{-}$ cells. Our results also suggest an involvement of myosin heavy chain kinase A (MHCK A) as a downstream regulator of the signalling cascade. We observe that cells that overexpress the GEF domain have higher levels of MHCK A recruited to the cytoskeletal fractions, which occurs when MHCK A is activated in response to cAMP. Furthermore, RasGEF Q is involved in cell sorting and developmental patterning and slug motility.

## 2.2. Materials and methods

### 2.2.1 Cell culture and development

*D. discoideum* cells of strain AX2 were grown either with *Klebsiella aerogenes* on SM agar plates or axenically in liquid nutrient medium (Claviez et al., 1982) in shaking suspension at 160 rpm at 21°C. *RasGEF Q*$^{-}$ cells were cultivated in nutrient medium containing 7 µg/ml G418 (Life Technologies, OH). To analyse development, cells were grown axenically to a density of 2-3 x $10^6$ cells /ml, washed twice in Soerensen phosphate buffer (17 mM Na-K phosphate, pH 6.0) and 5 x $10^7$ cells were plated on phosphate agar plates.

For phototaxis assays, 10 µl of cells at a density of 1 x $10^8$ cells / ml were transferred to the centre of a 90 mm phosphate agar plate and placed in a black opaque box with a slit to

provide a unidirectional light source and cells were allowed to develop to the migratory slug stage. Slime trails and cellular material were transferred onto a nitrocellulose membrane. Membranes were stained with staining solution (0.1% amido black in 20% iso-propanol and 10% acetic acid) for 10 minutes and destained twice with destaining solution (20% iso-propanol and 10% acetic acid) for 15 min, washed with water and air-dried.

For development in chimera, *RasGEF Q*$^{-}$ cells and wild type cells were transfected with pBsr-GFP for expression of GFP to mark the different cell types. 90% wild type cells were mixed with 10% *RasGEF Q*$^{-}$ cells expressing GFP or 90% *RasGEF Q*$^{-}$ cells were mixed with 10% GFP expressing wild type cells and allowed to co-develop. For control 10% GFP-expressing wild type cells were mixed with 90% wild type cells. Images were taken at the slug stage using a Leica DMR fluorescent microscope.

### 2.2.2 Generation of *RasGEF Q*$^{-}$ cells and cells expressing RasGEF Q domains

For generation of the knockout vector, cDNA clone SLH890 (procured from the *D. discoideum* cDNA project, Tsukuba) encompassing nucleotides 1798-3987 of *RasGEF Q* cloned in pSPORT (Invitrogen Inc.) was used. The plasmid was digested with *BsaBI* to release a 55 bp fragment and the Neomycin resistance cassette (Witke et al., 1987) was inserted by blunt end ligation. The resulting replacement vector was linearised by digesting with *SalI* and transformed into AX2 by electroporation. Transformants were selected in nutrient medium containing G418 (7 μg/ml). Independent clones were screened for the disruption of the *RasGEF Q* gene by PCR using genomic DNA, Southern blotting, immunofluorescence and western blot analysis. For Southern blot analysis a probe encompassing nucleotides 690 - 990 of the cDNA was used.

For expression of the N-terminal fragment Δ-GEF-GEFQ fused to green fluorescent protein (GFP) at its N-terminus, a 1.45 kb fragment encoding amino acid residues 172-654

was cloned into pBsr (Mohrs et al., 2000). For expression of the DEP domain as a GFP tagged protein fused at the N-terminus a 450 bp fragment encoding residues 683-833 was cloned into pMCS (Weber et al., 1999). The same fragment was recloned into pGEX-4T1 (GE Health Care) for expression of GST-DEP in bacteria. For expression of the C-terminal domain containing the catalytic GEF domain as a GFP-GEF fusion fused at the N-terminus, a 1.2kb fragment encoding residues 910-1298 was cloned into pMCS. The same fragment was recloned into pGEX-4T1 for expression of GST-GEF in bacteria.

### 2.2.3 Generation of RasGEF Q monoclonal antibodies

The procedure used to generate RasGEF Q monoclonal antibodies was as described before (Schleicher et al., 1984). The DEP domain of RasGEF Q (residues 683-833) was used for immunization of four female Balb/c mice (Lingnau et al., 1996). mAbs K-70-187-1 and K-70-102-1 are used in this study. They recognise a protein of 143 kDa in whole cell homogenates of wild type Ax2 cells, which is absent in *RasGEF Q*$^{-}$ cells.

### 2.2.4 Actin binding assay

All purified proteins used in the study were clarified by centrifugation at 120,000 *g* for 60 min at 4˚C. *Dictyostelium* actin was isolated as described before (Haugwitz et al., 1991). Actin sedimentation assays were performed as described (Jung et al., 1996). Briefly, G-actin (5 µM) was polymerized in the presence or absence of GST-GEF (60 µg/ ~ 1µM) or GST (20 µg/ ~ 1 µM) by addition of 0.1 volume of 10 x polymerization buffer (100 mM imidazol, pH 7.6, 20 mM $MgCl_2$, 10 mM EGTA, 1 M KCl, 5 mM ATP) for 30 min at room temperature. The final reaction volume was 70 µl. Binding to F-actin was determined by high-speed centrifugation at 120,000 *g* for 1 h at 4˚C. Crosslinking of filaments was analysed by low-

speed centrifugation at 12,000 *g* for 1 h at 4°C. Equal amounts of pellet and supernatant were resolved by SDS-PAGE (10% acrylamide) and proteins visualized by Coomassie Brilliant Blue staining.

### 2.2.5 *In vitro* binding assays with GST fusion protein and analysis of cAMP induced activation of RasB

For interaction with cytoskeletal proteins, 5 x $10^7$ AX2 cells were lysed in lysis buffer (LB: 25 mM Tris/HCl, pH 7.5, 150 mM NaCl, 5 mM EDTA, 0.5% Triton-X100, 1 mM DTT, supplemented with protease inhibitors (Sigma) with 5 mM ATP added) with or without a preincubation with 10 µM Latrunculin A for 1 hr (Lat A, Sigma) and incubated with equal amounts of GST-GEF bound to beads for 3 hrs at 4˚C. Beads were washed with wash buffer (25 mM Tris/HCl, pH 7.5, 150 mM NaCl, 5 mM EDTA) and the pulldown eluates were analysed in western blots. Monoclonal antibodies recognizing actin (Simpson et al., 1984) or myosin II (Pagh and Gerisch, 1986) and a polyclonal antibody against myosin II heavy chain kinase A (Kolman et al., 1996) were used.

For interaction of GST-GEF with RasB, 5 x $10^7$ AX2 cells were lysed by sonication in LB without Triton-X100 and membrane and nuclear enriched pellet fraction separated by centrifugation at 100,000 *g* for 30 min at 4˚C. The pellet fraction was resuspended in LB containing 1% Triton-X100. The pulldown reaction was done as described above. For analysis of binding preference of GST-GEF for GTP- or GDP-bound RasB, cell lysates from 5 x $10^7$ AX2 cells were lysed in 1 ml LB. One 1 ml aliquot was pretreated with 100 µM GDP and 5 mM $MgCl_2$ and another one with 100 µM GTPγS and 5 mM $MgCl_2$ for 1 hr and the pulldown reaction was done as above. Eluates were probed with RasB-specific polyclonal antibodies (Sutherland et al., 2001).

Activation of RasB was assayed by performing pulldown with beads coated with the GST fused Ras-binding domain of *S. pombe* Byr2 (Gronwald et al., 2001; Scheffzek et al., 2001). 5 x $10^7$ AX2 and *RasGEF* $Q^-$ cells harvested at the vegetative (t0) and aggregation-competent (t6) stages and GFP-GEF expressing cells at the vegetative stage. Cells were lysed in LB and incubated with equal amounts of GST-Byr2 bound beads. Pulldown eluates were immunoblotted and probed with RasB antibody.

cAMP induced activation of RasB in aggregation competent AX2 cells was done according to Kae (Kae et al., 2004). Cells were stimulated with 500 nM cAMP while shaking and immediately lysed 0, 10 or 60 s after cAMP stimulation. Lysates were incubated with equal amounts of glutathione-sepharose beads coated with GST-Byr2(RBD) to pulldown active Ras, and probed with RasB antibody .

### 2.2.6 Preparation of cytoskeletal ghosts

Cytoskeletal fractions were isolated as proteins insoluble in Nonidet P-40 (Chung and Firtel, 1999) or as proteins insoluble in Triton X-100 (Steimle et al., 2001). For isolation of cytoskeletal fractions for analysing myosin II levels, 1 x $10^7$ cells were harvested at either the vegetative or aggregation competent stage by centrifugation and lysed in NP-40 buffer (50 mM Tris/HCl, pH 7.6, 100 mM NaCl, 10 mM NaF, 1 mM EDTA, 1 mM EGTA, 1% NP-40, 10% glycerol, 1 mM DTT, supplemented with protease inhibitors (Sigma)). After vortexing tubes were kept on ice for 10 min followed by 10 min at room temperature. The samples were spun at 100,000 *g* for 4 min. Supernatants were discarded and pellet fractions washed once with NP-40 buffer. The pellet fractions were dissolved in 2x SDS-PAGE sample buffer (Laemmli, 1970) and proteins resolved by SDS-PAGE (8% acrylamide) and visualized by Coomassie Brilliant Blue staining. Protein bands were scanned and changes in myosin II content in the cytoskeleton quantified using NIH-Image J software. For isolation of

cytoskeletal fractions for analyzing MHCK A, 1.5 x $10^6$ cells were lysed in buffer containing 0.1 M MES, pH 6.8, 2.5 mM EGTA, 5 mM $MgCl_2$, 0.5 mM ATP, 0.5% Triton X-100 supplemented with protease inhibitors (Sigma), briefly vortexed and then spun at 100,000 *g* for 1 min. Supernatant fractions were precipitated with acetone. Pellet and supernatant fractions were resolved by SDS-PAGE and immunoblotted using MHCK A specific monoclonal antibody (Steimle et al., 2001). The level of MHCK A in both the pellet and supernatant fractions was quantified by densitometric analysis of the scanned blot using the ImageJ program (NIH). The percent MHCK A in the pellet fraction was determined by dividing the value obtained for the band in the pellet by the total from the bands in the pellet and supernatant.

### 2.2.7 Analysis of cell shape and cell migration

Aggregation competent AX2 and *RasGEF* $Q^-$ cells were plated onto glass coverslips and allowed to settle for 15 minutes and chemotaxis experiments performed with micropipettes filled with $10^{-4}$ M cAMP attached to a micromanipulator system. The micropipette tip was carefully moved to touch the surface of the glass coverslip. Images were recorded at intervals of 6 s using a Leica DM-IL inverse microscope (40X objective) and a conventional CCD video camera and analyzed using Dynamic Image Analysis Software (DIAS) (Wessels et al., 1998).

### 2.2.8 2-dimensional SDS-PAGE

2D-gel electrophoresis was performed using an adaptation of protocols as described before (Clemen et al., 2005). *Dictyostelium* cells were lysed in lysis buffer (7 M urea, 2 M thiourea, 4% CHAPS, 40 mM Tris, 2% IPG-buffer, 2% DTT, 1 mM PMSF, protease

inhibitors (Roche) containing bromophenol blue at room temperature and centrifuged at 16.000 *g* for 5 min. Samples of supernatants (250 µl) were diluted with rehydration buffer to a volume of 350 µl and applied to the IEF-strips (18 cm, pH 3-10 non-linear) via rehydration technique for 12 h at 50 V. The strips were then focused on the IPGphor system (Amersham Biosciences) with a current limit of 50 µA per strip at 20°C with the following program: 1 h at 200 V, 1 h at 500 V, 1 h at 1000 V, gradient to 8000 V in 1 h, and a final focusing step at 8000 V for 28 kVh. After IEF the strips were briefly rinsed with water and prepared for the second dimension by a two-step equilibration and cystine alkylation process. The strips were incubated two times in equilibration buffer (50 mM Tris/HCl, pH 8.8; 6 M urea; 30% v/v glycerol; bromophenol blue) for 12 min, in which 1% (w/v) DTT (step one) or 4% (w/v) iodoacetamide were added, respectively. Subsequently, the strips were loaded on SDS gels (8% acrylamide) and resolved in the second dimension. Gels were subjected to immunoblotting using myosin II specific monoclonal antibody mAb 56-396-2 (Pagh and Gerisch, 1986).

### 2.2.9 Miscellaneous methods

For treatment with Latrunculin A, cells were treated with 10 µM Lat A in nutrient medium with shaking for 40 min. Cells were fixed by 3% paraformaldehyde/picric acid and stained for F-actin using TRITC-labelled phalloidin (Sigma). For staining for myosin II, aggregation competent cells were allowed to settle on coverslips and fixed using methanol (-20ºC) and stained for myosin II using monoclonal antibody 56-396-2 (Pagh and Gerisch, 1986) and images captured using a Leica TCS-SP laser scanning confocal microscope. For quantitative analysis initial scans using AX2 cells was used to optimize scanning parameters, subsequently *RasGEF* $Q^{-}$ cells were scanned. The accompanying Leica software was used to

generate pseudo 3-D projections from 2D images in which the *z*-axis represents intensity distribution over the scanned area.

Monoclonal antibodies recognizing contact site A protein (csA) (Bertholdt et al., 1985), actin (Simpson et al., 1984), GFP (Noegel et al., 2004) were used for western blotting.

## 2.3 Results

### 2.3.1 Domain organization, expression pattern and functional dissection of RasGEF Q

RasGEF Q is a 1298 aa protein with a calculated molecular mass of 143.000. Apart from the RasGEF domains, it contains a DEP domain (a domain conserved among fly Dishevelled, worm Egl10 and mammalian Pleckstrin) separating the two RasGEF domains and a predicted coiled-coil region at the N-terminus (Figure 7.).

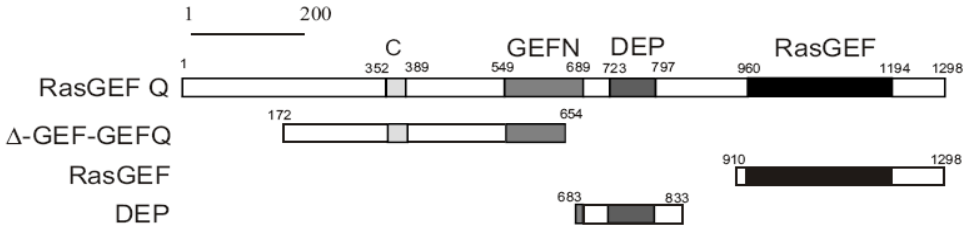


**Figure 7. Architecture of RasGEF Q and localization of RasGEF Q domains and generation of RasGEF Q null cells. (A) Schematic diagram of RasGEF Q depicting its domain organization and constructs used in the study.**

RasGEF Q mRNA as examined by RT-PCR analysis of cDNA is present throughout development with elevated levels during aggregation and the loose mound stage (t6-t8) (Figure 8 top, (Wilkins et al., 2005). Monoclonal antibody K-70-187-1 generated against the DEP domain of RasGEF Q recognized a protein of the expected size, which was present in

vegetative cells and in early development till the aggregation stage (t6) but could not be detected later (Figure 8 bottom). Instead, a smaller and less intense band was seen at subsequent stages (Figure 8 bottom *asterisk*). The smaller band could arise by translation from a downstream start (ATG) site at position 565. The sequence between both start sites is highly AT rich and could function as an alternative promoter.

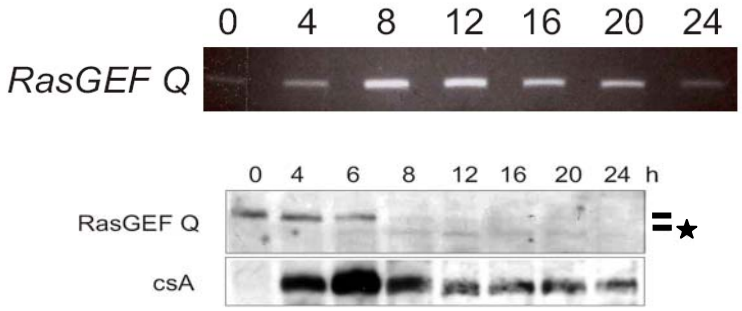


**Figure 8. Expression of RasGEF Q protein during development. Total cell lysates prepared at the indicated time points were immunoblotted and probed using mAb K-70-187-1 raised against RasGEF Q. In the lower panel expression of the developmentally regulated cell adhesion protein csA is shown for control.**

We used K-70-187-1 monoclonal antibodies to study the subcellular localization of endogenous RasGEF Q by immunofluorescence and found that the protein was present in the cytosol in wild type vegetative cells, whereas in *RasGEF Q*$^-$ cells the staining was strongly reduced (Figure 9).

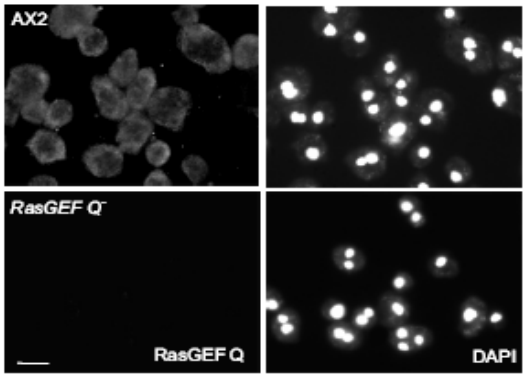


**Figure 9. Localization of endogenous RasGEF Q using purified RasGEF Q mAb K-70-187-4 in wild type and RasGEF Q null vegetative cells.**

To study the functions of different domains of RasGEF Q we expressed the corresponding GFP fusion proteins in AX2. In fixed cells the RasGEF domain (GFP-GEF) was present throughout the cytosol but was enriched at the cell cortex where it colocalized with F-actin (Figure 10, top panels, single arrow heads) and was also present in the nucleus (Figure 10, top panels, double arrow heads). Live cell analysis showed that the protein was present throughout the cells. It was also observed in the nucleus and in moving cells it accumulated in extending pseudopods. Cells expressing GFP-Δ–GEF-GEFQ, which corresponds to N terminal domain (amino acids 172-654) distributed throughout the cytoplasm with enrichment in the cortex (Figure 10, middle panels). The DEP domain was present throughout the cytoplasm but did not show a particular enrichment, neither in fixed nor in living cells (Figure 10, bottom panels).

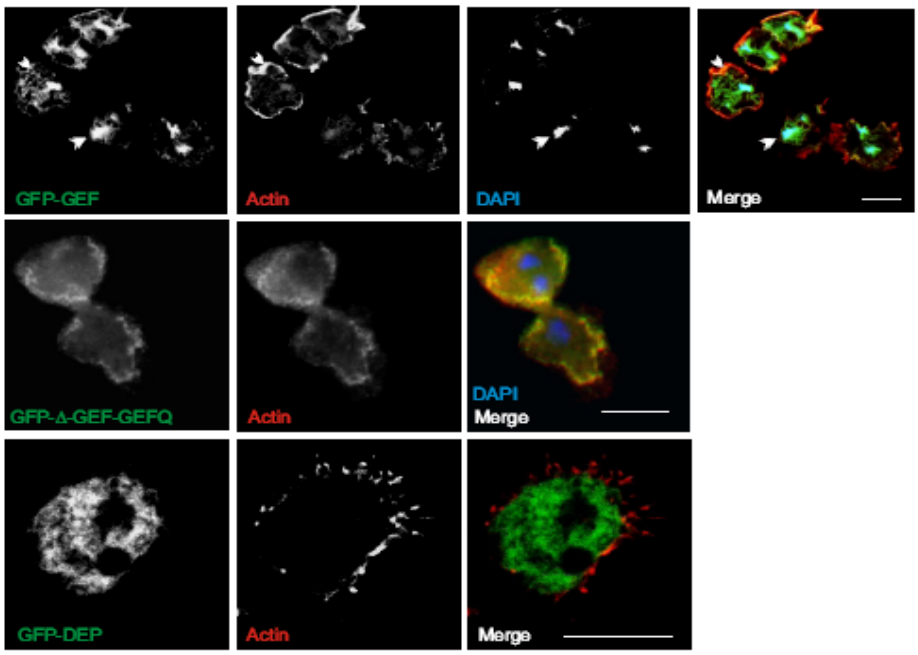


**Figure 10. Localization of GFP tagged RasGEF Q domains. Top panel, GFP-GEF localizes to the cell cortex (single arrowheads) and to the nucleus (double arrowheads). Middle panel, GFP-Δ-GEF-GEFQ localizes throughout the cytosol but is enriched in the cell cortex. Lower panel, the DEP domain is present throughout the cytoplasm. F-actin was stained by TRITC-labelled phalloidin, DNA with DAPI. Cells were fixed with picric acid/formaldehyde. Confocal images are shown. Bar, 10 µm.**

### 2.3.2 RasGEF Q association with the actin cytoskeleton

Small GTPases of the Ras superfamily and their regulatory GEFs are known to be directly involved in the regulation of the cytoskeleton (Lim et al., 2002). To investigate the colocalization of GFP-GEF with F-actin in the cortex further we used the F-actin depolymerizing drug latrunculin A (Lat A). Treatment with 10 µM Lat A for 40 min led to a loss of cortical F-actin. In parallel, the cortical localization of GFP-GEF was lost, whereas its nuclear localization and the cytoplasmic staining were not affected (Figure 11). This indicates that the GEF domain is recruited to the cortical region by F-actin.

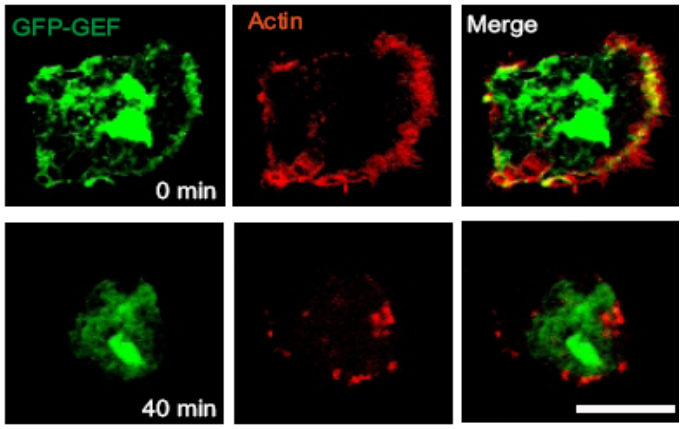


**Figure 11. Association of the C terminal part of RasGEF Q with F-actin. The cortical localization of GFP-GEF is sensitive to latrunculin A. Cells expressing GFP-GEF were incubated with Latrunculin A for 40 min and fixed with picric acid/formaldehyde and stained for actin using TRITC-labelled phalloidin. Bar, 10µm**

To test whether the GEF domain directly interacts with actin filaments, we performed co-sedimentation assays. We used the GST-tagged GEF domain in these assays and found that it co-sedimented with actin filaments by high speed centrifugation at 120,000 *g*, whereas the fusion protein alone stayed in the supernatant. The GST-GEF interaction with F-actin occurred even at high salt concentrations (100 mM KCl), which is known to drastically reduce the binding efficiency of several actin-binding proteins like α-actinin, comitin and plastin (Jung et al., 1996; Prassler et al., 1997) (Figure 12). In low speed sedimentation assays F-actin

could be pelleted in the presence of GST-GEF indicating the protein also possesses F-actin bundling activity (Figure 13). Together, our results imply that RasGEF Q binds to F-actin in vitro and in vivo and that the C-terminal region containing the RasGEF domain mediates this binding.

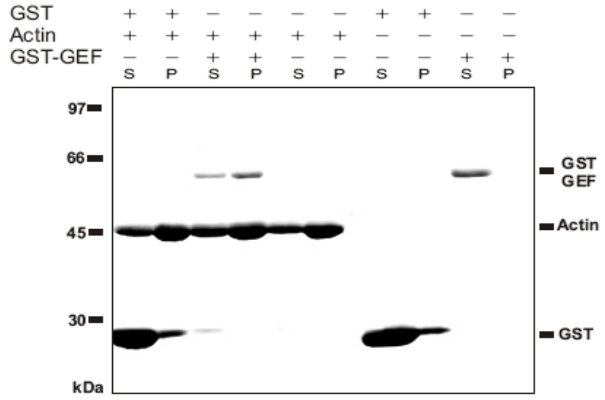


**Figure 12. Association of the C terminal part of RasGEF Q with F-actin.GST-GEF binds to F-actin in an *in vitro* cosedimentation assay using *Dictyostelium* actin. Pellet (P) and supernatant (S) were separated by high speed centrifugation and proteins in the fractions resolved by SDS-PAGE and stained with Coomassie-brilliant blue.**

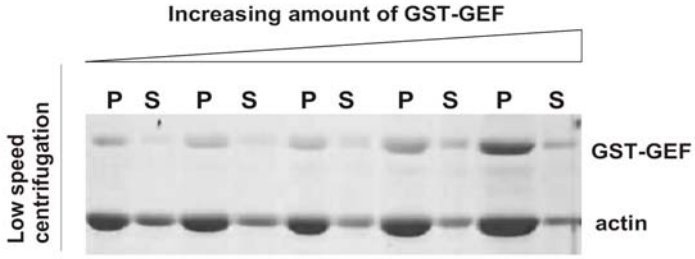


**Figure 13. F-actin bundling properties of GST-GEF in an *in vitro* cosedimentation assay using *Dictyostelium* actin. Pellet (P) and supernatant (S) were separated by low speed centrifugation at 12,000 *g* for 1 h at 4°C. Pellet and supernatant were resolved by SDS-PAGE (10% acrylamide) and proteins visualized by Coomassie Brilliant Blue staining.**

### 2.3.3 RasGEF Q null cells have defects in developmental patterning and slug motility

To study the functions of RasGEF Q in vivo we generated cells lacking RasGEF Q. *RasGEF Q*⁻ cells were generated by homologous recombination, screened by genomic PCR on

genomic DNA and confirmed by Southern and western blotting (Figure 14) and immunofluorescence analysis (Figure 8).

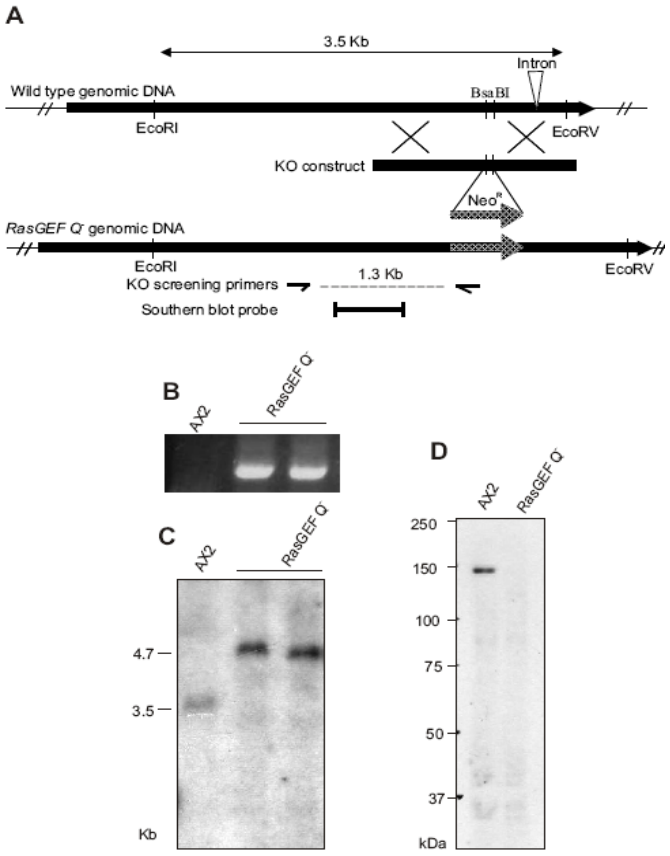


**Figure 14. Generation of RasGEF Q null cells. (A) Scheme for generation of *RasGEF Q*$^{-}$ cells. (B) Confirmation of mutant clones by PCR using genomic DNA of wild type AX2 and mutant clones. (C) Southern blot analysis using *EcoRI* and *EcoRV* digested genomic DNA confirms the recombination event. A probe encompassing nucleotides 690 - 990 of the cDNA was used. (D) Western blot analysis using cell lysates of vegetative cells from AX2 and *RasGEF Q*$^{-}$ cells were probed with mAb K-70-187-1.**

Multicellular morphogenesis can be described in its most basic form as a process where cells in a group undergo coordinated changes in cell shape and motility to form an organized structure to perform a particular function. The process of *D. discoideum* development is one such example of programmed multicellularization (Chisholm and Firtel, 2004). Involvement of the cytoskeleton in such processes that require continuous cellular changes is a prerequisite. When developed on nutrient deficient agar plates, AX2 cells form aggregates by 8 h and tipped mounds by 13 h. The tip elongates to form a standing finger that

falls down, becoming a migratory slug or pseudoplasmodium by 16 h. Development is completed by 20-24 hrs with the formation of fruiting bodies (Figure 15. Top panels). *RasGEF Q*$^{-}$ cells initiate the developmental programme, but in over 50% of the mounds multiple tips arise from a single mound by 13-14 h and as a result fruiting bodies are smaller than in AX2 (Figure 15, middle panels). Cells overexpressing GFP-GEF show normal development (Figure 15, bottom panels)

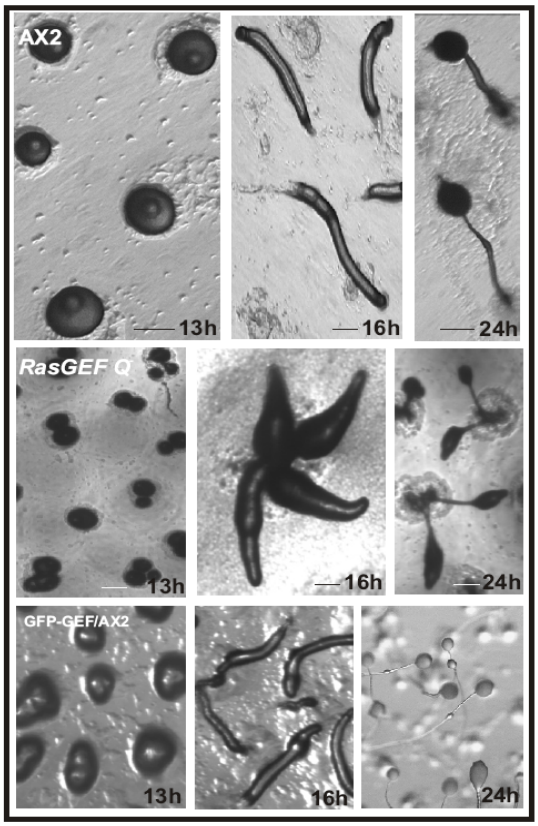


**Figure 15. Developmental defects in RasGEF Q null cells. Top panels, wild type tipped-aggregate (13 hours), migratory slug (16 h), fruiting body (24 h). Middle panels, *RasGEF Q*$^{-}$ aggregates break up into smaller aggregates (13 h), multiple tipped structures (16 h) and fruiting bodies (24h). Bottom panels, development of cells overexpressing GFP-GEF. Bars, 200 µm**.

*RasGEF Q*$^{-}$ cells form slugs that are relatively smaller and their ability to move was greatly reduced and they did not perform phototaxis towards a directed light source. In contrast, slugs from AX2 cells expressing GFP-GEF were able to move and perform phototaxis, but the migration was more disoriented compared to the parental AX2 strain.

GFP-GEF slugs migrated at an average angle of about 80˚, whereas AX2 slugs migrated at an average angle of 25˚ towards the light. *RasGEF Q*$^{-}$ cells expressing GFP-GEF or GFP-Δ-GEF-GEFQ showed slightly improved slug motility in phototaxis assays compared to *RasGEF Q*$^{-}$ cells; a proportion of the slugs formed could migrate towards the light source, although migration was greatly reduced, indicating that the RasGEF Q is important for slug motility (Figure 16).

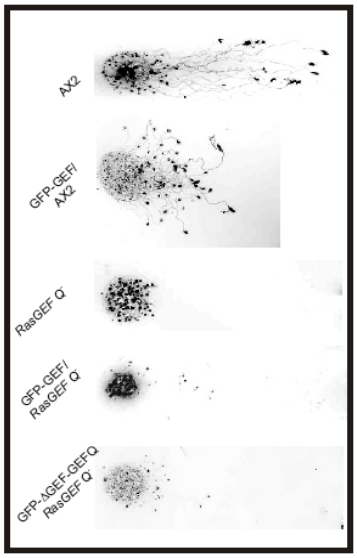


**Figure 16. Developmental defects in RasGEF Q null cells. Altered slug motility in phototaxis assays in *RasGEF Q*$^{-}$ and GFP-GEF expressing cells. Wild type AX2, GFP-GEF overexpressing AX2 cells *RasGEF Q*$^{-}$ cells as well as *RasGEF Q*$^{-}$ cells expressing GFP-GEF or GFP-Δ-GEF-GEFQ were allowed to develop on phosphate agar plates placed in a black opaque box for 36 h with a unidirectional light source from an open slit. Migratory pattern of slugs were determined by transferring slime trails and cellular materials onto nitrocellulose membrane. Membranes were stained with 0.1% amido black.**

*D. discoideum* serves as a model system to understand cell sorting. At the mound stage an asymmetry is established and a fixed proportion of cell types is generated where the majority of the cells (nearly 80%) are destined to become spore cells, and sort to the rear of a slug, and 20% occupy the anterior tip becoming the stalk cells that hold the spore mass in the fruiting body. Involvement of a particular protein in such cell-sorting mechanisms can be easily studied in *D. discoideum* by mixing strains together and allowing them to co-develop as

a chimera. When 10% GFP-expressing AX2 cells were mixed with 90% unlabelled AX2 cells, GFP-labelled cells distributed evenly throughout the slug. However, when 10% GFP-labelled AX2 cells were mixed with 90% unlabelled *RasGEF Q*$^{-}$ cells, wild type cells localized to the anterior prestalk region and mutants are present in the posterior prespore region of the slug. In a converse experiment where 10% GFP-labelled *RasGEF Q*$^{-}$ cells were mixed with 90% AX2 cells mutant cells also sorted to the posterior (Figure 17).

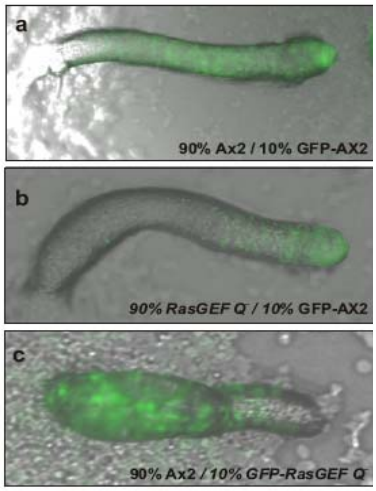


**Figure 17. Altered cell-type spatial patterning in *RasGEF Q*$^{-}$ mutants. (a) 10% AX2 cells labelled with GFP were mixed with 90% unlabelled wild type cells, (b) 10% labelled wild type cells were mixed with 90% unlabelled *RasGEF Q*$^{-}$ cells, (c) 10% labelled *RasGEF Q*$^{-}$ cells were mixed with 90% AX2 cells and were codeveloped as a chimera. Images were taken at the slug stage.**

### 2.3.4 Cytokinesis defect in suspension in cells overexpressing GFP-GEF and constitutively activated RasB

Further analysis revealed that the cells expressing GFP-GEF were defective in cytokinesis in suspension. When grown in suspension for six days they attain an average nuclei number of about 6 nuclei per cell, whereas wild type AX2 and *RasGEF Q*$^{-}$ cells are mostly mono- or binucleated (Figure 18 A-D). However, when grown on a plastic surface GFP-GEF cells are predominantly mono- or binucleated probably dividing by traction-

mediated cytofission as occurs in *mhcA*$^{-}$ cells (De Lozanne and Spudich, 1987; Neujahr et al., 1997).

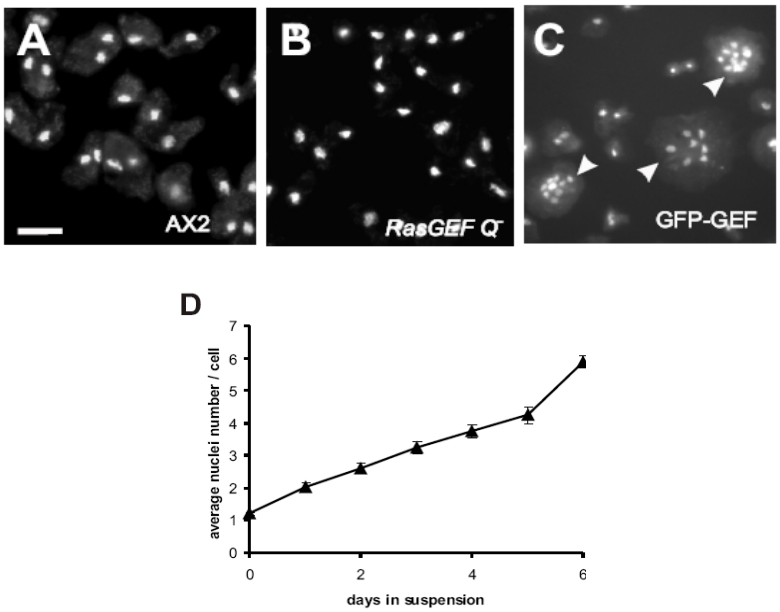


**Figure 18. Cells overexpressing GFP-GEF have a cytokinesis defect. (A and B) Cytokinesis is normal in wild type AX2 and *RasGEF Q*$^{-}$ cells but is defective in GFP-GEF cells (C). Arrowheads indicate multinucleated cells. Bar, 10 µm. (D) The increase in the number of nuclei in GFP-GEF cells. GFP-GEF cells were grown in suspension, fixed at the indicated times, stained with DAPI and the nuclei counted.**

Our results indicate that, although in GFP-GEF cells karyokinesis is normal, the following cytokinesis is impaired. We also confirmed previous data on the localization and phenotype of cells expressing constitutively activated RasB (RasB$^{G12T}$) (Sutherland et al., 2001). Overexpression of GFP-tagged RasB$^{G12T}$ caused cells to become multinucleated in suspension and was slightly enriched in the nucleus (Figure 19). Since overexpressors of the GEF domain and overexpressors of RasB$^{G12T}$ had phenotypic similarities we hypothesised that RasGEF Q could be an exchange factor for RasB, and overexpression of the GEF domain acts as an activated form of RasGEF Q, and a regulatory mechanism must exist.

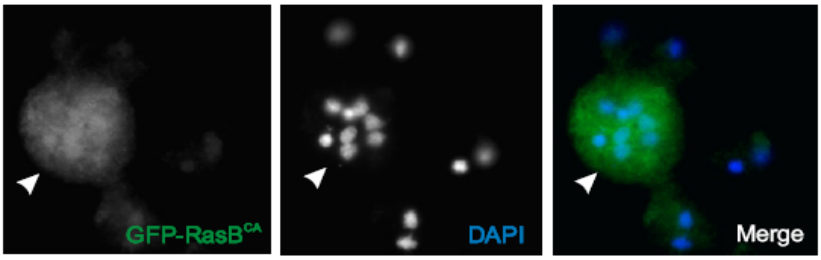


**Figure 19. Cytokinesis defect in cells overexpressing constitutively activated RasB$^{G12T}$ (GFP-RasB$^{CA}$). Cells were fixed with methanol and nuclei are visualized with DAPI. Arrowheads indicate a multinucleated cell.**

### 2.3.5 RasGEF Q activates RasB

To test whether RasGEF Q interacts with and activates RasB we performed several assays. In pulldown assays, GST-GEF bound to glutathione-sepharose beads could precipitate RasB from AX2 cell lysates (Figure 20 A). When cell lysates were pre-treated with 5 µM GDP or 5 µM GTPγS, we found that GST-GEF bound preferentially to the GDP-bound form of RasB (Figure 20 B) which is the preferred form for a RasGEF-Ras interaction.

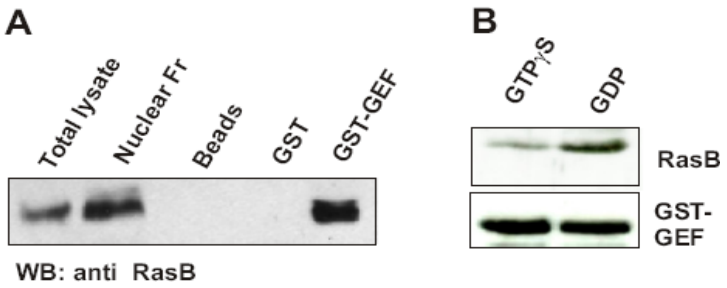


**Figure 20. Physical association of GST-GEF and RasB. (A) Glutathione-sepharose beads coated with either GST-GEF or GST or uncoated with any protein were incubated with AX2 cell lysates, pulldown eluates were immunoblotted with RasB antibody. (B) GST-GEF binds preferentially to GDP-bound RasB. Glutathione-sepharose beads coated with either GST-GEF were incubated with AX2 cell lysates preincubated with 100 µM GTPγS or 100 µM GDP. Pulldown eluates were immunoblotted with RasB antibody.**

To determine if RasGEF Q actually activates RasB we used GST-Byr2RBD (Ras Binding Domain) to pull down GTP-bound active RasB from AX2, *RasGEF Q*$^{-}$ or GFP-GEF cells. *S. pombe* Byr2 is a Ras effector (MEK kinase homolog) and binds to Ras in its

activated (GTP-bound) form (Gronwald et al., 2001; Scheffzek et al., 2001). Cell lysates of AX2 and *RasGEF Q*$^{-}$ at the growth (t0) and aggregation (t6) stage and GFP-GEF at t0 were incubated with equal amounts of GST-Byr2RBD bound to glutathione-sepharose beads. We found that RasB is activated only at t6 in AX2 cells, whereas *RasGEFQ*$^{-}$ cells are unable to activate RasB at either t0 or t6. GFP-GEF cells at t0 have a high level of activated RasB, indicating that RasGEF Q acts as an exchange factor for RasB (Figure 21). Expression of the GEF domain alone may act as a constitutively activated form of RasGEF Q. Our results also indicate that, although RasB is expressed throughout development (Daniel et al., 1993), it is activated upon starvation, thus implying a role for cAMP in its activation process. Since RasB is not activated in *RasGEFQ*$^{-}$ cells we can conclude that it is the only or the predominant exchange factor for RasB.

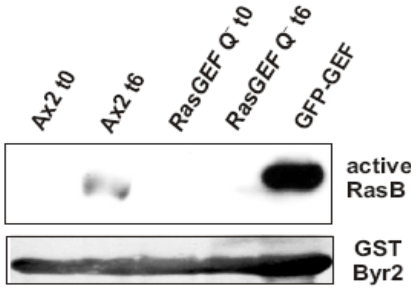


**Figure 21. RasB is activated upon starvation (t6) in wild type cells but is not activated in *RasGEF Q*$^{-}$ but is activated in cells overexpressing GFP-GEF (t0) as shown using beads coated with GST-Byr2(RBD).**

### 2.3.6 RasB is activated upon cAMP stimulation

To test whether RasB is activated upon response to cAMP, we used GST-Byr2(RBD) to pulldown activated Ras from cell lysates stimulated with cAMP. We observed an elevation in the levels of activated RasB within 10 s of stimulation with cAMP and decreasing by 60 sec (Figure 22 A, top lanes). We also observed that in cells overexpressing the DEP domain, the RasB activation was greatly reduced and delayed (Figure 22 A, bottom lanes). As

overexpression of the GEF domain acts as a constitutively activated form of RasGEF Q, the DEP domain that resides between the RasGEF domains might serve as a possible autoregulatory domain in the activation process of RasGEF Q. Further on, in a GST pulldown experiment GST-DEP could pulldown GFP-GEF from cell lysates of cells overexpressing GFP-GEF, indicating that the two domains can physically interact (Figure 22 B).

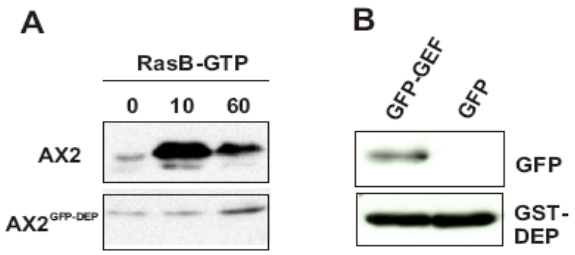


**Figure 22. Activation of RasB in response to cAMP. (A) Aggregation competent AX2 cells (top lanes) or wild type cells overexpressing GFP-DEP (lower lanes) were stimulated with 500 nM cAMP and the amount of activated RasB bound to GST-Byr2(RBD) was determined at the indicated time points. (B) Interaction between the DEP and the GEF domain of RasGEF Q. Glutathione sepharose beads coated with GST-DEP and incubated with cell free extracts from cells expressing GFP-GEF or GFP alone.**

### 2.3.7 Role of RasGEF Q in regulating myosin II function

Defects in Ras pathways result in chemotaxis defects (Charest and Firtel, 2006; Sasaki and Firtel, 2005; Sasaki and Firtel, 2006). To examine whether RasGEF Q had any effect on chemoattractant-induced cell migration, we compared the migration of aggregation competent *RasGEF Q*$^{-}$ and parental AX2 cells. During migration towards an exogenous cAMP source, wild type cells are well polarized and produce pseudopodia exclusively at the leading edge and very few lateral pseudopods. In contrast, *RasGEF Q*$^{-}$ cells produce more random pseudopodia (4.6 per cell /10 min) than wild-type cells (1.7 per cell / 10 min) (Table I) and have an increased frequency of turning (Figure 23 A and B), showing similarities to 3xALA myosin mutants. Surprisingly, the cell motility parameters (speed, persistence and direction change) were not significantly altered.

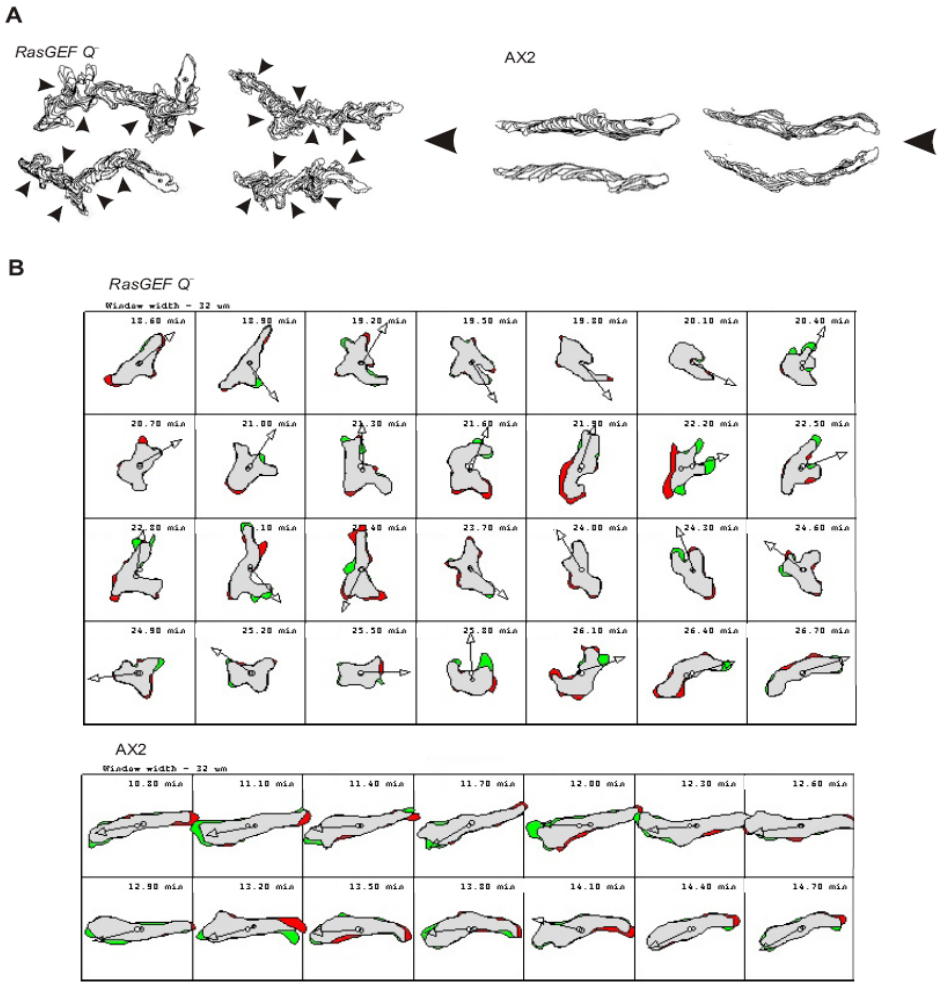


**Figure 23. Chemotactic behaviour of *RasGEF Q⁻* cells. (A) Computer generated cell tracks of *RasGEF Q⁻* and AX2 cells during chemotactic migration in a spatial cAMP gradient using DIAS. Arrows indicate turns initiated by formation of lateral pseudopods in *RasGEF Q⁻* cells. (B) Shape changes of aggregation competent *RasGEF Q⁻* and AX2 cells during chemotactic migration were analysed by DIAS. Images were taken every 6 s but only every third frame is shown. The green areas indicate new membrane protrusions and the red areas indicate retractions.**

Table. Lateral pseudopod formation by cells crawling in buffer and in a spatial cAMP gradient

| | Cell type | Number of cells | 0-2 lateral pseudopods per 10 minute (%) | 3-5 lateral pseudopods per 10 minute (%) | >5 lateral pseudopods per 10 minute (%) | Average frequency of lateral pseudopods per cell per 10 min |
|---|---|---|---|---|---|---|
| Buffer | AX2 | 31 | 9.6 | 45.16 | 45.16 | 5.19 |
| | RasGEF Q⁻ | 33 | -- | 21.21 | 78.78 | 7.03 |
| Gradient | Ax2 | 35 | 82.85 | 17.14 | -- | 1.71 |
| | RasGEF Q⁻ | 29 | 6.9 | 65.50 | 27.50 | 4.65 |

Images were taken at magnification of 40X every 30 s. In all cases cells were analysed for 10 min. Chi-square test performed between AX2 and RasGEF Q⁻ cells on data of the three categories of lateral pseudopods formed showed highly significant ( $p \geq 0.001$) difference between AX2 and RasGEF Q⁻ in both buffer and cAMP gradient.

In chemotaxing cells myosin II typically localizes to the posterior cortical regions of polarized cells where it is required for retraction of the cell body and suppression of lateral pseudopods. When we stained *RasGEF Q*$^{-}$ cells for myosin we observed an increased myosin staining in the cortex, that was not restricted to the rear, and also an elevated myosin level throughout the cytoplasm (Figure 24).

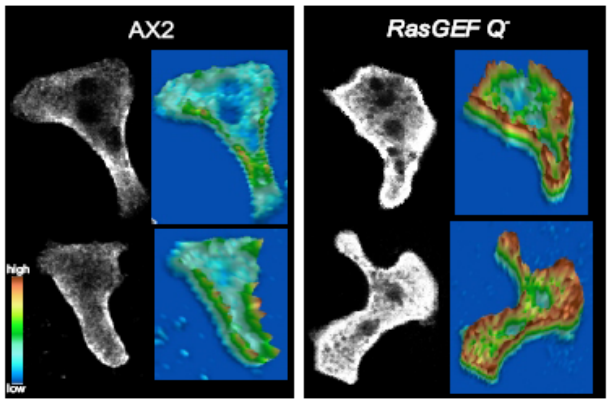


**Figure 24. RasGEF Q regulation of myosin II assembly. (A) Aggregation competent AX2 and *RasGEF Q*$^{-}$ cells were fixed and stained for myosin II. Images were taken with a confocal microscope. Every confocal section is accompanied by a pseudo 3-D projection in which the *z*-axis represents the intensity of myosin II staining over the scanned area.**

To test this further we measured the amounts of myosin II present in preparations of cytoskeletal ghosts of *RasGEF Q*$^{-}$ and AX2 cells both from growing and aggregation competent stages. In this assay the amount of myosin II recovered reflects the amount of filamentous myosin associated with the actin cytoskeleton in the living cell. Myosin II filament assembly and disassembly is an extremely dynamic process and in *D. discoideum* it depends largely on the levels of myosin heavy chain phosphorylation. Also, the level of myosin II in the cytoskeletal fractions in AX2 cells is significantly higher in aggregation competent cells than in growing cells. In contrast, *RasGEF Q*$^{-}$ cells had a high level of myosin II in the cytoskeletal fractions obtained from growing cells, which was comparable to that in aggregating AX2 cells and there was no significant rise upon reaching aggregation competence (Figure 25, top lanes). Total myosin II levels in both AX2 and *RasGEF Q*$^{-}$ cells were comparable in vegetative and aggregation competent cells (Figure 25, bottom lanes).

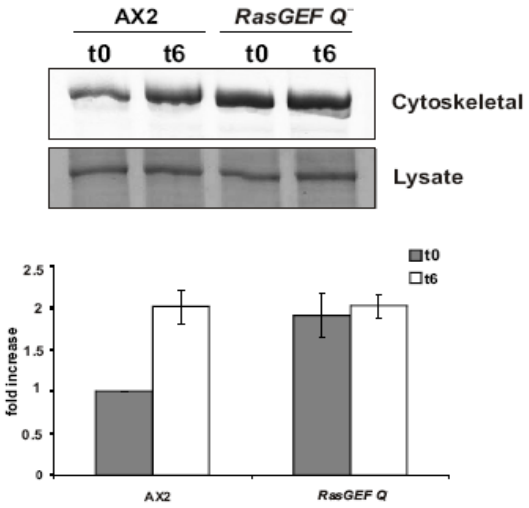


**Figure 25. RasGEF Q regulation of myosin II assembly. Myosin II levels in cytoskeletal ghosts from cells in vegetative and aggregation competent stages. The graph (below) represents an average of four independent experiments.**

The cause for higher levels of filamentous myosin II in *RasGEF Q*$^{-}$ cells could be due to higher levels of unphosphorylated myosin II that can spontaneously form filaments. To test this hypothesis we determined the phosphorylation status of myosin II in vegetative AX2 and

*RasGEF Q*$^{-}$ cells. We used 2-dimensional gel electrophoresis to examine the changes in the isoelectric point (pI) of phosphorylated versus unphosphorylated myosin II. We observed myosin II as a distinct spot in a western blot using myosin II antibodies. We found that in *RasGEF Q*$^{-}$ cells myosin II had a higher pI than myosin II in AX2 cells, implying that in *RasGEF Q*$^{-}$ cells myosin was predominantly in the unphosphorylated state (Figure 26). From these results we conclude that the higher levels of unphosphorylated myosin II in *RasGEF Q*$^{-}$ cells lead to higher levels of filamentous myosin II and involve myosin heavy chain kinases in the process.

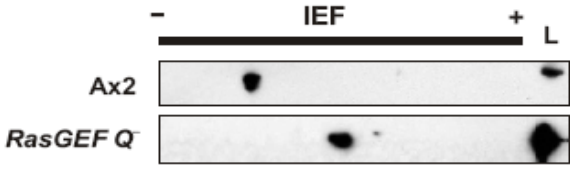


**Figure 26. RasGEF Q regulation of myosin II assembly. Lysates from vegetative wildtype AX2 and *RasGEF Q*$^{-}$ cells were subjected to 2-D SDS-PAGE analysis for determining the phosphorylation status of myosin II.**

### 2.3.8 RasGEF Q regulates Myosin II through MHCK A

The presence of higher amounts of unphosphorylated myosin II in *RasGEF Q*$^{-}$ cells indicated that probably myosin phosphorylation is affected. MHCK A is a major kinase regulating myosin II phosphorylation. In GST-pulldown experiments we found that GST-GEF could co-precipitate myosin II and myosin heavy chain kinase A (MHCK A) from cell lysates under conditions that dissociate actin-myosin complexes by addition of 5 mM ATP. Actin was absent from the precipitate. When cell lysates were preincubated with Lat A to disrupt the cytoskeleton, the association with myosin II and MHCK A was totally abolished (Figure 27). These results indicate that an intact cytoskeleton is required for bringing a signalling complex together, where RasGEF Q can bind to MHCK A and myosin II in an F-actin dependent manner.

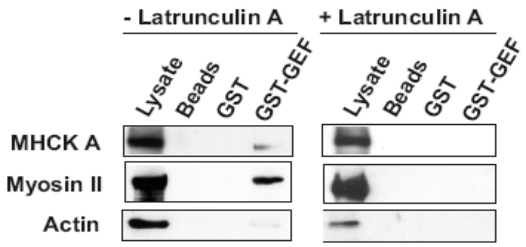


**Figure 27. RasGEF Q regulates myosin II through MHCK A. (A) GST-GEF can associate with myosin II and myosin heavy chain kinase A (MHCK A) in a manner that is sensitive to Latrunculin A treatment.**

We then examined MHCK A in *RasGEF Q*$^{-}$ cells and in cells overexpressing GFP-GEF. Under normal conditions MHCK A is localized throughout the cytosol, upon chemoattractant stimulation MHCK A associates with the cytoskeleton and localizes to the cell cortex (Steimle et al., 2001). Association with the actin cytoskeleton causes a drastic increase in the autophosphorylation activity of MHCK A which is then activated (Egelhoff et al., 2005). Using a monoclonal antibody that detects both the phosphorylated (~145 kDa) and the unphosphorylated (130 kDa) form of MHCK A (Steimle et al., 2001), we found that *RasGEF Q*$^{-}$ cells and cells overexpressing GFP-GEF have both unphosphorylated and autophosphorylated MHCK A. We then analyzed the amounts of MHCK A associated with cytoskeletal fractions as the cytoskeleton associated protein represents the active autophosphorylated form of MHCK A. We found that *RasGEF Q*$^{-}$ cells and AX2 cells have similar amounts of MHCK A associated with the cytoskeletal fractions. In contrast, cells overexpressing the GEF domain had at least two fold higher levels of MHCK A associated with the cytoskeletal fractions (Figure 28).

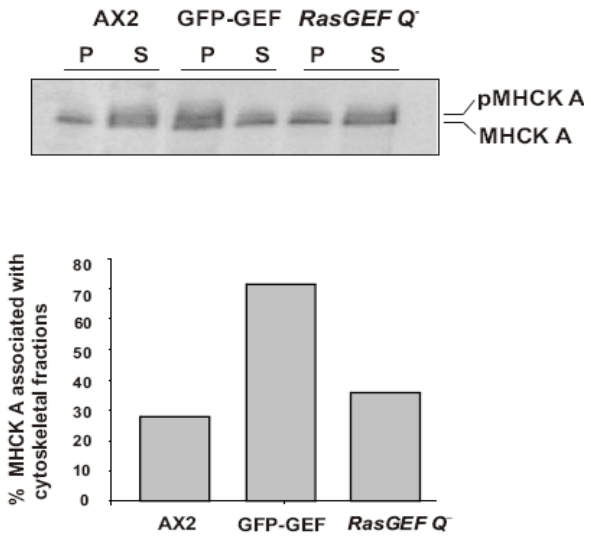


**Figure 28. RasGEF Q regulates myosin II through MHCK A. Cytoskeletal fractions from wild type AX2, AX2 cells overexpressing GFP-GEF and *RasGEF Q*$^{-}$ cells were prepared as described in Materials and methods. Supernatant and pellet fractions were resolved by SDS-PAGE and immunoblotted using MHCK A specific monoclonal antibody. The graph below represents the average of two independent experiment and shows the amount of MHCK A present in the pellet fractions as the percentage of the total MHCK A content.**

To investigate if activated Ras could transduce signals for regulation of myosin II, we used the GST-Byr2(RBD) to pulldown active Ras from GFP-GEF cells at t6 and found MHCK A in pulldown eluates with active RasB (Figure 29). Pulldown eluates did not contain myosin II. Thus, MHCK A, which directly regulates myosin II phosphorylation, may either bind directly to active Ras or associate with complexes containing active Ras, suggesting that it might be regulated by Ras upon activation.

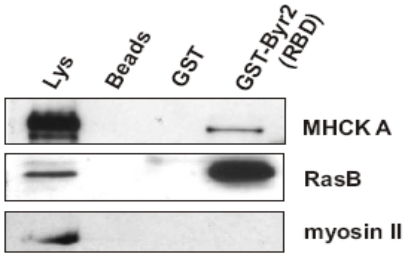


**Figure 29. RasGEF Q regulates myosin II through MHCK A. Presence of MHCK A in fractions containing active RasB. Active RasB was pulled down from GFP-GEF (t6) cells**

**using GST-Byr2(RBD). The precipitates were tested for the presence of myosin heavy chain kinase A (MHCK A) and myosin II heavy chain.**

## 2.4 Discussion

### 2.4.1 RasGEF Q in regulation of myosin II functions

Our studies on RasGEF Q reveal that it is required for regulation of myosin II based cellular functions like cytokinesis and cell shape during chemotaxis and also affects late developmental decisions. We provide evidence for RasB being a substrate for RasGEF Q and propose that regulation of myosin II functions by RasGEF Q occurs predominantly through RasB. Cells lacking RasGEF Q show myosin II overassembly associated with the inability to suppress lateral pseudopods similar to that observed in 3XALA myosin II mutants. We show that the myosin overassembly is due to higher levels of unphosphorylated myosin II in these cells, so the defect in myosin phosphorylation might arise from an inability to activate myosin heavy chain kinases. Cells that overexpress the GEF domain of RasGEF Q have a cytokinesis defect in suspension and these cells also have high levels of constitutively activated RasB. We identified RasB as the substrate for RasGEF Q through in vivo and in vitro binding assays and found that RasB is activated upon cAMP, which indicates an involvement of cAMP and cAMP receptors (seven transmembrane G-protein coupled receptors, GPCR) in the process of activation.

We ruled out the possibility that RasGEF Q might activate RasG. Cells lacking RasG show a cytokinesis defect (Tuxworth et al., 1997), whereas in cells that overexpress the GEF domain of RasGEF Q resulting in constitutively high levels of active Ras we see a cytokinesis defect, and thus activation of RasG might be independent of RasGEF Q. We also provide a function for the less well understood function of the DEP domain in RasGEF Q as our results

point to the DEP domain acting as an autoregulatory domain of RasGEF Q. Under vegetative conditions when RasB is not activated, the DEP domain can bind to the GEF domain and RasGEF Q is in an inactive conformation. On starvation, GPCRs upon cAMP binding can induce a conformational change whereby the DEP domain inhibition is released and thus activate RasGEF Q, which activates RasB.

We observed that myosin in *RasGEF Q*$^{-}$ cells has a higher pI, possibly due to higher levels of unphosphorylated myosin II. A higher level of unphosphorylated myosin II is the cause of myosin overassembly in the cortex in *RasGEF Q*$^{-}$ cells. This also implies a role of MHCK in the process. In *D. discoideum* the most immediate regulators of myosin II are MHCKs. *D. discoideum* has four MHCKs (A-D), among which MHCK A has been most extensively studied. *MKCK A*$^{-}$ cells exhibit a partial, but significant level of myosin II overassembly due to higher levels of unphosphorylated myosin II. Overexpression of MHCK A elicits defects comparable to those observed in myosin II null cells, namely a blocked cytokinesis in suspension and arrested development in the mound stage (Kolman et al., 1996). In chemotaxing cells MHCK A relocalizes to the actin rich cortex in the anterior of the cell, where it presumably functions to phosphorylate and disassemble myosin II at the leading edge (Steimle et al., 2001). The GEF domain of RasGEF Q has the ability to co-precipitate MHCK A and myosin II in an F-actin dependent manner. In accordance with the fact that RasGEF Q regulates myosin II functions by regulating MHCK A, we observed that cells overexpressing the GEF domain have a two fold higher level of MHCK A associated with cytoskeletal fractions. This is the result of MKCK A activation by autophosphorylation where upon it associates with the actin-cytoskeleton in aggregation competent cells that are stimulated with cAMP (Steimle et al., 2001). Thus overexpression of the GEF domain causes larger amounts of MHCK A to be activated. On the other hand, MHCK A distribution in cytoskeletal fractions is normal in *RasGEF Q*$^{-}$ cells indicating that RasGEF Q plays a role in facilitating MHCK A recruitment to the cytoskeleton, and that other (probably passive) processes are

important for returning the kinase to the cytosol. Furthermore, the C terminus of RasGEF Q, which harbours the GEF domain, has the potential to bind to F-actin directly in F-actin co-sedimentation assays. These results also suggest that the actin cytoskeleton may serve as a scaffold to recruit a signalling complex at the leading edge. RasB, which is activated by RasGEF Q may promote myosin II phosphorylation by regulating the activity of myosin heavy chain kinase A (Figure 30) which leads to phosphorylation of myosin II followed by elimination of filamentous myosin II from the leading edge. In a mutant situation where RasGEF Q is absent, RasB would not be active and MHCK A activation would be limited and would result in higher levels of unphosphorylated myosin and thus myosin II overassembly in the cortex in these cells. In a situation where we overexpress the catalytic GEF domain of RasGEF Q we see constitutively high levels of activated RasB which activates MHCK A leading to higher levels of phosphorylated myosin II. Since phosphorylated myosin II cannot assemble into filaments that are required to provide force during cytokinesis, these cells fail to divide in suspension. Such a system may be very useful for *D. discoideum* and the expansion of the functional roles for Ras proteins may compensate for the lack of Rho GTPases or its effector molecule ROCK, which regulate myosin II functions in higher eukaryotes (Somlyo and Somlyo, 2000).

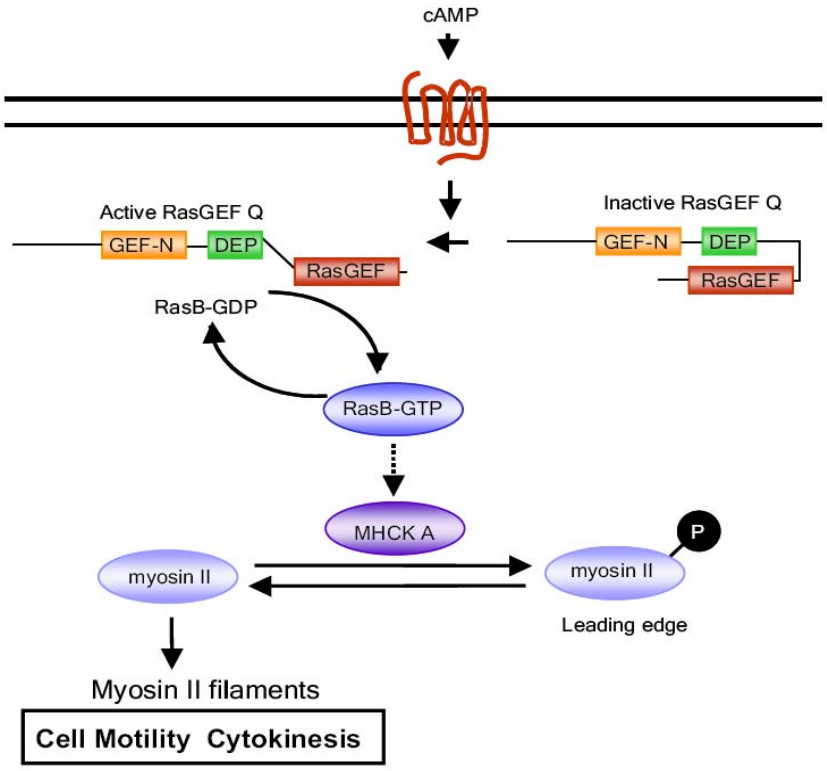


**Figure 30. Model for a role of RasGEF Q in regulating Myosin II functions**

### 2.4.2 RasGEF Q in *D. discoideum* development

The process of *D. discoideum* development is an example of programmed multicellularization (Chisholm and Firtel, 2004), where cells that form and organize the multicellular organism undergo continuous coordinated changes in shape and motility which require the cytoskeleton. *D. discoideum* tip formation is an event that can serve as a model to understand similar developmental processes in other organisms. Normally only one tip arises from a mound and this apical tip serves as an organizer to control morphogenesis of the organism by acting as a cAMP oscillator from which waves are initiated and propagated posteriorly (Siegert and Weijer, 1992; Siegert and Weijer, 1995). Mounds from *RasGEF Q*$^{-}$ cells give rise to supernumerary tips and as a result smaller fruiting bodies are formed. Besides *RasGEF Q*$^{-}$ cells mutations in other components of signal transduction cascades lead

to similar defects. A defect in Scar, a WASP-related protein identified in a mutant screen that suppresses phenotypes of *cAR2*$^{-}$ cells, also leads to a multiple tipped phenotype (Bear et al., 1998) as does overexpression of an activated RasD$^{G12T}$ (Reymond et al., 1986). Similarly, a double knockout of two isoforms of phosphatidylinositol-3-kinase (*PI3K*$^{1-/2-}$) and overexpression of the phosphotyrosine phosphatase PTP1 also resulted in the multiple tip phenotype (Howard et al., 1992; Zhou et al., 1995).

Multiple tips arising from *RasGEF Q*$^{-}$ mounds may result from the formation of more than one oscillator (or embryogenic organizer). It is also possible that a single embryogenic organizer subdivides to form multiple organizers causing the multiple tip phenotype. The tip of the slug is also critical in sensing light and phototactic migration of the slugs. *RasGEF Q*$^{-}$ mounds gave rise to slugs, but when analyzed for their ability to migrate in phototaxis assays they showed severe impairment. On the other hand, slugs from cells overexpressing GFP-GEF formed migratory slugs but their orientation towards the light source was severely impaired. Several proteins in Ras signaling have been implicated in phototaxis, with *RasD*$^{-}$ and *RasGEF E*$^{-}$ cells having totally impaired phototaxis (Wilkins et al., 2000; Wilkins et al., 2005).

Our data also suggests that a RasGEF Q mediated pathway is required for proper spatial patterning in the slug. In chimeric experiments with *RasGEF Q*$^{-}$ cells and wild type cells, *RasGEF Q*$^{-}$ cells are predominant in the posterior prespore region of the slug. Absence of RasGEF Q may cause defects in proper directional movement of cells within the slug necessary to maintain proper spatial patterning. The cell-autonomous nature of this defect in *RasGEF Q*$^{-}$ mutants may suggest a role of RasGEF Q in processing external signals. Similar patterns of mutant cell distributions in chimeras have been reported for cells lacking the GPCR CrlA, G protein Gα5 or the ERK1 protein kinase, suggesting these components might function in the same or in related pathways (Gaskins et al., 1996; Natarajan et al., 2000;

Raisley et al., 2004). The findings that myosin heavy chain and myosin light chain are required for cell patterning during *D. discoideum* development may also be relevant for RasGEF Q regulating myosin II (Chen et al., 1998; Eliott et al., 1993; Springer et al., 1994). Cells lacking myosin heavy chain can aggregate but fail to proceed beyond the mound stage of development. The regulatory light chain of myosin has also been thought to be required for directional sorting of prestalk EcmAO cells at the tip of a developing mound (Clow et al., 2000). Though RasGEF Q transcripts are present throughout development, a protein of higher molecular weight is present in the first six hours of development and smaller isoform generated by an alternative promoter is present in low amounts during later stages of development. This smaller form of the protein might have functions in regulating processes in late development.

# Chapter 2

## GxcDD, a putative RacGEF, is important for *Dictyostelium* development

*Rho subfamily GTPases are implicated in a large number of actin related processes. They shuttle from an inactive GDP-bound form to an active GTP-bound form. This reaction is catalysed by Guanine nucleotide exchange factors (GEFs). GTPase activating proteins (GAPs) help the GTPase return to the inactive GDP-bound form. Compared to our understanding of the downstream effects of Racs our understandings of upstream mechanisms that activate Rac GTPases are relatively poor. We report on GxcDD (**G**uanine e**x**change factor for Ra**c** GTPases), a Dictyostelium RacGEF. GxcDD is 180-kDa multidomain protein containing a CH domain, two IQ motifs, three PH domains, a RhoGEF domain and an ArfGAP domain. Inactivation of the gene results in defective streaming during development under different conditions and a delay in developmental timing. Characterizations of single domains revealed that the CH domain of GxcDD functions as a membrane association domain, the RhoGEF domain can physically interact with a subset of Rac GTPases and the ArfGAP-PH tandem accumulates in cortical regions of the cell and in phagosomes. Our results also suggest that a conformational change is required for activation of GxcDD, which would be important for its downstream signaling.*

## 3.1 Introduction

Rho GTPases are small monomeric GTPases of the Ras superfamily. Like any other GTPase Rho GTPases act as binary molecular switches cycling between a GTP-bound active and a GDP-bound inactive form. Guanine nucleotide exchange factors (GEFs) catalyze the activation reaction, and GTPase activating proteins (GAPs) convert the active to an inactive form. Further regulators, guanine nucleotide dissociation inhibitors (GDIs), block spontaneous activation and regulate cycling between membrane and cytosol. When activated, Rho GTPases undergo a conformational change enabling them to interact with their effector molecules and transduce signals for downstream events. Rho GTPases have been implicated in a large number of actin-related processes like motility, adhesion, morphogenesis, membrane trafficking and cytokinesis (Etienne-Manneville and Hall, 2002; Ridley, 2001).

The human genome codes for 21 Rho GTPases and functions of most of them are only poorly understood. Of these, three, namely RhoA, Rac1 and Cdc42 are more extensively studied. RhoA generates myosin-based contractility and formation of adhesion complexes; Rac1 and Cdc42 are primarily involved in formation of protrusive structures, Rac1 regulates formation of lamellipodia and Cdc42 regulates filopodia formation and establishment of cell polarity (Etienne-Manneville and Hall, 2002; Ridley, 2001).

Sequencing of the genome of the social amoeba *D. discoideum* revealed the presence of 18 Rac related GTPases, whereas a typical Rho or Cdc42 were absent (Eichinger et al., 2005; Vlahou and Rivero, 2006). Only a few of the Rac related GTPases have been characterized in detail. Rac1A, 1B and 1C (Dumontier et al., 2000; Faix, 2002) and Rac E are required for cytokinesis (Larochelle et al., 1996), Rac1A was also shown to be involved in a formin-dependent pathway for filopodia formation (Schirenbeck et al., 2005), RacB is required for chemotaxis and morphogenesis (Park et al., 2004) and RacC has been implicated in phagocytosis (Seastone et al., 1998) and plays an important role in PI 3-kinase activation

and WASP activation for the dynamic regulation of F-actin assembly during chemotaxis (Han et al., 2006). RacG is required for cell shape, motility, and phagocytosis (Somesh et al., 2006b) and RacH has been implicated in vesicular trafficking (Somesh et al., 2006a).

Compared to our understanding of the downstream effects of Rac GTPases less is known about the mechanisms that activate Rac GTPases controlled by GEFs, GAPs or GDIs. In *Dictyostelium* at least 45 proteins contain a RhoGEF-PH module and most of them have a unique domain composition. The RhoGEF-PH (or diffuse B-cell lymphoma homology DH/ pleckstrin homology PH) module is the structural feature that mediates the nucleotide exchange activity on Rho GTPases. Five of these RacGEFs have been studied in some detail. DdRacGap1 (DRG) containing both RhoGEF and Rho-GAP domains acts as a GEF for Rac1 and simultaneously acts as a GAP for RacE and Rab GTPases (Knetsch et al., 2001). RacGEF1 has a specificity for RacB in regulating chemoattractant stimulation, F-actin polymerization, and chemotaxis (Park et al., 2004). The tail domain of MyoM, an unconventional myosin has been shown to catalyse nucleotide exchange on Rac1 GTPases and can induce actin-driven surface protrusions (Geissler et al., 2000). More recently Trix, a three CH domain containing RacGEF, has been suggested to regulate the endocytic pathway (Strehle et al., 2006). Finally, Darlin, an armadillo repeat protein homologous to the mammalian GEF smgGDS (small G-protein dissociation stimulator, a guanine nucleotide exchange factor for numerous Ras and Rho family GTPases (Williams, 2003)), has been shown to physically interact with RacE and RacC and may modulate chemotactic responses during early development (Vithalani et al., 1998). Nucleotide exchange activity on Rho GTPases are also displayed by CZH (CDM-zizimin homology) domain proteins (Cote and Vuori, 2002). Presently only a few members of the family have been studies in other organisms like the mammalian Dock180 and CED-5 in *C. elegans*. *Dictyostelium* has 8 members of this family, the functions of them remain to be elucidated.

In this study we focus on GxcDD, a novel multidomain RacGEF that contains a calponin homology (CH) domain, two IQ motifs, a DH domain, three PH domains and an ArfGAP domain. We show that, though dispensable for growth and development, GxcDD is required for proper streaming early in *Dictyostelium* development. The RacGEF domain of GxcDD can physically interact with several RacGTPases. Characterization of the individual domains revealed that the CH domain can act as a membrane anchor and the ArfGAP-PH tandem accumulates at cortical regions and on phagosomes. Our data also suggest that a conformational change is possibly required to activate GxcDD.

## 3.2 Materials and Methods

### 3.2.1 Strain growth and development

*D. discoideum* cells of strain AX2 were grown either with *Klebsiella aerogenes* on SM agar plates or axenically in liquid nutrient medium in shaking suspension at 160 rpm at 21°C (Claviez et al., 1982). *gxcDD*$^{-}$ cells were cultivated in axenic medium containing 3.5 µg/ml blasticidin (ICN Biochemicals, OH). To analyse development, cells were grown axenically to a density of 2-3 x $10^6$/ml, washed twice in Soerensen phosphate buffer (17 mM Na-K phosphate, pH 6.0) and 5 x $10^7$ cells were plated on phosphate agar plates. The streaming pattern was studied by allowing 1 ml of 2 x $10^6$ cells/ml to settle on a well of a NUNC six-well plate and observed at 3 min intervals with Leica DM-IL Inverse microscope.

### 3.2.2 Generation of *gxcDD*$^{-}$ cells and molecular cloning

For disruption of the *GxcDD* gene in AX2 cells, a *GxcDD* gene replacement vector was constructed using the plasmid pBSBsrΔBam (Sutoh, 1993). A 1.1-kb 5' fragment was PCR amplified using the forward primer 5-ATGCAACCCAAAGATTATATG-3'and reverse

primer 5-ACTATTGTAATGGATGAT-3' and a 1.0-kb 3' fragment was PCR amplified using forward primer 5'-TTAATGAGTTGTATGAGAAGA-3' and reverse primer 5'-TGTGCAGAATGTGGAGCATCA-3' from AX2 genomic DNA. The PCR products obtained were cloned into pGEM-T Easy cloning vector (Promega GmbH). The gene fragments were released and cloned into pBSBsr△Bam. The resulting replacement vector was linearised by digesting with PvuII and transformed into AX2 by electroporation. Transformants were selected in nutrient medium containing blasticidin (3.5 μg/ml). Independent clones were screened for the disruption of the GxcDD gene by PCR using genomic DNA, Southern blotting and western blot analysis. For Southern blot analysis a probe encompassing nucleotides 3807-4860 was used.

For expression of the CH domain of GxcDD fused to green fluorescent protein (GFP) at the N-terminus, a 0.4-kb fragment encoding the first 134 residues of GxcDD was amplified from AX2 cDNA and cloned into pBsr-GFP (Mohrs et al., 2000; Westphal et al., 1997). A 1-kb fragment encoding residues 395-707 containing the RacGEF domain was amplified and cloned in pGEX-4T1 (Amersham Biosciences) for expression in *E. coli*. The C-terminal 1-kb fragment encoding residues 1269-1619 containing the ArfGAP-PH tandem was amplified and cloned into pBsr-GFP for expression in AX2 cells and in pGEX-4T3 for expression in *E. coli*. Generation of strains expressing RacF1, RacG, RacH fused to GFP has been described elsewhere (Rivero et al., 1999; Somesh et al., 2006a; Somesh et al., 2006b). For expression of Rac1a, RacA (GTPase domain), RacB, RacC, RacD, RacE, RacI and RacJ were fused to the C-terminus of GFP, PCR was performed on corresponding cDNAs. PCR products were cloned into pDEX-GFP and the sequence verified. These vectors were introduced into AX2 cells and clones were selected by visual inspection under a fluorescent microscope.

### 3.2.3 Generation of polyclonal antibodies specific for GxcDD

Polyclonal antibodies specific for GxcDD were obtained by immunising female white New Zealand rabbits with GST-ArfGAP-PH (100 µg/animal; Pineda Antikörper-Service, Berlin), followed by two boosts of 100 µg each at two weeks intervals. The antiserum was affinity purified by incubating with GST-ArfGAP-PH bound glutathione-sepharose beads.

### 3.2.4 Subcellular fractionation

For separating membrane and cytosolic fractions cells were washed in Soerensen buffer and resuspended at a density of 1 x $10^8$ cells/ml in MES buffer (20 mM MES, pH 6.5, 1 mM EDTA, 250 mM sucrose supplemented with protease inhibitor cocktail (Sigma)). Cells were lysed by sonication and membrane and cytosolic fractions separated by centrifugation at 100,000 *g* for 30 min at 4˚C.

Triton X-100 was used for preparing cytoskeletal fractions. Cells were washed as before and resuspended in Soerensen buffer at a density of 5 x $10^7$ cells/ml and 300 µl of cell suspension were lysed using an equal volume of TIC buffer (2% Triton X-100, 20 mM KCl, 20 mM imidazol, pH 7.0, 20 mM EGTA, 4 mM $NaN_3$) and incubated on ice for 10 min followed by incubation at RT for 10 min. The insoluble cytoskeleton fraction was separated by centrifugation at 10,000 *g* for 4 min. Supernatant and pellet fractions were subjected to western blot analysis.

### 3.2.5 GST pulldown assays

GST-RacGEF and GST-ArfGAP-PH were expressed in *E. coli* and bound to glutathione-sepharose beads. For interaction of GxcDD with Rac proteins, 4 x $10^7$ AX2 cells expressing *Dictyostelium* Racs as GFP fusions were lysed in lysis buffer (25 mM Tris, pH 7.5, 150 mM NaCl, 5mM EDTA, 0.5% Triton X-100, 1 mM NaF, 0.5 mM $Na_3VO_4$, 1 mM DTT, supplemented with protease inhibitors (Sigma)) and incubated with equal amounts of GST-

RacGEF bound beads for 3 hrs at 4˚C. Beads were washed with wash buffer (25 mM Tris, pH 7.5, 150 mM NaCl, 5 mM EDTA). The eluate of the pulldown was immunoblotted and the Rac protein detected using a GFP specific monoclonal antibody (Noegel et al., 2004). Cells expressing only GFP were used as a control. For interaction studies of the ArfGAP-PH domain GST-ArfGAP-PH bound to glutathione-sepharose beads was incubated with AX2 cell lysates. GST bound beads were used as a control.

### 3.2.6 Miscellaneous methods

Immunoflorescence was done by fixing cells using cold methanol for 10 min followed by staining for actin using actin-specific monoclonal antibody Act1-7 (Simpson et al., 1984) and Cy3 conjugated secondary antibody. Live cell imaging of fluorescent cells in suspension or during phagocytosis of TRITC labelled yeast particles was done by laser scanning confocal microscopy essentially as described (Rivero and Maniak, 2006). Capillary chemotaxis was done as described using a Leica DM-IL inverse microscope and analyzed using DIAS (Wessels et al., 1998).

Monoclonal antibodies recognizing α-actinin (Schleicher et al., 1984), contact site A (Bertholdt et al., 1985), pspA (Gregg et al., 1982) and comitin (Weiner et al., 1993) were used for western blotting.

F-actin levels upon cAMP stimulation were determined as described (Hall et al., 1988). Briefly, aggregation competent cells resuspended at 2 x $10^7$ cells/ml were stimulated with 1 µM cAMP and 50 µl samples were taken at various timepoints. Samples were immediately lysed in lysis buffer (3.7% formaldehyde, 0.1% Triton X-100, 0.25 µM TRITC-phalloidin in 20 mM potassium phosphate, 10 mM PIPES, pH 6.8, 5 mM EGTA, 2 mM $MgCl_2$) and stained for 1 hr and centrifuged at 10,000g for 5 min. Pellets were extracted with 1 ml methanol overnight and fluorescence (540/565) measured in a fluorimeter.

For crosslinking experiment GST-ArfGAP-PH was thrombin cleaved on glutathione sepharose beads and the purified protein subjected to dialysis against PBS, pH 7.4, for 6hr at 4˚C. To equal amount of protein increasing amount of glutaraldehyde (0-0.1% v/v) was added. The final reaction volume was 40 µl. Crosslinking was carried at 4˚C for 30 min, the reaction was stopped by addition of 5 µl 1 M glycine. Samples were subjected to imunoblotting.

For cell aggregation in suspension *gxcDD*$^{-}$ and AX2 cells were allowed to starve in Soerensen buffer at a density of 1 x $10^7$ cells/ml and samples were withdrawn at the indicated times. The percentage of aggregated cells was determined by measuring the $OD_{600}$.

For northern blot analysis total RNA was isolated from AX2 cells of different developmental stages as described previously and separated in agarose gels containing 6% formaldehyde (Noegel et al., 1985; Rivero et al., 1996a). The blot was probed with a fragment derived from the 3' end of GxcDD cDNA (nt 3807-4860)

## 3.3 Results

### 3.3.1 Expression pattern and domain characterization of GxcDD

The gene coding for the RacGEF GxcDD (**G**uanine e**X**change factor for ra**C**) is located on chromosome 3. GxcDD is 1619 residues long with a calculated molecular mass of 179.652. It is a multidomain protein containing a CH domain, two IQ motifs, three PH domains, a RhoGEF domain and an ArfGAP domain (Figure 31). The calponin homology (CH) domain is located at the N terminus and resides between residues 18-122, the two IQ motifs between residues 390-417 and 432-461. The DH domain of RhoGEFs is the region required for mediating guanine nucleotide exchange on the Rho family GTPases. In general, a pleckstrin homology (PH) domain follows the DH (*d*iffuse B-cell lymphoma *h*omology) domain and this tandem DH-PH module is the signature motif of the Dbl family of guanine

nucleotide exchange factors (GEFs). Similarly, in GxcDD, a DH domain responsible for the catalytic RacGEF activity resides between residues 464-637. There are three PH domains in GxcDD, a comparatively large and less defined PH domain between residues 664-910 and two more between residues 941-1038 and 1520-1618. An ArfGAP domain, which shows highest homology to centaurin-α is placed between residues 1258-1376. Centaurins are ArfGAPs with functions in intracellular trafficking and contain a PH domain. They act downstream of PI 3 kinases and are targets for PtdIns(3,4,5)$P_3$ (Jackson et al., 2000).

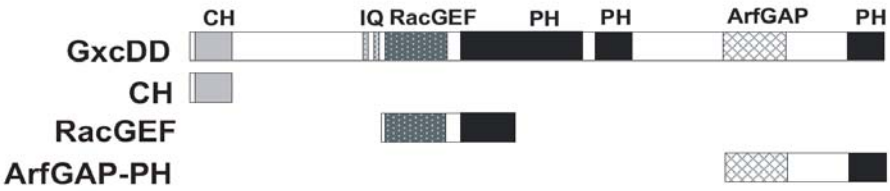


**Figure 31. Schematic representation of the domain organization of GxcDD and the domain constructs used in the study.**

We analysed the expression profile of GxcDD during *D. discoideum* development at the transcript level with a specific cDNA probe (Figure 32 A) and at the protein level with polyclonal antibodies (Figure 32 B), respectively. We found that GxcDD is expressed throughout development and that the protein levels do not vary greatly.


**Figure 32. Expression profile of GxcDD during *D. discoideum* development. (A) Northern blot showing the expression profile of GxcDD during *D. discoideum* development on phosphate agar plates. Cells were harvested at the indicated time points and RNA isolated by phenol-chloroform method and probed using a fragment derived from the 3' end of the GxcDD cDNA (nt 3807-4860). (B) Western blot showing the**

**accumulation of GxcDD during development. Total cellular proteins were harvested at the indicated time points and subjected to western blot analysis using polyclonal antibodies raised against GxcDD. Taken from Dhamodaran N, *Ph.D thesis*, University of Cologne, 2004.**

As the polyclonal antibodies that had been raised against the ArfGAP-PH domain of GxcDD, were unsuitable for immunofluorescence, we addressed the subcellular localization of the protein by means of subcellular fractionation and Triton X-100 treatment of the cells. We found GxcDD to be equally present in the cytosolic and membranous fractions. It also associated with the Triton X-100 insoluble cytoskeletal fraction (Figure 33).

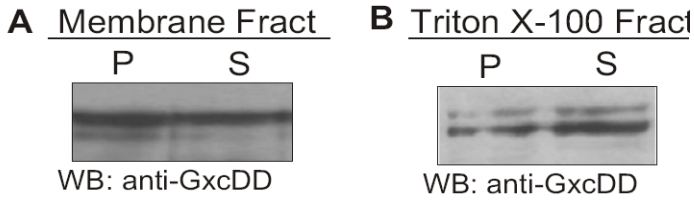


**Figure 33. Localization of GxcDD. (A) Membrane or cytosolic fractions and (B) Triton X-100 soluble (S) and insoluble (P) cytoskeletal fractions (bottom) were prepared and subjected to immunodetection using GxcDD polyclonal antibodies. Taken from Dhamodaran N, *Ph.D thesis*, University of Cologne, 2004.**

### 3.3.2 The CH domain of GxcDD functions as a membrane association domain

To study the function of the CH domain in GxcDD we expressed it as a fusion with GFP in *D. discoideum*. Live cell imaging of GFP-CH showed that it almost completely localized to the cortical regions of the cell, suggesting it may either be associated with the cortical actin cytoskeleton or the plasma membrane. When GFP-CH expressing cells were stained for actin, we observed only a partial overlap at certain places, which might be due to the close proximity of cortical actin and the plasma membrane (Figure 34 A). Furthermore,

subcellular fractionation revealed that GFP-CH was completely recovered in the membrane fraction (Figure 34 B, lanes 1 and 2). When Triton-insoluble cytoskeletons were prepared we found GFP-CH exclusively in the supernatant fraction indicating that it does not associate with actin (Figure 34 B, lanes 3 and 4). For control we used comitin, a membrane and actin cytoskeleton associated protein, and α-actinin, an F-actin crosslinking protein. Comitin is present in the membrane fraction and also in the cytoskeletal fraction, whereas α-actinin does not associate with the Triton-insoluble cytoskeleton due to its low affinity for F-actin. These findings demonstrate that the CH domain of GxcDD does not interact with actin but, surprisingly, associates with membranes. The CH domain of GxcDD thus can act as a membrane anchor for GxcDD.

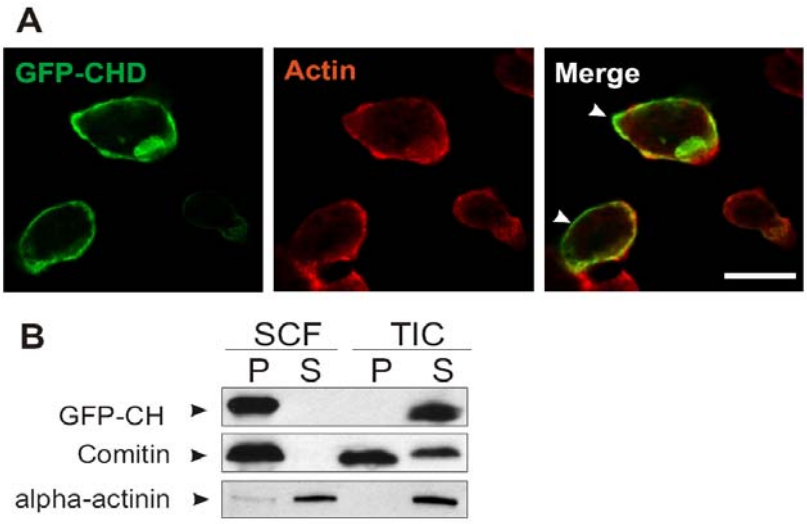


**Figure 34. The CH domain of GxcDD acts as a membrane anchor. (A) Cells expressing GFP-CH were fixed and stained with actin specific mAb act1-7. GFP-CH and actin co-localized only partially as indicated by arrows. (B) Subcellular fractionation (SCF) and Triton X-100 insoluble fractionation (TIC) of cells expressing GFP-CH. Proteins were immunodetected using a GFP monoclonal antibody. Comitin is used as a marker for the membrane fraction and α-actinin as a marker for the cytosolic fraction. GFP-CH was exclusively found in the membrane fractions and did not associate with the cytoskeleton.**

### 3.3.3 Association of GxcDD with *D. discoideum* Rac GTPases

As the *D. discoideum* genome lacks typical Rho or Cdc42 small GTPases, but has several Rac related GTPases we checked for a direct physical interaction of the DH domain of GxcDD with *Dictyostelium* Rac GTPases. We expressed the DH domain of GxcDD as a GST fusion protein (GST-DH) in *E. coli*, bound the protein to glutathione-sepharose beads and used them for incubation with lysates derived from *D. discoideum* cells expressing different Rac GTPases as GFP fusion proteins. Rac GTPases interacting with GST-DH were identified by immunoblotting with GFP monoclonal antibodies (Figure 35). The expression levels of the Rac proteins varied, and RacF1, G and J were not expressed in very high amounts, whereas Rac1a, A, B, C, D, E, H and I were highly expressed. We found that Rac1a, A, C, E, H and I bound to the DH domain of GxcDD, whereas RacB and RacD, that were expressed in very high amounts, did not bind to the DH domain, indicating specificity in the pulldown assay. The data indicate that GxcDD can activate more than one Rac. It is however also likely that it is not the only exchange factor for these interacting proteins.

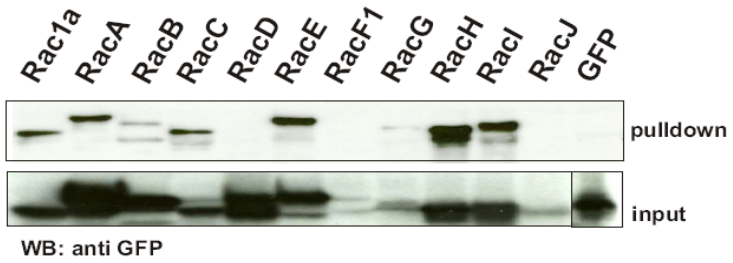


**Figure 35. Association of GxcDD with *D. discoideumm* Rac GTPases. GST-RacGEF was expressed in *E. coli* and bound to glutathione-sepharose beads. Equal amounts of washed beads were incubated with cell lysates of AX2 cells expressing GFP fusions of 11 of 18 *D. discoideum* Racs. Pulldown eluates were resolved by 12% SDS-PAGE and the Rac proteins detected using a GFP monoclonal antibody.**

### 3.3.4 The C terminal domain of GxcDD is enriched in the cortex and relocates to the membrane during phagocytosis

At the C terminus GxcDD possesses an ArfGAP domain followed by a PH domain. Arfs are small GTPases known to be required for vesicular trafficking. An ArfGAP domain would be required to inactivate the activated form of Arf (Randazzo and Hirsch, 2004). Similar to the association of PH domains with DH domains, the ArfGAP domain in GxcDD is associated with a PH domain. To examine the functions of these domains we expressed the C-terminal part containing the ArfGAP-PH tandem as a GFP fusion protein in AX2 cells. GFP-ArfGAP-PH was targeted to the cell cortex where it colocalized with actin (Figure 36 A). Live-cell imaging experiments where GFP-ArfGAP-PH expressing cells were incubated with TRITC labelled yeast particles showed a strong enrichment of the fusion protein on phagosomes and at the leading edges of the cell (Figure 36 B). Cell fractionation using Triton X-100 indicated a distribution of GFP-ArfGAP-PH in both the Triton-insoluble cytoskeleton fraction and in the supernatant (Figure 36 C). These results suggest that unlike the N-terminal CH domain, which is totally membrane bound, the C-terminal part can also associate with the actin cytoskeleton.

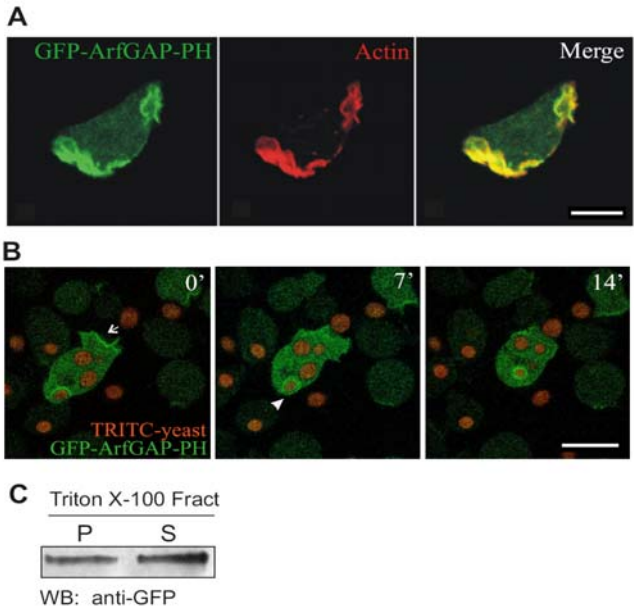


**Fig. 36. Cortical localization of the C-terminus of GxcDD containing the ArfGAP-PH tandem and enrichment on phagosomes. (A) Wild type *D. discoideum* cells expressing GFP-ArfGAP-PH were fixed and stained with actin specific mAb act1-7, showing complete overlap of the two. (B) Live cell imaging of cells expressing GFP-ArfGAP-PH**

**incubated with TRITC labelled yeast. GFP-ArfGAP-PH enriches at the phagocytic cup (arrow head) and also at the leading cortical edges of the cell (arrow). (C) Cells expressing GFP-ArfGAP-PH were subjected to Triton X-100 extraction. Fractions were separated by 10% SDS-PAGE and the protein detected using GFP specific mAb K3-184-2. GFP-ArfGAP-PH was equally distributed in both the Triton X-100 insoluble cytoskeleton and the soluble fraction. Figure A and C taken from Dhamodaran N, *Ph.D thesis*, University of Cologne, 2004.**

When we used GST-ArfGAP-PH to identify interacting proteins we could co-precipitate full length GxcDD from AX2 cell lysates. The precipitated proteins were resolved on SDS polyacrylamide gels and one of the unique bands analysed by MALDI-TOF mass spectroscopy identified GxcDD as an interacting protein. Co-precipitation of GxcDD was also confirmed by western blot analysis (Figure 37 A). To test whether the ArfGAP-PH domain interacts with itself and forms higher oligomers, we purified the ArfGAP-PH domain by thrombin cleavage from the GST fusion protein and treated it with increasing amounts of glutaraldehyde to promote crosslinking of associated proteins. The proteins were resolved on SDS polyacrylamide gels, blotted and probed with the GxcDD specific polyclonal antibodies. We did not observe formation of higher oligomers (Figure 37 B), indicating that the association of ArfGAP-PH with the full length GxcDD is through an interaction with other domains in the protein. We then checked if the N-terminal CH domain could interact with either the RacGEF domain or the ArfGAP-PH tandem in a GST-pulldown experiment using cells expressing GFP-CH domain. We found that beads coated with ArfGAP-PH tandem could pulldown significant amounts of GFP-CH domain, as compared to beads coated with the RacGEF domain (Figure 37 C). Thus the CH domain at the N terminus can be an interacting domain of the ArfGAP-PH tandem and this interaction might regulate either the activity or the localization of the protein.

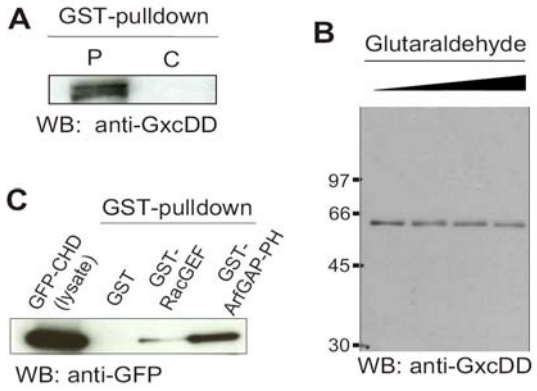


**Figure 37. Interaction of ArfGAP-PH with full length GxcDD. (A) Glutathione-sepharose beads coated with GST-ArfGAP-PH were incubated with wild type cell lysates (P). GST coated beads were used as a control (C). Pulldown eluates were resolved by 10% SDS-PAGE, western blots revealed GxcDD as an interacting protein. (B) GST-ArfGAP-PH was cleaved by thrombin to liberate the ArfGAP-PH protein and the purified protein was tested for oligomerization using increasing amounts of glutaraldehyde as a crosslinking agent (0 – 0.1 % v/v). (C) The CH domain has the potential to bind to the GEF domain and the ArfGAP-PH domain. Lysates from cells expressing GFP-CH domain (GFP-CHD) were used in pulldown assays employing GST-RacGEF or GST-Arf-GAP-PH bound to glutathione sepharose beads. The blots were probed with a GFP-specific monoclonal antibody.**

PH domains bind to phosphatidylinositol phosphates (PtdIns) and mediate the recruitment of proteins to membranes. When we tested whether the PH domain in the ArfGAP-PH domain could bind to PtdIns using a dot blot assay we found that the protein bound to PtdIns(3,4)$P_2$ and PtdIns(4,5)$P_2$, but highest binding was observed with PtdIns(3,4,5)$P_3$, the product of PI3K (Figure 38).

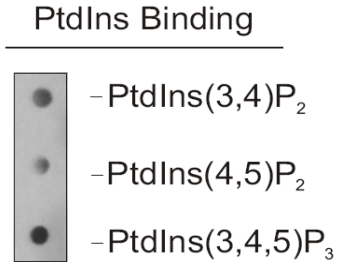


**Figure 38. Interaction of ArfGAP-PH with phosphoinositides. PtdIns(3,5)$P_2$, PtdIns(4,5)$P_2$, PtdIns(3,4,5)$P_3$ were spotted on a PVDF membrane and incubated with**

**ArfGAP-PH protein and binding detected using GxcDD specific polyclonal antibodies. Taken from Dhamodaran N, *Ph.D thesis*, University of Cologne, 2004.**

### 3.3.5 Characterization of *gxcDD⁻* cells

To gain knowledge about the physiological role of GxcDD we disrupted the gxcDD gene by homologous recombination in wild type AX2 cells (Figure 39 A). The disruption of the gene was confirmed by PCR analysis using genomic DNA of individual clones and verified by Southern blot analysis and by western blotting of total cell lysates using polyclonal antibodies (Figure 39 B-C).

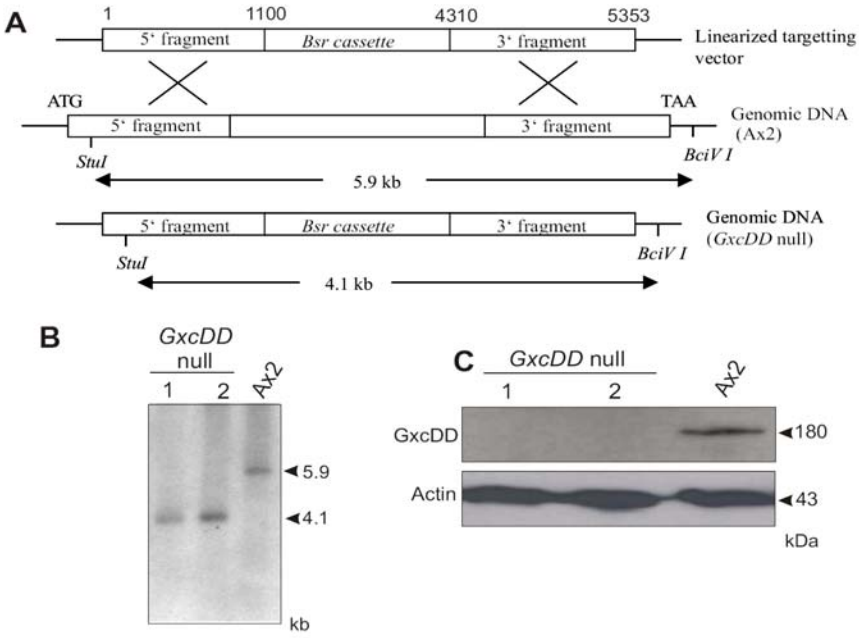


**Figure 39. Generation of *gxcDD⁻* cells. (A) Schematic representation of the strategy to generate *gxcDD⁻* cells. (B) Southern blot analysis of *StuI* and *BciVI* digested genomic DNA to confirm the recombination event in *gxcDD⁻* cells. Two independent clones were analysed. (C) Western blot analysis indicates the complete loss of GxcDD protein in *gxcDD⁻* cells (upper panel). The blot was reprobed with actin specific mAb act1-7 as a loading control (lower panel). Taken from Dhamodaran N, *Ph.D thesis*, University of Cologne, 2004.**

*gxcDD⁻* cells did not show severely altered phenotypes when examined for growth on a bacterial lawn or in suspension, cytokinesis or actin organization in the cortex (not shown).

The enrichment of the ArfGAP-PH domain at macropinosomes (Figure 36 B) suggested that GxcDD might have a role in endosomal processes like phagocytosis and pinocytosis. Quantitative phagocytosis and pinocytosis assays did however not reveal significant differences with the parental strain (not shown).

### 3.3.6 *gxcDD*$^{-}$ cells show a delay in development and defects in streaming behaviour

*D. discoideum* is a soil living organism feeding on bacteria; upon sensing starvation a developmental programme is initiated as a survival strategy. cAMP serves as the master regulator for development. In this process unicellular amoebae aggregate to form a mound, and the mound forms a tipped aggregate or an optional slug stage which shows phototactic and thermotactic behaviour. The developmental programme is completed upon reaching culmination and formation of the fruiting body. The entire process is well coordinated and programmed and wild type AX2 cells complete development by 20-24 hrs upon starvation when allowed to develop on nutrient deficient phosphate agar plates. *gxcDD*$^{-}$ cells enter the developmental programme timely when starved and complete the developmental process by forming fruiting bodies. However the developmental programme is delayed, and fruiting bodies are formed only after 28 hrs (Figure 40 A). A closer analysis showed that the early developmental stages took place timely until cells had formed aggregates, however from t12 onward development was delayed by more than 4 hours. Tipped aggregates had formed only after 20 hours and slugs at t24 as compared to t16 for AX2. Moreover, not all aggregates had transformed into fruiting bodies at t28. This delay in development was also confirmed by analysing the expression profile of the prespore specific protein pspA which is recognized by mAb Mud1. In AX2 highest levels of pspA are observed between t12 and t20, whereas in *gxcDD*$^{-}$ cells pspA reached similar levels from t20 to t28. By contrast, the aggregation

specific cell adhesion protein contact site A (csA) had its peak expression at t8 in wild type and mutant (Figure 40 B) confirming the defect in later developmental stages.

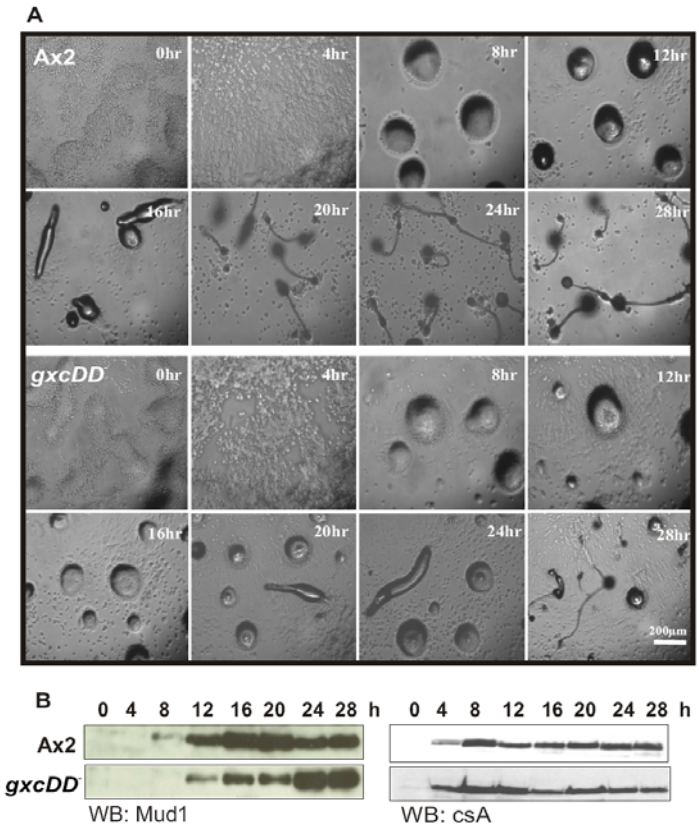


**Figure 40. Developmental delay in *gxcDD*⁻ cells. (A) Parental wild-type AX2 and *gxcDD*⁻ cells were allowed to develop on nutrient deficient agar plates. Images were recorded every 4 hrs. *gxcDD*⁻ cells did develop to form fruiting bodies but were delayed in development by at least 4 hrs. (B) Cells were collected at 4 hr intervals for total protein and analysed by western blot. The appearance of the prespore marker pspA (detected by Mud1 monoclonal antibody) and the aggregation specific csA protein (detected using monoclonal antibody 33-294-17) were monitored.**

When wild type AX2 cells are starved in a monolayer, cells polarize and form long streams. *gxcDD*⁻ cells were not able to form such long streams. Cells polarized and began to form streams, but soon the streams broke apart and were left behind as aggregates (Figure 41 A). Streaming of aggregation competent *D. discoideum* cells can also be observed in a capillary chemotaxis assay by applying an exogenous source of cAMP. *gxcDD*⁻ cells

migrated towards the cAMP source but did not form characteristic streams as in wild type cells (Figure 41 B).

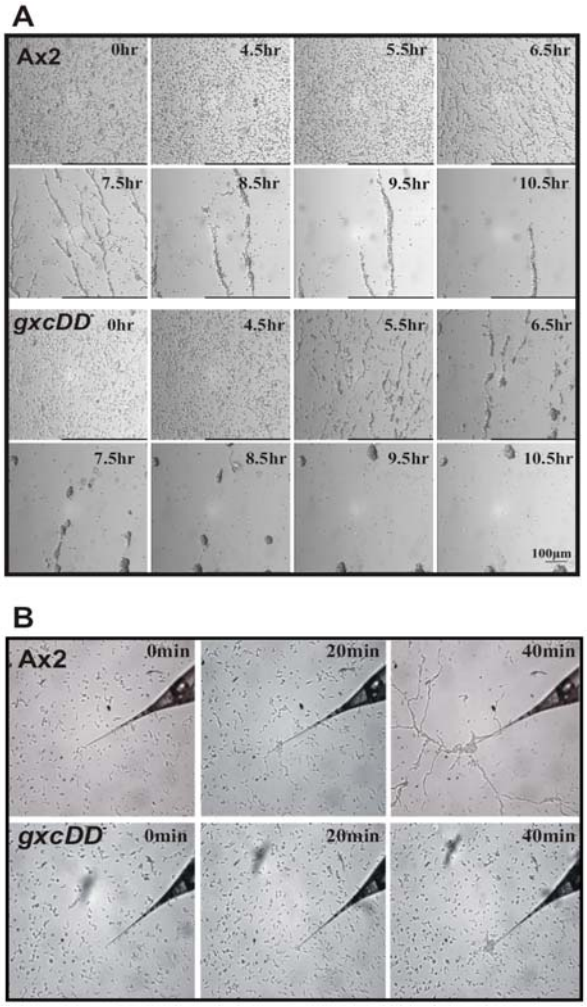


**Figure 41. Streaming defect in *gxcDD⁻* cells. (A) AX2 and *gxcDD⁻* cells were allowed to starve on plastic plates. Images were continuously recorded. Streams formed in *gxcDD⁻* cells broke down to aggregates. (B) Streaming was also recorded in wild type and *gxcDD⁻* cells using an exogenous source of cAMP in a capillary chemotaxis assay. *gxcDD⁻* cells did migrate towards the cAMP source but did not form streams. Figure B taken from Dhamodaran N, *Ph.D thesis*, University of Cologne, 2004.**

We then assayed aggregate formation in suspension, which can be determined by following the decrease in optical density of the suspension due to aggregate formation. We found that the degree of aggregation was reduced in *gxcDD⁻* cells (Figure 42) and a large majority of cells stayed as single cells and did not form aggregates.

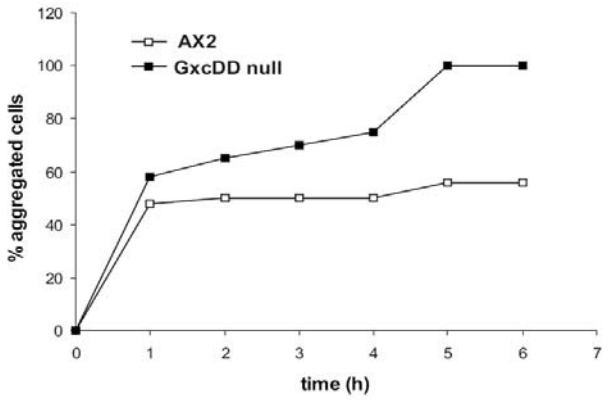


**Figure 42. *gxcDD*$^{-}$ and AX2 cells were allowed to starve in Soerensen buffer at a density of 1 x $10^7$ cells/ml and samples were withdrawn at the indicated times. Percentage of aggregated cells was determined by measuring the $OD_{600}$. The data represent the average of three independent experiments. Taken from Dhamodaran N, *Ph.D thesis*, University of Cologne, 2004.**

A quantitative analysis of chemotaxis parameters in chemotaxing *gxcDD*$^{-}$ cells showed that speed, persistence and directionality were similar to the AX2 wild type cells (Table 1).

Table1. Analysis of cell motility of GxcDD null cells

| | AX2 | *gxcDD*$^{-}$ |
|---|---|---|
| **Buffer** | | |
| Speed (μm/min) | 6.65 ± 2.61 | 5.53 ± 1.89 |
| Persistance (μm/min-deg) | 1.71 ± 1.19 | 1.38 ± 0.59 |
| Directionality | 0.31 ± 0.19 | 0.32 ± 0.18 |
| Direction change (deg) | 47.81 ± 11.94 | 49.06 ± 14.28 |
| **cAMP Gradient** | | |
| Speed (μm/min) | 14.56 ± 3.81 | 15.03 ± 3.75 |
| Persistance (μm/min-deg) | 5.55 ± 2.25 | 5.52 ± 2.27 |
| Directionality | 0.71 ± 0.26 | 0.83 ± 0.14 |
| Direction change (deg) | 24.49 ± 17.76 | 17.32 ± 8.93 |

Time-lapse image series were captured at 30 s intervals. The DIAS software was used to trace individual cells along the image series and calculate motility parameters.

In agreement with these results quantitative measurement of F-actin levels upon cAMP stimulation gave results similar to the one obtained for AX2 (Figure 43). Our observations of the subtle defects in development and streaming behaviour in *gxcDD*$^{-}$ cells indicate that, although GxcDD is dispensable for development, it acts at various stages of development.

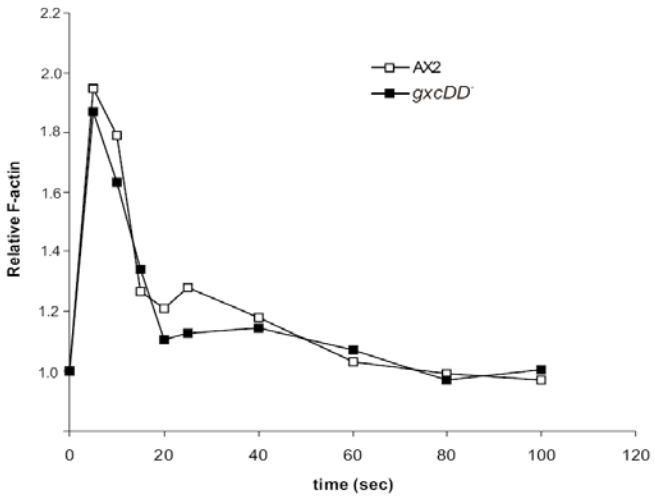


**Figure 43. cAMP induced actin polymerization response in mutant and wild type cells. Aggregation competent cells at 2 x $10^7$ cells/ml were stimulated with 1 µM cAMP and samples were taken at the indicated times. The F-actin content was determined as described in Materials and methods. The data is the average of three independent experiments.**

## 3.4 Discussion

In the present study we have analysed GxcDD, a novel putative *D. discoideum* RacGEF that has a unique domain organization containing a CH domain, two IQ motifs, a RhoGEF domain followed by two PH domains and an ArfGAP domain followed by one more PH domain. Seven other *Dictyostelium* RacGEFs contain a CH domain (Vlahou and Rivero, 2006). The Calponin homology (CH) domain is a protein module of about 100 amino acids present in the actin-binding protein calponin that controls smooth muscle contraction and cytoskeletal organization in non-muscle cells. The CH domain of calponin is however not responsible for its interaction with actin. In contrast, the actin-binding domain (ABD) of several proteins is comprised of two CH domains in a tandem arrangement. CH domains are classified into at least five classes based on the degree of sequence similarity (Gimona et al., 2002; Korenbaum and Rivero, 2002). CH1 in association with CH2 can interact with actin.

Isolated CH2 and CH3 domains do not interact with actin at all (Gimona and Mital, 1998; Stradal et al., 1998). CH4 and CH5 are found in the actopaxin/parvin family of actin-binding proteins implicated in linking integrins with intracellular pathways that regulate the actin cytoskeleton (Legate et al., 2006). Most RhoGEFs from *Dictyostelium* and other species like mammalian Vav and α-PIX contain one type 3 CH domain and have thus been implicated in signal transduction. The CH domain of GxcDD is also a type 3 CH domain and our studies indicate that this domain is targeted to membranes exclusively and does not interact with actin. The membrane targeting of the CH domain may regulate the association of GxcDD with membranous fractions. CH3 domain containing proteins are the group of CH domain containing proteins that have the most diverse functions among the CH domains. Our findings are consistent with the hypothesis that although the five CH domains are homologous and have structural similarity, they may have evolved to perform different functions (Banuelos et al., 1998).

The DH domain of RhoGEFs regulate their nucleotide exchange activity. The associated PH domain is required for full catalytic activity and for phosphoinositide binding and localization of the protein. Recent studies in yeast have shown that only a small fraction of PH domains are capable of independent membrane targeting of a protein and those that do often require phosphoinositides and non-phosphoinositide determinants like Arf GTPases in some cases for subcellular localization (Lemmon, 2004). GxcDD possesses a DH domain which is followed by two PH domains, the first being comparatively large and poorly conserved. We found that the DH domain can bind to a set of Rac GTPases (Rac1a, RacA, RacC, RacE, RacH and RacI) with sufficient affinity. However, our data need to be handled with caution, as mere physical interaction does not imply that all the above-mentioned Racs would be substrates for GxcDD *in vivo*. Further characterization of the interaction by enzymatic exchange assays needs to be performed for deeper understanding of its GEF activity. It is also possible that some of the interacting Racs and GxcDD might never see each

other *in vivo* because of their subcellular localization e.g., RacH is mostly located at endosomes and not at the plasma membrane (Somesh et al., 2006a).

A conformational change or binding of bioactive lipids to proteins are mechanisms known to activate a signal transducing protein (Huttelmaier et al., 1998; Parker, 2004). Our observation of the ArfGAP-PH tandem binding to GxcDD but not being able to form higher oligomers indicates that the ArfGAP-PH may interact with some other part of the protein and exist as an inactive form. A conformational change would then be required to convert it to its active form. A possible activator could be PtdIns(3,4,5)P which binds to the ArfGAP-PH tandem with significant affinity. In the ArfGAP ASAP1, a member of the centaurin family, which has an ArfGAP-PH tandem like GxcDD, the PH domain is known to function as an autoinhibitory domain and upon activation by PtdIns the ArfGAP domain is activated (Kam et al., 2000). A similar activation mechanism may also exist for GxcDD. The recruitment of the ArfGAP-PH tandem to the cortical regions of the cell and the phagocytic cup indicates a possible role in endocytic processes.

To understand the physiological role of GxcDD, we generated *gxcDD*$^{-}$ cells. Our observations indicate that although cells lacking GxcDD grow normally under laboratory conditions, undergo development and complete it with the formation of fruiting bodies, streaming behavior during chemotaxis is altered and development delayed. *D. discoideum* cells can form streams during the aggregation process, which is the result of a cAMP relay mechanism. In this process certain cells, the pacemaker cells, have the ability to produce cAMP. The secreted cAMP can bind to cARs (cAMP receptors, which are G-protein coupled receptors), which induce a multitude of signaling events. Activation of cARs leads to dissociation of the heterotrimeric G-proteins and membrane localization of CRAC (*c*ytosolic *r*egulator of *a*denylyl *c*yclase) followed by activation of adenylyl cyclase (ACA), cAMP production and secretion (Chen et al., 1997). The neighboring cell then senses cAMP and streams of cells moving towards the aggregation centre are generated. It has been found that

ACA localized to the rear of a migrating cell is required for formation of streams (Kriebel et al., 2003). ACA is possibly localized to the rear by a vesicular system that would require Arf function and GxcDD might be a part in its regulation. As GcxDD contains several functional and regulatory domains, it is likely to regulate signal transduction downstream of cAMP receptors. Binding of cAMP to the surface ligand activates PI3K whose products may use GxcDD as adaptor protein to bring about downstream signalling. GxcDD at the membrane may have either a function in conjunction with GTPases with its GEF and GAP domain or may act along with another combination of functional domains. Interference with such a complex network of intricate signalling is a possible mechanism for the delay in developmental timing in *gxcDD*$^{-}$ cells.

# Chapter 3

## Association of IQGAP related protein GAPA with actin crosslinking proteins Filamin and Cortexillin I in cytoskeletal regulation

*Filamin and cortexillin are F-actin cross-linking proteins allowing actin filaments to form three-dimensional networks. We identified the IQGAP related protein GAPA as an interactor for D. discoideum Filamin and Cortexillin I, and provide evidence that GAPA might exist as a trimer in vivo. GAPA has been shown to be required for cytokinesis. Expression of GFP-tagged GAPA completely rescued the strong cytokinesis defect in GAPA null cells. We found that it interacts through the GAP domain with the actin binding domain (ABD) of Filamin. We observe in both Filamin and GAPA null cells nuclei free particles arising due to membrane blebbing presumably due to weakening of the actin cytoskeleton. We also observed that GAPA is required for phototaxis as is filamin. GAPA is enriched in the cleavage furrow in dividing cells and its recruitment to the cleavage furrow requires cortexillin I.*

## 4.1 Introduction

The dynamics and three-dimensional structure of the actin cytoskeleton largely depends on the activity of different actin-binding proteins and is implicated in a variety of key cellular processes including locomotion, endocytosis, cytokinesis and morphogenesis. F-actin crosslinking proteins stabilize the three-dimensional networks or densely packed bundles of actin filaments. Crosslinkers must have two-actin binding sites in order to connect neighbouring actin filaments. Two actin binding sites can be present in a single polypeptide chain as in ABP34 and fimbrin or can be formed by dimerization (filamin, cortexillin, α-actinin). The spatial arrangement of the two actin-binding sites along with the length and flexibility of the spacer elements determines whether a crosslinking protein induces bundling or network formation (Noegel and Schleicher, 2000; Schleicher et al., 1995).

Several actin crosslinking proteins have been identified in *D. discoideum* (Eichinger et al., 2005). These include a number of CH domain containing proteins. In α-actinin, filamin and cortexillin two CH domains (CH1 and CH2) form the actin binding domain, in fimbrin the actin binding domain is formed by four fimbrin-type CH domains (CHf1-CHf4) (Korenbaum and Rivero, 2002). Actin crosslinking proteins with different actin binding sites are ABP34, translational elongation factor 1α (ABP50), villin-related proteins and dynacortin (Girard et al., 2004; Gloss et al., 2003; Hofmann et al., 1992; Lim et al., 1999; Robinson et al., 2002; Yang et al., 1990).

Filamin crosslinks actin filaments, promotes orthogonal branching and plays an important role in maintaining the cortical actin network (Stossel et al., 2001). *Dictyostelium* filamin is 120 kDa in size having a conserved N-terminal actin binding domain formed by two CH domains resembling those of the α-actinin/spectrin superfamily proteins. The rest of the protein forms 6 repeated domains of antiparallel β-sheets adopting an immunoglobulin fold,

and is also termed as rod repeats. Filamins are present as dimmers and the dimerization is mediated through rod repeat 6 (Figure 44).

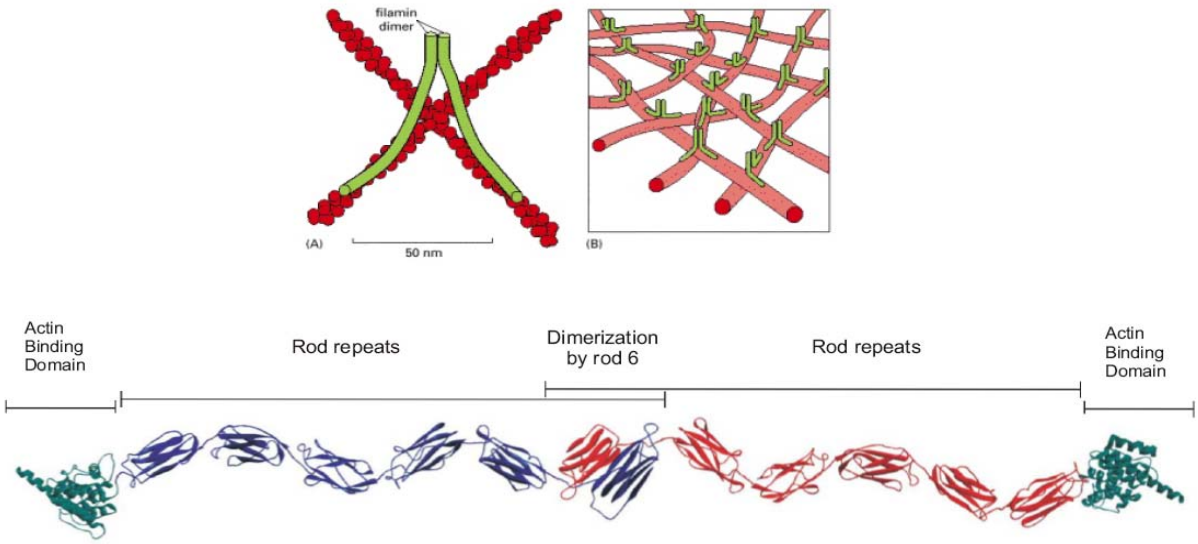


**Figure 44. Structural organization of Dictyostelium filamin. (Top) Mechanism how filamin dimers crosslinks actin filaments to orthogonal network (Molecular Biology of the Cell, Garland Science, 4th Edition). (Bottom) Structure of dictyosstelium filamin as a dimmer (Popowicz et al., 2006). The CH1-CH2 domains forming the actin binding domain (green), the immunoglobulin fold rod repeats from two monomers (blue and red) and the dimerization between rod repeat 6 from either monomer are indicated.**

A growing body of evidence from mammalian cells suggests role for filamin in intracellular trafficking and in signal transduction and has been implicated in several disease in humans (Feng and Walsh, 2004; Stossel et al., 2001). Filamin interacts with caveolin-1 which is implicated in caveolae biogenesis, cholesterol transport and endocytic events (Conner and Schmid, 2003). Involvement of filamin in signal transduction is inferred by its interaction with several compoments of the NF-κB pathway and with the small GTPases RhoA, Rac, Cdc42 and RalA and also with regulators and effectors of small GTPases like Trio, FilGAP, Pak 1 and ROCK, β1 integrin (Bellanger et al., 2000; Calderwood et al., 2001; Ohta et al., 2006; Ohta et al., 1999; Vadlamudi et al., 2002). Over 50 interactors of filamin have been identified in mammalian system, but only one interactor of filamin has been

reported for *Dictyostelium* filamin, namely Filamin interacting protein FIP, which in association with filamin is suggested to be required for development (Knuth et al., 2004).

Cortexillins (cortexillin I and II) are closely related actin crosslinking proteins (having 60 % identity at the amino acid level) specific for *D. discoideum*, which were isolated from contracted actomyosin complexes (Faix et al., 1996). In the Cortexillins the actin binding domain is followed by a coiled-coil domain essential for dimerization. Cortexillin I and II differ in the C terminal domains, Cortexillin I has a $PIP_2$ binding site in the C terminal (Stock et al., 1999). Cortexillins form parallel heterodimers and organize actin filaments into anti-parallel bundles and a three-dimensional meshwork. They are distributed in the cell cortex during interphase, but localize to the cleavage furrow with the onset of cytokinesis, where they remain till the daughter cells separate (Weber et al., 1999). Translocation to the cleavage furrow is controlled by Rac1 and IQGAP-related proteins establishing a direct link between signaling and cytoskeletal components. Cortexillins have an essential role in cytokinesis. Ablation of one of the cortexillins results in moderate cytokinesis defects, deletion of both cortexillins results is a dramatic defect in cytokinesis, often resulting is large multinucleated cells containing up to 100 nuclei. Interestingly, in cortexillin I a C-terminal 92 aa which includes a nine aa residue basic stretch reminiscent of $PIP_2$ binding found in other actin regulatory proteins is crutial for localization of Cortexillin I to the cleavage furrow and rescues the cytokinesis defect. This domain is also important for the actin bundling activity of cortexillin I, and that this activity is negatively regulated by $PIP_2$ (Stock et al., 1999).

IQGAP-related proteins constitute a conserved family of scaffolding proteins that interact with cytoskeletal and signaling proteins. They contain a conserved RasGAP homology domain (GRD) followed by a RasGAP C-terminal domain (RGCT). GRD domains do not exhibit RasGAP activity but interacts with activated Rho GTPases and in contrast inhibits their GTPase activity (Brown and Sacks, 2006). Here we report that GAPA, an IQGAP related protein, is a filamin and cortexillin I interacting protein. Interaction of Filamin

and GAPA is through the GAP domain of GAPA and the actin-binding domain of filamin. We show that GAPA exists as a trimer in vivo. We also show that GAPA is enriched at the cleavage furrow during cytokinesis and that recruitment to the cleavage furrow requires cortexillin I.

## 4.2 Materials and Methods

### 4.2.1 Cloning of full length GAPA and GAP domain of GAPA

Full length GAPA was amplified from *D. discoideum* cDNA and cloned into pGEM-TE (Promega), and recloned into pBsrN2 vector (R. Blau-Wasser, unpublished) for expression in *D. discoideum* cells and pGEX-4T1 (GE Healthcare) for expression in bacterial cells. A fragment encompassing nucleotide residues 604-1671 encoding the catalytic GAP domain was amplified from cDNA and cloned in pGEX-4T1 (GE Healthcare) for expression in bacteria.

### 4.2.2 Cell culture, cell lines and transformation of *D. discoideum* cells

Cells of *D. discoideum* AX2 wild type strain and of transformants were cultivated in liquid nutrient medium at 21°C on polysterene plates or in shaking culture at 160 rpm or on SM agar plates with *Klebsiella aerogenes* (Claviez et al., 1982). Cells were transformed by electroporation as described (Knecht and Pang, 1995).

The following cell lines were used in this study. Wild type AX2 cells, AX2-derived myosin II$^-$ strain HS2205 (Manstein et al., 1989), AX2-derived GAPA$^-$ strain (Faix et al., 2001), AX2-derived Filamin$^-$ strain HG1264 (Brink et al., 1990), AX2-derived cortexillin I$^-$ (Faix et al., 1996) and cells expressing GAPA fused to green fluorescent protein (GFP) in the above mentioned strains (this work). Different GFP-tagged filamin expressing cells used in this study: GFP-ABD (Pang et al., 1998), HG1264 cells expressing the actin binding domain (ABD) of filamin; GFP-ABD + rod1-2, HG1264 cells expressing ABD and first two rod

repeats of filamin; GFP-rod 1-6, HG1264 cells expressing the six rod repeats of filamin (Khaire et al., 2007); GFP-FLN, HG1264 cells expressing full-length filamin, GFP-Fil$^{S174A}$, HG1264 cells expressing filamin mutated at position 174 in the ABD.

For phototaxis assays, 10 µl of cells at a density of 1 x $10^8$ cells / ml were transferred to the centre of a 90 mm phosphate agar plate and placed in a black opaque box with a slit to provide a unidirectional light source and were allowed to develop to the migratory slug stage. Slime trails and cellular material were transferred onto a nitrocellulose membrane. Membranes were stained with staining solution (0.1% amido black in 20% iso-propanol and 10% acetic acid) for 10 minutes and destained twice with destaining solution (20% iso-propanol and 10% acetic acid) for 15 min, washed with water and air-dried.

### 4.2.3 Oligomerization of GAPA

Analytical gel filtration was done on a Sephadex G200 for cell free lysates containing GFP-GAPA or on a Saphadex G75 column for the purified GAP domain using the SMART system (GE Healthcare). Native gel electrophoresis was done at 4°C in the absence of SDS where proteins migrate corresonding to the protein's charge and hydrodynamic size. Protein samples were either heated at 65°C or unheated and resolved under native conditions. Proteins were visualized by silver staining.

### 4.2.4 Protein-protein interaction studies

Interaction between GAPA and Filamin was studied using GST-pulldown assays. Glutathione sepharose beads coated with GST-GAPA or GST-GAP were incubated with cell free lysates from wild type cells at 4°C to pulldown endogenous filamin. Pulldown eluates were resolved by SDS-PAGE and immunoblotted with filamin monoclonal antibody 82-454-12 (Brink et al., 1990). Glutathione sepharose beads or beads coated with GST were used as a control. To map the domain in filamin interacting with GAPA, beads coated with GST-GAP

were incubated with cell free lysates from HG1264 expressing the actin binding domain (ABD), the actin binding domain along with first two rod repeats (ABD+rod1-2) or the six rod repeats (rod1-6) or full length Filamin or a mutated Filamin(S174A) as GFP-fusion. Pulldown eluates were resolved by SDS-PAGE and immunoblotted with GFP monoclonal antibody K3-184-2 (Noegel et al., 2004).

Interaction between GAPA and cortexillin was done by immunoprecipitation of GFP-GAPA using GFP monoclonal antibody mAb K3-184-2 from cell free extracts of cells expressing GFP-GAPA. Pulldown eluates were resolved by SDS-PAGE and immunoblotted with polyclonal antibodies against cortexillin I. Also, Glutathione sepharose beads coated with GST-GAPA were incubated with cell lysates to pulldown endogenous cortexillin I. Pulldown eluates were resolved by SDS-PAGE and immunoblotted with cortexillin I polyclonal antibodies.

### 4.2.5 Fluorescence microscopy

Live cell imaging of cells expressing GFP-GAPA migrating in a chemotactic gradient was performed in chemotactic chambers (Ibidi Biosciences, Munich). Images were captured by confocal microscope.

To observe localization of GFP-GAPA during cytokinesis in different cell types, cells were first seeded on glass coverslips and synchronized using nocodazol (10 μM / ml) for 3 hrs to block cell division in mitosis. The block was then released by washing away the nocodazole and allowing the cell cycle to progress for 1 hr. Cells were then fixed by ice cold methanol. α-tubulin staining (Piperno and Fuller, 1985) was used to identify cells as mitotic. The nuclear DNA was stained using DAPI. Images were captured using epifluorescence microscope (Leica).

## 4.3 Results

### 4.3.1 Localization of GAPA

Cells lacking GAPA show a cytokinesis defect (Adachi et al., 1997; Faix et al., 2001). This prompted us to analyze the localization of GAPA during cytokinesis. We expressed full length GAPA as a GFP fusion in wild type AX2 and *GAPA*$^{-}$ cells. Expression of GFP-GAPA completely rescued the strong cytokinesis defect in *GAPA*$^{-}$ cells indicating that the recombinant protein is functionally active (Figure 45).

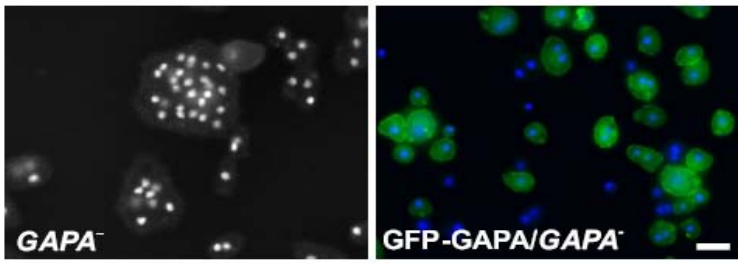


**Figure 45. Expression of GFP-GAPA rescues cytokinesis defect in *GAPA*$^{-}$ cells. (left) *GAPA*$^{-}$ cells are multinucleated, but the cytokinesis defect is rescued on introduction of GFP-GAPA (right). Nuclei stained with DAPI. Bar 10 µm.**

We then analyzed localization of GAPA under different cellular conditions by imaging of live cells and fixed cells. Under vegetative conditions we noted that GFP-GAPA is present throughout the cytosol and is enriched at the cell cortex (Figure 46 A) whereas in migrating aggregation competent cells the membrane localization was lost and the protein was distributed throughout the cytosol (Figure 46 B).

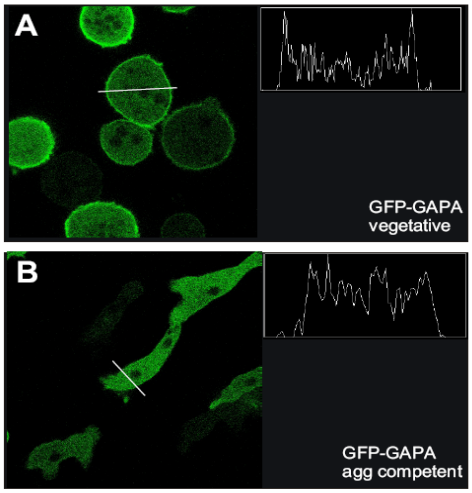


**Figure 46. Localization of GAPA in vegetative and aggregation competent cells. (A) Vegetative wild type cells expressing GFP-GAPA were observed using confocal microscopy. (B) Aggregation competent wild type cells expressing GFP-GAPA were seeded in a chemotaxis chamber and migration in the direction of a chemotaxis gradient was observed using confocal microscopy. (Inset) Fluorescence intensity profiles of GFP-GAPA distribution (measured using Image J software) through an arbitrary position in the cell marked by the white line.**

To study the localization of GFP-GAPA during cytokinesis in fixed cells AX2 cells expressing GFP-GAPA were fixed after a release from the nocodazol block. α-Tubulin staining was used to identify a cell as mitotic (Piperno and Fuller, 1985). Initially, GFP-GAPA is present uniformly in the cytosol and at the plasma membrane, but with progression of cytokinesis it translocates to the cleavage furrow (Figure 47).

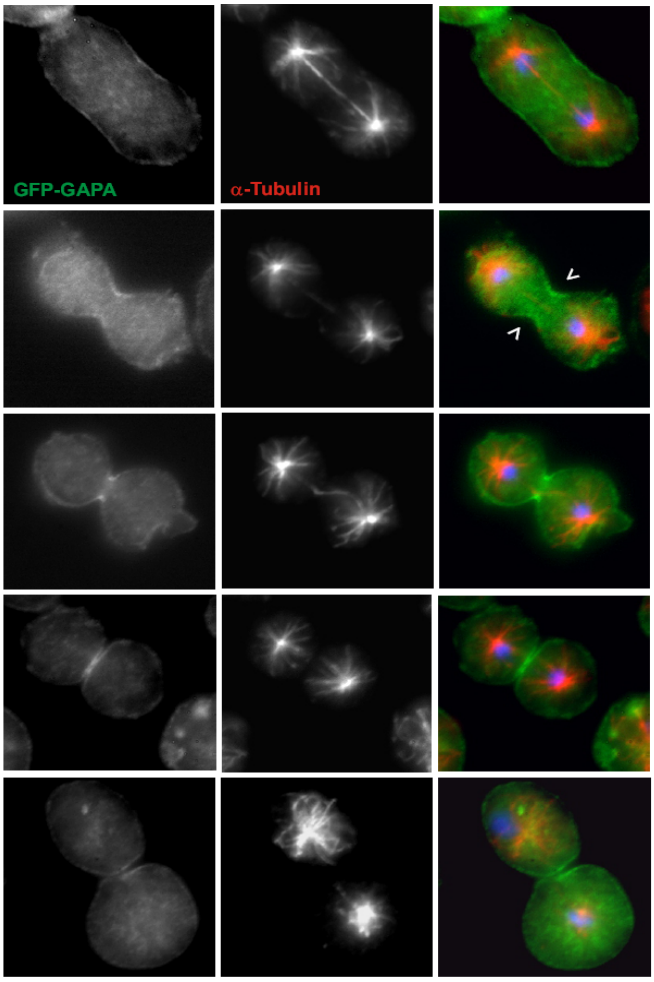


**Figure 47. Localization of GAPA to the cleavage furrow during cytokinesis. Cells expressing GFP-GAPA (green) were synchronized using nocodazol to block progression of the cell cycle and then released, and then fixed using cold methanol. Tubulin (red) antibody is used to identify mitotic cells. Nuclei (blue) are stained with DAPI.**

As myosin II is essential for cytokinesis and localizes to the clavage furrow during cytokinesis, we analyzed localization of GFP-GAPA in *mhcA*$^-$ (myosin II heavy chain null) cells. We found that localization of GFP-GAPA to the cleavage furrow during cytokinesis was unaltered in these cells (Figure 48). This is consistent with previous results that show that in GAPA$^-$ cells undergoing cytokinesis myosin II is localized in the cleavage furrow (Adachi et al., 1997), indicating that localization of either GAPA or myosin II to the cleavage furrow during cytokinesis is not dependent on each other.

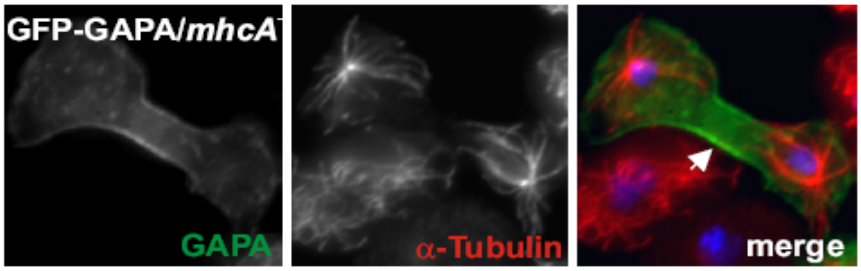


**Figure 48. Localization of GAPA to the cleavage furrow is independent of myosin II. Myosin II null cells expressing GFP-GAPA were synchronized using nocodazol to block progression of cell cycle and then released, and then fixed using cold methanol. Tubulin (red) antibody is used to identify mitotic cells. Nuclei (blue) are stained with DAPI.**

### 4.3.2 Oligomerization of GAPA

In a GST-pulldown experiment where glutathione sepharose beads were coated with GST-GAP and incubated with cell free extracts from cells expressing GFP-GAPA, we found that GST-GAP could pulldown GFP-GAPA indicating the possibility of GAPA to form oligomers (Figure 49).

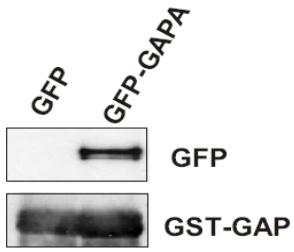


**Figure 49. Oligomerization of GAPA. Glutathione-sepharose beads coated with GST-GAP were incubated with cell free extacts from cells expressing GFP-GAPA or GFP. Pulldown eluates were probed with GFP antibody mAb K3-184-2. GST-GAP pulls down GFP-GAPA.**

To study this further, we analyzed the ability of GAPA to form oligomers using cell-free extracts from AX2 cells expressing GFP-GAPA and size fractionated the proteins by gel-filtration using a Superdex-200 column. Recombinant GFP-GAPA, which has a molecular mass of ~ 120 kDa, largely eluted in fractions around 440 kDa, indicating the possibility of trimer formation in vivo (Figure 50).

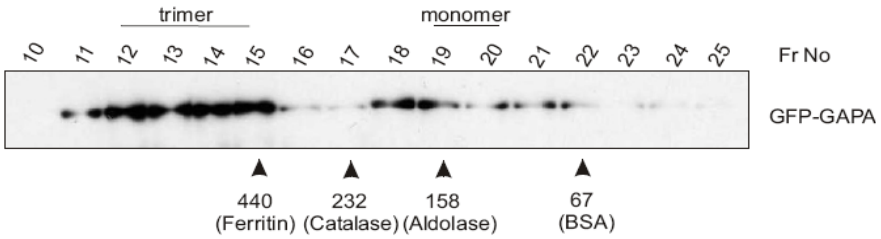


**Figure 50. Oligomerization of GAPA. Cell free extracts from cells expressing GFP-GAPA were subjected to analytical gel filtration. The eluates were analysed by western blotting using GFP-specific mAb K3-184-2. The fraction number of elutions of corresponding molecular weight markers are indicated with arrowheads.**

To rule out the possibility that GFP tagged to GAPA at the N-terminus might effect oligomerization we analysed the oligomerization potential of the GAP domain of GAPA. The GAP domain is a 37 kDa polypeptide, free of any tag. We performed gel electrophoresis under native conditions and gel filtration chromatography and found that in native gel analysis the GAP domain was largely present as a diffuse band at sizes between 90 – 140 kDa, again indicating formation of a trimer under native conditions (Figure 51 A). In gel filtration analysis using a Superdex 75 column GAP consistently eluted in fractions corresponding to a trimer in solution (Figure 51 B). These results support that GAPA exists as a trimer in vivo.

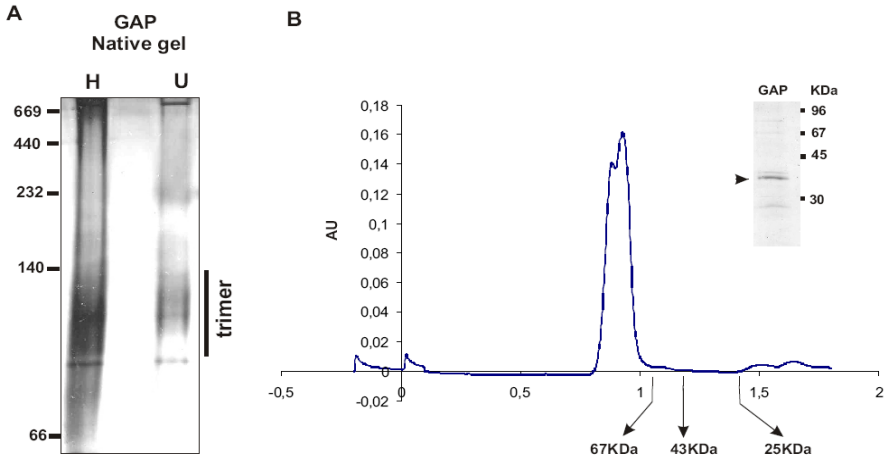


**Figure 51. Oligomerization of the GAP domain of GAPA. (A) Oligomerization of the GAP domain of GAPA using native gels. The GAP polypeptide was either heated at 65°C (H) or unheated (U) and then resolved by native PAGE (8% acrylamide) and visualized using silver staining. (B) Oligomerization of the GAP domain of GAPA using**

**gel filtration chromatography. The GAP polypeptide was subjected to gel filtration chromatography and the $OD_{280}$ recorded to detect the protein.**

### 4.3.3 GAPA interacts with Filamin

We initially found GAPA as a filamin interacting protein in immunoprecipitation assays with filamin monoclonal antibodies and subsequent identification by MALDI-TOF mass spectroscopy (N.K Khaire, *Ph.D. thesis*, University of Cologne, 2003). We next confirmed the association between filamin and GAPA using different GAPA and filamin polypeptides and identified the interaction domains. We expressed the actin bindining domain (ABD), the ABD along with the first two rod repeats (ABD+rod 1-2) and only the rod domains (rod1-6) as GFP fusion proteins in cells lacking filamin (HG1264) (Khaire et al., 2007). We also expressed GAPA or only the GAP domain as GFP fusion proteins in *D. discoideum* cells or as GST fusion proteins in bacteria (Figure 52).

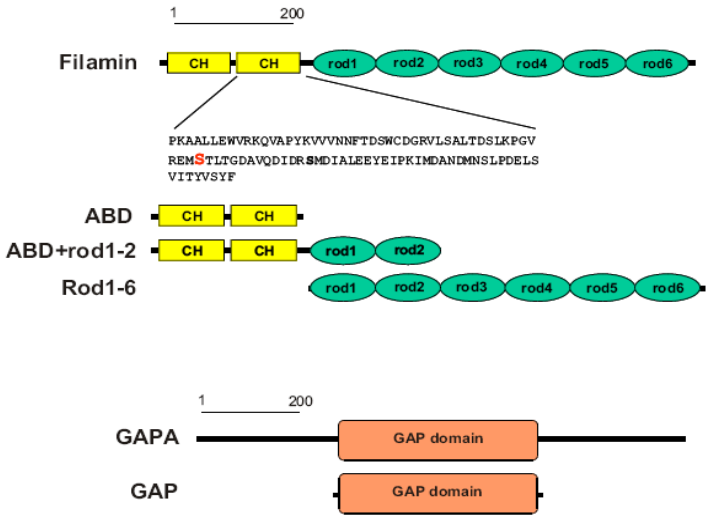


**Figure 52. Filamin and GAPA constructs used in this study. The filamin proteins were expressed as GFP fusions in $FLN^-$ strain HG1264 and GAPA proteins as GST fusions in bacteria or GFP fusions in *D. discoideum* cells. In the upper part the location of a putative phosphorylation site in CH-domain 2 is shown.**

In GST-pulldown experiments we found that both full length GAPA and the GAP domain could pulldown filamin from cell lysates (Figure 53 A). Filamin is very sensitive to

proteolysis and often appears as a smear in western blots. Since the GAP domain alone was sufficient to pulldown filamin, we used GST-GAP to map the GAPA interacting part in filamin. Glutathione sepharose beads coated with GST-GAP were incubated with cell lysates from HG1264 cells expressing GFP-ABD, GFP-ABD+rod1-2 and GFP-rod1-6. The pulldown eluates were resolved by SDS-PAGE and immunoblotted using GFP-specific mAb K3-184-2. We found that only GFP-ABD and GFP-ABD+rod1-2 could bind to GST-GAP but not GFP-rod1-6 indicating that the actin-binding domain (ABD) in filamin represents the GAPA interacting domain (Figure 53 B). Analysis of the actin-binding domain revealed the presence of a putative protein kinase A (PKA) phosphorylation site (S174). PKA is a cAMP effector protein and cAMP serves as a master regulator at different points during *D. discoideum* development. Several investigations indicated that filamin null mutants have an altered expression of components of the cAMP signaling system. In filamin null mutants cAMP phosphodiesterase (PDE) is down-regulated and its inhibitor (PDI) is upregulated which might lead to a rise of the cAMP levels in these mutants (N.K. Khaire, *Ph.D. thesis*, University of Cologne, 2003). Elevated cAMP levels in filamin null mutants might be the cause of defects in phototactic migration that may arise due to interference with the formation of three-dimensional scroll waves. Therefore we were tempted to analyze if the putative PKA phosphorylation site in the ABD of filamin is critical for its interaction with GAPA. Glutathione sepharose beads coated with GST-GAP were incubated with cell lysates of HG1264 expressing either GFP-full length filamin (GFP-Fil) or GFP-full length filamin carrying the S174A mutation (GFP-FLN$^{S174A}$). Eluates when analyzed by westen blotting revealed that the PKA phosphorylation site S174 is not critical for interaction with GAPA, but confirmed the GAPA-filamin interaction (Figure 53 C).

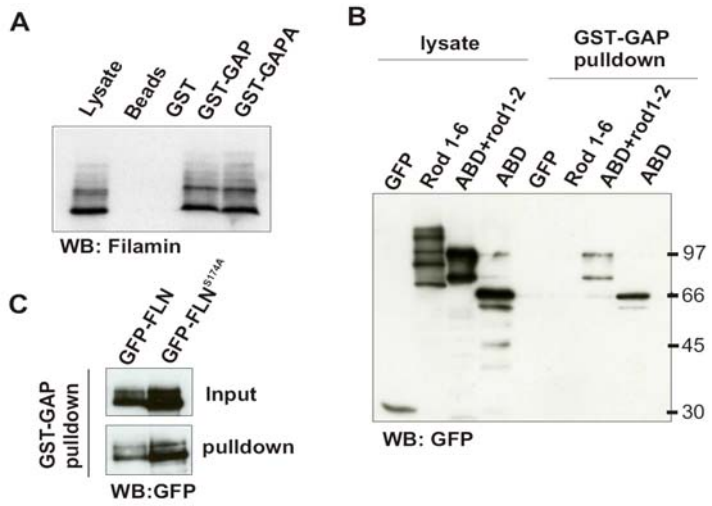


**Figure 53. Interaction of GAPA with Filamin. (A) Glutathione sepharose beads coated with GST-GAPA or GST-GAP has the ability to pulldown endogenous Filamin using monoclonal antibody (Brink et al., 1990) against filamin. (B) GST-pulldown experiment showing the ability of GST-GAP to bind specifical to GFP-tagged ABD or ABD+rod1-2, but not to rod1-6 constructs of Filamin. (C) GST-GAP binding to GFP fused full-length Filamin (GFP-FLN) is unaffected in a Filamin mutant (GFP-FLN$^{S174A}$) where a PKA phosphorylatable Serine residue is mutated to Alanine.**

### 4.3.4 GAPA null cells show a slug phototaxis defect

Slugs of cells lacking filamin show defects in phototaxis, migrating shorter distances in the darkness and migrating at angles larger than 45° to the incident light (Fisher et al., 1997; Wallraff and Wallraff, 1997). Wild type slugs on the other hand migrate along a fairly straight path towards the incident light. Several small GTPases and their regulators have also been implicated in phototaxis (Wilkins et al., 2005). Since GAPA interacts with Filamin we investigated whether phototaxis is affected in slugs from GAPA null cells. We found that slugs from GAPA null cells were able to form migrating slugs. However, in comparison to wild type slugs GAPA null slugs move towards the light source is an extremely disoriented fashion (Figure 54). This reveals a new role for GAPA and a possible role of GAPA in regulating Filamin in phototactic functions.

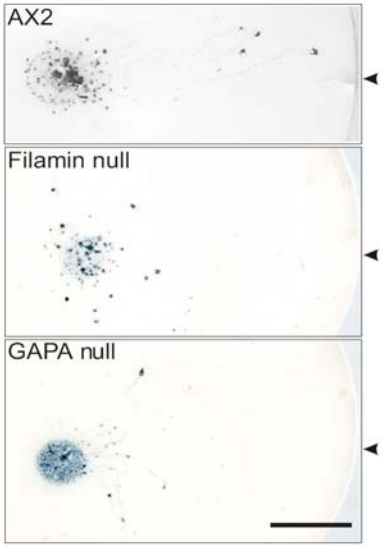


**Figure 54. Altered phototaxis in GAPA null cells. Wild type AX2, Filamin null and GAPA null cells were allowed to develop on phosphate agar plates in a black opaque box for 36 h with a unidirectional light source from an open slit. Migratory pattern of slugs were determined by transferring slime trails and cellular materials onto nitrocellulose membrane. Membranes were stained with 0.1% amido black. Bar, 1 cm.**

### 4.3.5 Filamin and cytokinesis

Since we found filamin as interaction partner of GAPA and as GAPA localizes to the cleavage furrow during cytokinesis we tested if filamin is enriched in the cleavage furrow during cytokinesis. We found that during cytokinesis, as in interphase, filamin had a cortical localization and was not enriched in the cleavage furrow (Figure 55 A). We then examined the localization of GAPA in the absence of filamin by expressing GFP-GAPA in HG1264 cells. The localization of GAPA during cytokinesis was unaltered which is consistent with the above results that showed that no enrichment of filamin in cleavage furrow during cytokinesis (Figure 55 B).

Filamin null mutants have a substantial shedding of cellular material during growth in shaking suspension. These particles contain cytosolic proteins but are devoid of nuclei (Rivero et al., 1996b). We observed such nuclei free particles in GAPA$^{-}$ cells and also in GAPA$^{-}$ cells expressing GFP-GAPA (Figure 55 C-E). Nuclei free particles could arise either by membrane blebbing due to weakening of the actin cytoskeleton or due to formation of an ectopic

cleavage furrow. We also observed the formation of ectopic cleavage furrows in HG1264 cells undergoing cytokinesis (Figure 55 F), indicating that nuclei free particle may be generated from both routes. Our results indicate that though filamin is not recruited to the cleavage furrow, it is required for maintaining the actin-cytoskeleton during cytokinesis.

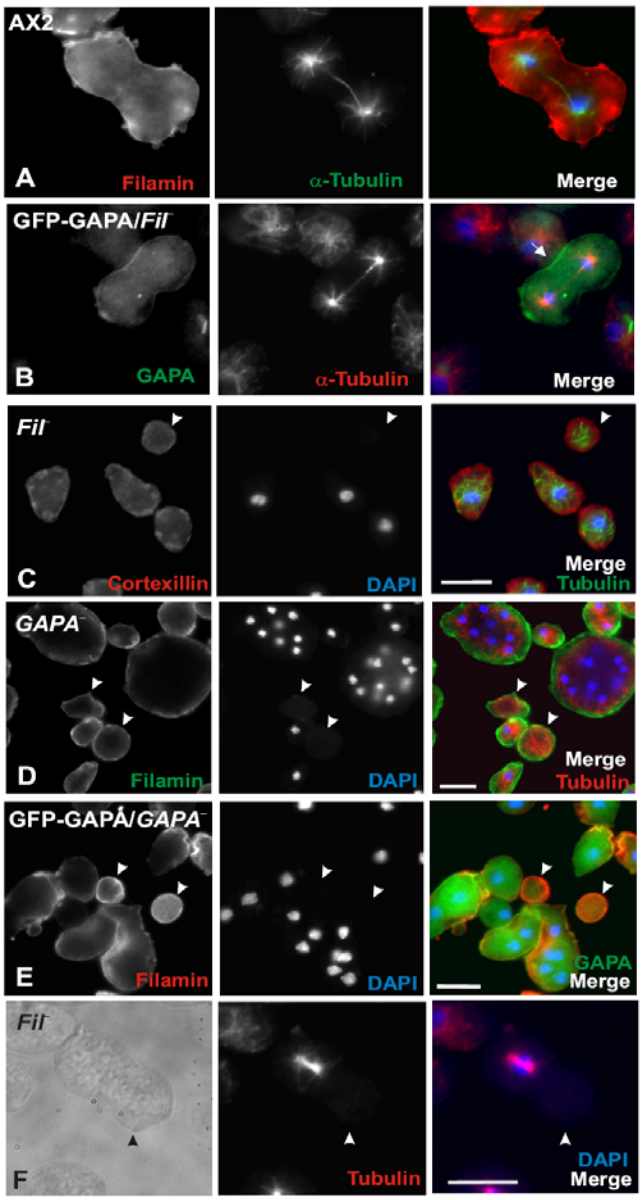


**Figure 55. (A) Filamin has a cortical localization during cytokinesis. (B) GFP-GAPA localizes to the cleavage furrow in filamin null cells. (C) Nucleus free particles in Filamin null cells. (D) Nucleus free particles in GAPA null cells. (E) Nucleus free particles in GAPA null cells expressing GFP-GAPA. (F) Formation of an ectopic cleavage furrow in Filamin null cells. Cells were fixed in ice-cold methanol, Filamin and α-tubulin was stained using monoclonal antibodies, nucleus stained with DAPI, Bar 10 µm.**

### 4.3.6 GAPA recruitment to the cleavage furrow requires cortexillin I

Cortexillins are enriched in the cortex during interphase and in the cleavage furrow during cells division (Faix et al., 1996). Since GAPA also localizes to the cleavage furrow during cytokinesis consistent with previous finding that GAPA$^-$ cells have a strong cytokinesis defect (Adachi et al., 1997; Faix et al., 2001), we investigated if a direct interaction between GAPA and cortexillin exists. Glutathione sepharose beads coated with GST-GAP could pulldown cortexillin I from cell lysates, but not another IQGAP related protein DGAP1, which is also required for cytokinesis and recruitment of cortexillin I to the cleavage furrow (Figure 56 B). In immunoprecipitation experiments using cells expressing GFP-GAPA with anti-GFP mAb K3-184-2 we could also pulldown cortexillin I, indicating the formation of a complex between GAPA and cortexillin I in vivo (Figure 56 C).

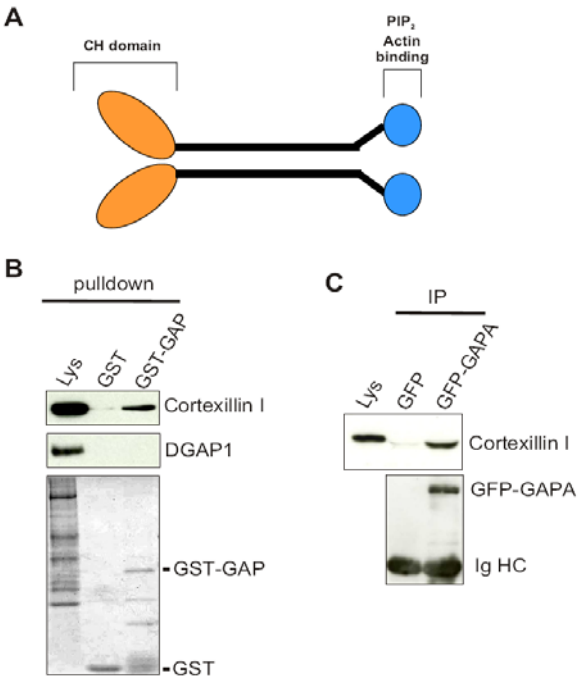


**Figure 56. Association between Cortexillin I and GAPA. (A) Architecture of Cortexillin I. (B) Glutathione sepharose beads coated with GST-GAP has the ability to pulldown endogenous Cortexillin I. (C) GFP monoclonal antibody was used to precipitate GFP-GAPA from cells overexpressing GFP-GAPA, the immunoprecipitaes were resolved by SDS-PAGE and probed for cortexillin I.**

Since GAPA and cortexillin I interact with each other and are recruited to the cleavage furrow during cytokinesis we investigated if GAPA localized to cleavage furrow in a Cortexillin I dependent manner. Previous studies showed that cortexillin localized to the cleavage furrow in the absence of either GAPA or DGAP1, but localization to the cleavage furrow was dramatically affected in cells lacking both GAPA and DGAP1 (Faix et al., 2001). When we expressed GFP-GAPA in cells lacking cortexillin I, the localization of GAPA to the cleavage furrow during cytokinesis was lost (Figure 57).

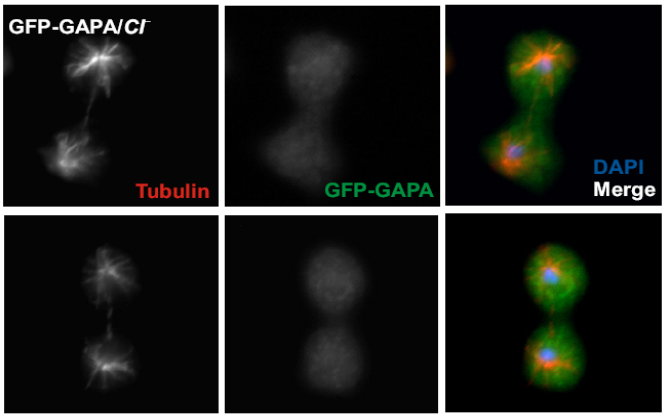


**Figure 57. Loss of localization of GFP-GAPA in the cleavage furrow in cortexillin I null cells. Cortexillin I null cells expressing GFP-GAPA were synchronized using nocodazol to block progression of the cell cycle and then released, and fixed using cold methanol. Tubulin (red) antibody was used to identify mitotic cells. Nuclei (blue) are stained with DAPI. Images were captured using florescence microscope.**

## 4.4 Discussion

### GAPA-Filamin interaction in regulating cytoskeletal organization

Studies from mammalian system have revealed a direct role of filamin to regulation of small GTPases Rho and Rac signaling in regulating cell polarity. Trio, and possibly other GEFs for Rac activate Rac, which leads to activation of PI5-kinase and PAK (p21 activated kinase) that promote actin-filament nucleation and cofilin inactivation, respectively. Activation of Rho by Lbc (a RhoGEF) stimulates ROCK, active ROCK phosphorylates FilGAP to inactivate Rac inhibiting elongation of actin-filaments and promotion of actin-filament disassembly. ROCK also phosphorylates myosin light chain and induces myosin filament formation and cell contraction. Several of these components of Rac-Rho signaling pathways are Filamin interactors like, RhoA, Trio, PAK, FilGAP (Bellanger et al., 2000; Ohta et al., 2006; Ohta et al., 1999; Vadlamudi et al., 2002). Thus filamin acts as an integrator for signal transduction pathways has thus been well characterized in mammalian system, but still remains to be understood completely in *D. discoideum*.

The *D. discoideum* genome lacks a typical Rho GTPase and also Rho activated kinase ROCK and the role of filamin as an integrator of signal transduction pathways still remains unanswered. Here we characterize the association between an IQGAP related protein, GAPA and *D. discoideum* Filamin, which shows that filamin in *D. discoideum* can also act as integrator of signaling cascades. We show that the actin binding domain of filamin formed by CH1 and CH2 domains mediate association with the GAP domain of GAPA. We have been able to show that in cells lacking either filamin or GAPA, the cytoskeleton is weak and gives rise to nuclei-less particles formed by membrane blebs. The association of GAPA to the actin-binding domain of filamin prompted us to analyze if GAPA plays any role in regulating rates of actin crosslinking mediated by filamin, which is currently under investigation.

The cytoskeleton plays a key role in *D. discoideum* morphogenesis. Both filamin and GAPA null cells undergo normal development forming normal fruiting bodies consisting of a stalk and a spore head with viable spores. In this process an event of cellular differentiation occurs, wherein undifferentiated vegetative cells upon entry into the developmental process

commit to either become a prestalk or a prespore cell, and is sorted in an anterior-posterior axis. The tip of an emerging fruiting body serves as the organizer for the developmental process generating oscillatory cAMP waves that are propagated through out the slug and are also responsible for slug migration behaviors. Filamin is required for phototaxis and filamin null mutants show defects in their phototactic abilities. And expression of filamin at the tip of a migrating slug rescues the phototaxis defects (Khaire et al., 2007). We also observed that GAPA null cells also show altered phototaxis behavior, indicating a possible role of filamin as an integrator in bringing a signaling complex required for phototaxis. PKA, a cAMP effector protein is a key signaling molecule in *D. discoideum* development in relaying signals to induce expression of developmentally regulated genes. We also analyzed the role of a PKA phosphorylable serine residue in the actin-binding domain of filamin, which is also the GAPA interaction domain, but we did not observe that mutations converting it into an unphosphorylabe alanine affect between GAPA and Filamin.

**GAPA-cortexillin I interaction in cytokinesis**

Cytokinesis is under intricate control of small GTPases and its effector proteins. In mammalian cells RhoA and its effector molecules ROCK and citron kinase are localized to the cleavage furrow (Matsumura, 2005). In *D. discoideum* cells lacking small GTPases RacE or RasG show cytokinesis defects (Larochelle et al., 1997; Tuxworth et al., 1997), also IQGAP related protein, which are Rac effector proteins are also critical for cytokinesis. Lack of GAPA or overexpression of DGAP1 causes defects in cytokinesis (Adachi et al., 1997; Faix and Dittrich, 1996). Among cytoskeletal proteins, a primary role of myosin II in cytokinesis is well established, where it interacts with membrane-associated actin filaments to form a ring that separates daughter cells by contraction (Matsumura, 2005; Satterwhite and Pollard, 1992). But the singular importance of myosin in cytokinesis was questioned when it

was observed that *D. discoideum* cells lacking myosin II can still divide when they attach on a surface. These finding provoked search for proteins responsible for cytokinesis in the absence of myosin II. Cortexillins were identified as actin crosslinking proteins which localize to the cleavage furrow during cytokinesis (Weber et al., 1999). It was also established that IQGAP proteins, GAPA and DGAP1 are required for recruitment of cortexillins to the cleavage furrow (Faix et al., 2001).

Here we show that GAPA is also recruited to the cleavage furrow during cytokinesis. Overexpression of the protein in did not lead to cytokinesis defects as observed when overexpressing DGAP1, probably indicate they have unique roles to play. We also did not observe a direct association between GAPA and DGAP1 in binding assays. We also observed that in cells lacking myosin II GAPA is still localized to the cleavage furrow, indicating a role of GAPA in a myosin II-independent mechanism in regulating cytokinesis. We also observed that in cells lacking cortexillin I, GAPA localization to the cleavage furrow is lost. On the other hand cortexillin I localizes to the cleavage furrow in cells lacking GAPA (Faix et al., 2001). These results imply that localization of GAPA to the cleavage furrow requires association with cortexillin I. It remains to be understood how Rac GTPases could regulate the process.

# Epilogue

*From my work which revolved around three proteins related to regulation of small GTPases, RasGEF Q, an exchange factor for Ras GTPase, GxcDD, a putative exchange factor for Rac GTPase and an IQGAP-related protein, GAPA it can be appreciated the diversity of cellular processes regulated by small GTPases. Using biochemical, cell biological or genetic approaches I could show the complexity of small GTPase signaling components*

*and the apparent simplicity of the organism. Though most of these signaling components are multi-domain proteins and there are many instances of such proteins with unique domain architecture in different organism, principles of cellular regulation are often conserved.*

Since the discovery that mutated Ras proteins are the transforming elements borne by certain cancer causing retroviruses (Der et al., 1982), the Ras family of small GTPases has been subjected to intensive study. Over 25 years of study has expanded our understanding on several aspects of cellular processes regulated by them and has extended the Ras family to a superfamily including five broad subfamilies: Ras, Rho Ran, Rab and Arf.

The *Dictyostelium* genome revealed that it encodes representatives of each of the subfamilies (though not containing any typical Rho or Cdc42 small GTPases it encodes for numerous Rac related GTPases). It also revealed the large number of proteins that contain regulatory domains for small GTPases; Guanine exchange factors (GEFs), which convert an inactive small GTPase to an active, GTPase and GTPase activating protein (GAPs), which inactivate them by increasing the rate of GTP hydrolysis (Vlahou and Rivero, 2006). My thesis dealt with three proteins involved in small GTPase signaling; RasGEF Q, an exchange factor for Ras GTPase, GxcDD, a putative exchange factor for Rac GTPases and an IQGAP related protein GAPA, a Rac effector protein.

RasGEF Q, one of the 25 RasGEFs, was found to be the prodominent exchange factor for one of the 15 Ras isoform in *Dictyostelium*, RasB. cAMP signaling though membrane receptors would activate RasGEF Q, which in turn activated RasB. Activated RasB then would regulate myosin II phosphorylation by activating myosin II heavy chain kinase A (MHCK A). This pathway is the first direct evidence of role of Ras small GTPase in regulation of myosin II functions in *Dictyostelium*. Myosin II, is crucial for processes like cell migration, cytokinesis and development. Deleting RasGEF Q or overexpressing the GEF domain of RasGEF Q or a constitutively activated RasB could phenocopy myosin II mutants.

These were supported by strong biochemical data where we observe defects in myosin phosphorylation and a role of MHCK A in the pathway. Rho GTPase and its effector kinase ROCK have been well characterized as a regulator of myosin in metazoan systems, in the absence of Rho and ROCK, *Dictyostelium* would have expanded the functions of its several GTPase to complement their role.

GxcDD, a multidomain protein containing CH domain, IQ motifs, PH domains, RhoGEF domains and ArfGAP domain is predicted to be a putative RacGEF. Inactivation of the gene resulted in delayed development and abnormal streaming behavior. We also examine the function of different domains, where we find the CH domain to act as a membrane anchor, the RhoGEF domain to have the ability to interact with several Rac GTPases and the ArfGAP-PH tandem to accumulate in cortical region of the cell and in phagosomes. We propose that GxcDD is not only a component of Rac signaling pathway in *Dictyostelium*, but is also involved in integrating different cellular signals.

GAPA, an IQGAP related protein was found enriched in the cleavage furrow and support previous findings that it is required for cytokinesis. We also identified it as an interactor of filamin and cortexillin. Association with filamin also reveals a role of *Dictyostelium* filamin acting as an integrator of signaling components. The interaction between GAPA and Filamin is through the GAP homology domain of GAPA and the Actin binding domain of Filamin. This finding has prompted investigation of a possible role GAPA in regulating filamin mediated actin crosslinking, which is currently ongoing. Our findings have also revealed a role of GAPA in phototaxis, which might involve a role of filamin as an integrator in signaling complex. Association with cortexillin also strengthens role of GAPA and Cortexillin-GAPA complex in cytokinesis. We show that GAPA is not required for myosin II independent cytokinesis but localization of GAPA to the cleavage furrow requires Cortexillin I.

From these above studies it is evident that small GTPases regulate a very broad spectrum of cellular processes. Many studies dealing with chemotaxis, cell polarity and cytokinesis have traditionally used *Dictyostelium* as a model. A comparison of signal transduction pathways, in particular those that involve small GTPases during chemotaxis have revealed though details of the process may differ, principles of organization and several components are shared throughout eukaryotic evolution.

## References


Adachi, H., Y. Takahashi, T. Hasebe, M. Shirouzu, S. Yokoyama, and K. Sutoh. 1997. Dictyostelium IQGAP-related protein specifically involved in the completion of cytokinesis. *J Cell Biol*. 137:891-8.

Arigoni, M., E. Bracco, D.F. Lusche, H. Kae, G. Weeks, and S. Bozzaro. 2005. A novel Dictyostelium RasGEF required for chemotaxis and development. *BMC Cell Biol*. 6:43.

Banuelos, S., M. Saraste, and K.D. Carugo. 1998. Structural comparisons of calponin homology domains: implications for actin binding. *Structure*. 6:1419-31.

Bear, J.E., J.F. Rawls, and C.L. Saxe, 3rd. 1998. SCAR, a WASP-related protein, isolated as a suppressor of receptor defects in late Dictyostelium development. *J Cell Biol*. 142:1325-35.

Bellanger, J.M., C. Astier, C. Sardet, Y. Ohta, T.P. Stossel, and A. Debant. 2000. The Rac1- and RhoG-specific GEF domain of Trio targets filamin to remodel cytoskeletal actin. *Nat Cell Biol*. 2:888-92.

Bertholdt, G., J. Stadler, S. Bozzaro, B. Fichtner, and G. Gerisch. 1985. Carbohydrate and other epitopes of the contact site A glycoprotein of Dictyostelium discoideum as characterized by monoclonal antibodies. *Cell Differ*. 16:187-202.

Bosgraaf, L., and P.J. van Haastert. 2006. The regulation of myosin II in Dictyostelium. *Eur J Cell Biol*. 85:969-79.

Bosgraaf, L., A. Waijer, R. Engel, A.J. Visser, D. Wessels, D. Soll, and P.J. van Haastert. 2005. RasGEF-containing proteins GbpC and GbpD have differential effects on cell polarity and chemotaxis in Dictyostelium. *J Cell Sci*. 118:1899-910.

Brink, M., G. Gerisch, G. Isenberg, A.A. Noegel, J.E. Segall, E. Wallraff, and M. Schleicher. 1990. A Dictyostelium mutant lacking an F-actin cross-linking protein, the 120-kD gelation factor. *J Cell Biol*. 111:1477-89.

Brown, M.D., and D.B. Sacks. 2006. IQGAP1 in cellular signaling: bridging the GAP. *Trends Cell Biol*. 16:242-9.

Calderwood, D.A., A. Huttenlocher, W.B. Kiosses, D.M. Rose, D.G. Woodside, M.A. Schwartz, and M.H. Ginsberg. 2001. Increased filamin binding to beta-integrin cytoplasmic domains inhibits cell migration. *Nat Cell Biol*. 3:1060-8.

Charest, P.G., and R.A. Firtel. 2006. Feedback signaling controls leading-edge formation during chemotaxis. *Curr Opin Genet Dev*. 16:339-47.

Charest, P.G., and R.A. Firtel. 2007. Big roles for small GTPases in the control of directed cell movement. *Biochem J*. 401:377-90.

Chen, M.Y., Y. Long, and P.N. Devreotes. 1997. A novel cytosolic regulator, Pianissimo, is required for chemoattractant receptor and G protein-mediated activation of the 12 transmembrane domain adenylyl cyclase in Dictyostelium. *Genes Dev*. 11:3218-31.

Chen, T.L., W.A. Wolf, and R.L. Chisholm. 1998. Cell-type-specific rescue of myosin function during Dictyostelium development defines two distinct cell movements required for culmination. *Development*. 125:3895-903.

Chisholm, R.L. 1997. Cytokinesis: a regulatory role for Ras-related proteins? *Curr Biol*. 7:R648-50.

Chisholm, R.L., and R.A. Firtel. 2004. Insights into morphogenesis from a simple developmental system. *Nat Rev Mol Cell Biol*. 5:531-41.

Chung, C.Y., and R.A. Firtel. 1999. PAKa, a putative PAK family member, is required for cytokinesis and the regulation of the cytoskeleton in Dictyostelium discoideum cells during chemotaxis. *J Cell Biol*. 147:559-76.
Claviez, M., K. Pagh, H. Maruta, W. Baltes, P. Fisher, and G. Gerisch. 1982. Electron microscopic mapping of monoclonal antibodies on the tail region of Dictyostelium myosin. *Embo J*. 1:1017-1022.
Clemen, C.S., D. Fischer, U. Roth, S. Simon, P. Vicart, K. Kato, A.M. Kaminska, M. Vorgerd, L.G. Goldfarb, B. Eymard, N.B. Romero, B. Goudeau, T. Eggermann, K. Zerres, A.A. Noegel, and R. Schroder. 2005. Hsp27-2D-gel electrophoresis is a diagnostic tool to differentiate primary desminopathies from myofibrillar myopathies. *FEBS Lett*. 579:3777-82.
Clow, P.A., T. Chen, R.L. Chisholm, and J.G. McNally. 2000. Three-dimensional in vivo analysis of Dictyostelium mounds reveals directional sorting of prestalk cells and defines a role for the myosin II regulatory light chain in prestalk cell sorting and tip protrusion. *Development*. 127:2715-28.
Conner, S.D., and S.L. Schmid. 2003. Regulated portals of entry into the cell. *Nature*. 422:37-44.
Cooper, J.A. 1991. The role of actin polymerization in cell motility. *Annu Rev Physiol*. 53:585-605.
Cote, J.F., and K. Vuori. 2002. Identification of an evolutionarily conserved superfamily of DOCK180-related proteins with guanine nucleotide exchange activity. *J Cell Sci*. 115:4901-13.
Daniel, J., G.B. Spiegelman, and G. Weeks. 1993. Characterization of a third ras gene, rasB, that is expressed throughout the growth and development of Dictyostelium discoideum. *Oncogene*. 8:1041-7.
de Hostos, E.L., C. Rehfuess, B. Bradtke, D.R. Waddell, R. Albrecht, J. Murphy, and G. Gerisch. 1993. Dictyostelium mutants lacking the cytoskeletal protein coronin are defective in cytokinesis and cell motility. *J Cell Biol*. 120:163-73.
De Lozanne, A., and J.A. Spudich. 1987. Disruption of the Dictyostelium myosin heavy chain gene by homologous recombination. *Science*. 236:1086-91.
Der, C.J., T.G. Krontiris, and G.M. Cooper. 1982. Transforming genes of human bladder and lung carcinoma cell lines are homologous to the ras genes of Harvey and Kirsten sarcoma viruses. *Proc Natl Acad Sci U S A*. 79:3637-40.
Devreotes, P., and C. Janetopoulos. 2003. Eukaryotic chemotaxis: distinctions between directional sensing and polarization. *J Biol Chem*. 278:20445-8.
Dormann, D., and C.J. Weijer. 2006. Chemotactic cell movement during Dictyostelium development and gastrulation. *Curr Opin Genet Dev*. 16:367-73.
Dumontier, M., P. Hocht, U. Mintert, and J. Faix. 2000. Rac1 GTPases control filopodia formation, cell motility, endocytosis, cytokinesis and development in Dictyostelium. *J Cell Sci*. 113 ( Pt 12):2253-65.
Egelhoff, T.T., D. Croft, and P.A. Steimle. 2005. Actin activation of myosin heavy chain kinase A in Dictyostelium: a biochemical mechanism for the spatial regulation of myosin II filament disassembly. *J Biol Chem*. 280:2879-87.
Egelhoff, T.T., R.J. Lee, and J.A. Spudich. 1993. Dictyostelium myosin heavy chain phosphorylation sites regulate myosin filament assembly and localization in vivo. *Cell*. 75:363-71.
Egelhoff, T.T., T.V. Naismith, and F.V. Brozovich. 1996. Myosin-based cortical tension in Dictyostelium resolved into heavy and light chain-regulated components. *J Muscle Res Cell Motil*. 17:269-74.
Eichinger, L., J.A. Pachebat, G. Glockner, M.A. Rajandream, R. Sucgang, M. Berriman, J. Song, R. Olsen, K. Szafranski, Q. Xu, B. Tunggal, S. Kummerfeld, M. Madera, B.A. Konfortov, F. Rivero, A.T. Bankier, R. Lehmann, N. Hamlin, R. Davies, P. Gaudet, P. Fey, K. Pilcher, G. Chen, D. Saunders, E. Sodergren, P. Davis, A. Kerhornou, X. Nie, N. Hall, C. Anjard, L. Hemphill, N. Bason, P. Farbrother, B. Desany, E. Just, T. Morio, R. Rost, C. Churcher, J. Cooper, S. Haydock, N. van Driessche, A. Cronin, I. Goodhead, D. Muzny, T. Mourier, A. Pain, M. Lu, D. Harper, R. Lindsay, H. Hauser, K. James, M. Quiles, M. Madan Babu, T. Saito, C. Buchrieser, A. Wardroper, M. Felder, M. Thangavelu, D. Johnson, A. Knights, H. Loulseged, K. Mungall, K. Oliver, C. Price, M.A. Quail, H. Urushihara, J. Hernandez, E. Rabbinowitsch, D. Steffen, M. Sanders, J. Ma, Y. Kohara, S. Sharp, M. Simmonds, S. Spiegler, A. Tivey, S. Sugano, B. White, D. Walker, J. Woodward, T. Winckler, Y. Tanaka, G. Shaulsky, M. Schleicher, G. Weinstock, A. Rosenthal, E.C. Cox, R.L. Chisholm, R. Gibbs, W.F. Loomis, M. Platzer, R.R. Kay, J. Williams, P.H. Dear, A.A. Noegel, B. Barrell, and A. Kuspa. 2005. The genome of the social amoeba Dictyostelium discoideum. *Nature*. 435:43-57.
Eliott, S., G.H. Joss, A. Spudich, and K.L. Williams. 1993. Patterns in Dictyostelium discoideum: the role of myosin II in the transition from the unicellular to the multicellular phase. *J Cell Sci*. 104 ( Pt 2):457-66.
Etienne-Manneville, S., and A. Hall. 2002. Rho GTPases in cell biology. *Nature*. 420:629-35.
Faix, J. 2002. The actin-bundling protein cortexillin is the downstream target of a Rac1-signaling pathway required for cytokinesis. *J Muscle Res Cell Motil*. 23:765-72.
Faix, J., and W. Dittrich. 1996. DGAP1, a homologue of rasGTPase activating proteins that controls growth, cytokinesis, and development in Dictyostelium discoideum. *FEBS Lett*. 394:251-7.
Faix, J., M. Steinmetz, H. Boves, R.A. Kammerer, F. Lottspeich, U. Mintert, J. Murphy, A. Stock, U. Aebi, and G. Gerisch. 1996. Cortexillins, major determinants of cell shape and size, are actin-bundling proteins with a parallel coiled-coil tail. *Cell*. 86:631-42.

Faix, J., I. Weber, U. Mintert, J. Kohler, F. Lottspeich, and G. Marriott. 2001. Recruitment of cortexillin into the cleavage furrow is controlled by Rac1 and IQGAP-related proteins. *Embo J*. 20:3705-15.
Feng, Y., and C.A. Walsh. 2004. The many faces of filamin: a versatile molecular scaffold for cell motility and signalling. *Nat Cell Biol*. 6:1034-8.
Fisher, P.R., A.A. Noegel, M. Fechheimer, F. Rivero, J. Prassler, and G. Gerisch. 1997. Photosensory and thermosensory responses in Dictyostelium slugs are specifically impaired by absence of the F-actin cross-linking gelation factor (ABP-120). *Curr Biol*. 7:889-92.
Franca-Koh, J., Y. Kamimura, and P. Devreotes. 2006. Navigating signaling networks: chemotaxis in Dictyostelium discoideum. *Curr Opin Genet Dev*. 16:333-8.
Gaskins, C., A.M. Clark, L. Aubry, J.E. Segall, and R.A. Firtel. 1996. The Dictyostelium MAP kinase ERK2 regulates multiple, independent developmental pathways. *Genes Dev*. 10:118-28.
Geissler, H., R. Ullmann, and T. Soldati. 2000. The tail domain of myosin M catalyses nucleotide exchange on Rac1 GTPases and can induce actin-driven surface protrusions. *Traffic*. 1:399-410.
Gimona, M., K. Djinovic-Carugo, W.J. Kranewitter, and S.J. Winder. 2002. Functional plasticity of CH domains. *FEBS Lett*. 513:98-106.
Gimona, M., and R. Mital. 1998. The single CH domain of calponin is neither sufficient nor necessary for F-actin binding. *J Cell Sci*. 111 ( Pt 13):1813-21.
Girard, K.D., C. Chaney, M. Delannoy, S.C. Kuo, and D.N. Robinson. 2004. Dynacortin contributes to cortical viscoelasticity and helps define the shape changes of cytokinesis. *Embo J*. 23:1536-46.
Gloss, A., F. Rivero, N. Khaire, R. Muller, W.F. Loomis, M. Schleicher, and A.A. Noegel. 2003. Villidin, a novel WD-repeat and villin-related protein from Dictyostelium, is associated with membranes and the cytoskeleton. *Mol Biol Cell*. 14:2716-27.
Gregg, J.H., M. Krefft, A. Haas-Kraus, and K.L. Williams. 1982. Antigenic differences detected between prespore cells of Dictyostelium discoideum and Dictyostelium mucoroides using monoclonal antibodies. *Exp Cell Res*. 142:229-33.
Gronwald, W., F. Huber, P. Grunewald, M. Sporner, S. Wohlgemuth, C. Herrmann, and H.R. Kalbitzer. 2001. Solution structure of the Ras binding domain of the protein kinase Byr2 from Schizosaccharomyces pombe. *Structure*. 9:1029-41.
Hall, A.L., A. Schlein, and J. Condeelis. 1988. Relationship of pseudopod extension to chemotactic hormone-induced actin polymerization in amoeboid cells. *J Cell Biochem*. 37:285-99.
Han, J.W., L. Leeper, F. Rivero, and C.Y. Chung. 2006. Role of RacC for the regulation of WASP and phosphatidylinositol 3-kinase during chemotaxis of Dictyostelium. *J Biol Chem*. 281:35224-34.
Haugwitz, M., A.A. Noegel, D. Rieger, F. Lottspeich, and M. Schleicher. 1991. Dictyostelium discoideum contains two profilin isoforms that differ in structure and function. *J Cell Sci*. 100 ( Pt 3):481-9.
Heid, P.J., D. Wessels, K.J. Daniels, D.P. Gibson, H. Zhang, E. Voss, and D.R. Soll. 2004. The role of myosin heavy chain phosphorylation in Dictyostelium motility, chemotaxis and F-actin localization. *J Cell Sci*. 117:4819-35.
Hofmann, A., L. Eichinger, E. Andre, D. Rieger, and M. Schleicher. 1992. Cap100, a novel phosphatidylinositol 4,5-bisphosphate-regulated protein that caps actin filaments but does not nucleate actin assembly. *Cell Motil Cytoskeleton*. 23:133-44.
Howard, P.K., B.M. Sefton, and R.A. Firtel. 1992. Analysis of a spatially regulated phosphotyrosine phosphatase identifies tyrosine phosphorylation as a key regulatory pathway in Dictyostelium. *Cell*. 71:637-47.
Huttelmaier, S., O. Mayboroda, B. Harbeck, T. Jarchau, B.M. Jockusch, and M. Rudiger. 1998. The interaction of the cell-contact proteins VASP and vinculin is regulated by phosphatidylinositol-4,5-bisphosphate. *Curr Biol*. 8:479-88.
Insall, R.H., J. Borleis, and P.N. Devreotes. 1996. The aimless RasGEF is required for processing of chemotactic signals through G-protein-coupled receptors in Dictyostelium. *Curr Biol*. 6:719-29.
Jackson, T.R., B.G. Kearns, and A.B. Theibert. 2000. Cytohesins and centaurins: mediators of PI 3-kinase-regulated Arf signaling. *Trends Biochem Sci*. 25:489-95.
Jung, E., P. Fucini, M. Stewart, A.A. Noegel, and M. Schleicher. 1996. Linking microfilaments to intracellular membranes: the actin-binding and vesicle-associated protein comitin exhibits a mannose-specific lectin activity. *Embo J*. 15:1238-46.
Kae, H., A. Kortholt, H. Rehmann, R.H. Insall, P.J. Van Haastert, G.B. Spiegelman, and G. Weeks. 2007. Cyclic AMP signalling in Dictyostelium: G-proteins activate separate Ras pathways using specific RasGEFs. *EMBO Rep*. 8:477-82.
Kae, H., C.J. Lim, G.B. Spiegelman, and G. Weeks. 2004. Chemoattractant-induced Ras activation during Dictyostelium aggregation. *EMBO Rep*. 5:602-6.
Kam, J.L., K. Miura, T.R. Jackson, J. Gruschus, P. Roller, S. Stauffer, J. Clark, R. Aneja, and P.A. Randazzo. 2000. Phosphoinositide-dependent activation of the ADP-ribosylation factor GTPase-activating protein ASAP1. Evidence for the pleckstrin homology domain functioning as an allosteric site. *J Biol Chem*. 275:9653-63.

Khaire, N., R. Muller, R. Blau-Wasser, L. Eichinger, M. Schleicher, M. Rief, T.A. Holak, and A.A. Noegel. 2007. Filamin-regulated F-actin assembly is essential for morphogenesis and controls phototaxis in Dictyostelium. *J Biol Chem*. 282:1948-55.
Knecht, D., and K.M. Pang. 1995. Electroporation of Dictyostelium discoideum. *Methods Mol Biol*. 47:321-30.
Knetsch, M.L., N. Schafers, H. Horstmann, and D.J. Manstein. 2001. The Dictyostelium Bcr/Abr-related protein DRG regulates both Rac- and Rab-dependent pathways. *Embo J*. 20:1620-9.
Knuth, M., N. Khaire, A. Kuspa, S.J. Lu, M. Schleicher, and A.A. Noegel. 2004. A novel partner for Dictyostelium filamin is an alpha-helical developmentally regulated protein. *J Cell Sci*. 117:5013-22.
Kolman, M.F., L.M. Futey, and T.T. Egelhoff. 1996. Dictyostelium myosin heavy chain kinase A regulates myosin localization during growth and development. *J Cell Biol*. 132:101-9.
Korenbaum, E., and F. Rivero. 2002. Calponin homology domains at a glance. *J Cell Sci*. 115:3543-5.
Kriebel, P.W., V.A. Barr, and C.A. Parent. 2003. Adenylyl cyclase localization regulates streaming during chemotaxis. *Cell*. 112:549-60.
Laemmli, U.K. 1970. Cleavage of structural proteins during the assembly of the head of bacteriophage T4. *Nature*. 227:680-5.
Larochelle, D.A., K.K. Vithalani, and A. De Lozanne. 1996. A novel member of the rho family of small GTP-binding proteins is specifically required for cytokinesis. *J Cell Biol*. 133:1321-9.
Larochelle, D.A., K.K. Vithalani, and A. De Lozanne. 1997. Role of Dictyostelium racE in cytokinesis: mutational analysis and localization studies by use of green fluorescent protein. *Mol Biol Cell*. 8:935-44.
Lee, S., R. Escalante, and R.A. Firtel. 1997. A Ras GAP is essential for cytokinesis and spatial patterning in Dictyostelium. *Development*. 124:983-96.
Legate, K.R., E. Montanez, O. Kudlacek, and R. Fassler. 2006. ILK, PINCH and parvin: the tIPP of integrin signalling. *Nat Rev Mol Cell Biol*. 7:20-31.
Lemmon, M.A. 2004. Pleckstrin homology domains: not just for phosphoinositides. *Biochem Soc Trans*. 32:707-11.
Lim, R.W., R. Furukawa, S. Eagle, R.C. Cartwright, and M. Fechheimer. 1999. Three distinct F-actin binding sites in the Dictyostelium discoideum 34,000 dalton actin bundling protein. *Biochemistry*. 38:800-12.
Lingnau, A., T. Chakraborty, K. Niebuhr, E. Domann, and J. Wehland. 1996. Identification and purification of novel internalin-related proteins in Listeria monocytogenes and Listeria ivanovii. *Infect Immun*. 64:1002-6.
Luck-Vielmetter, D., M. Schleicher, B. Grabatin, J. Wippler, and G. Gerisch. 1990. Replacement of threonine residues by serine and alanine in a phosphorylatable heavy chain fragment of Dictyostelium myosin II. *FEBS Lett*. 269:239-43.
Manstein, D.J., M.A. Titus, A. De Lozanne, and J.A. Spudich. 1989. Gene replacement in Dictyostelium: generation of myosin null mutants. *Embo J*. 8:923-32.
Matsumura, F. 2005. Regulation of myosin II during cytokinesis in higher eukaryotes. *Trends Cell Biol*. 15:371-7.
Mohrs, M.R., K.P. Janssen, T. Kreis, A.A. Noegel, and M. Schleicher. 2000. Cloning and characterization of beta-COP from Dictyostelium discoideum. *Eur J Cell Biol*. 79:350-7.
Mullins, R.D., W.F. Stafford, and T.D. Pollard. 1997. Structure, subunit topology, and actin-binding activity of the Arp2/3 complex from Acanthamoeba. *J Cell Biol*. 136:331-43.
Natarajan, K., C.A. Ashley, and J.A. Hadwiger. 2000. Related Galpha subunits play opposing roles during Dictyostelium development. *Differentiation*. 66:136-46.
Neujahr, R., C. Heizer, and G. Gerisch. 1997. Myosin II-independent processes in mitotic cells of Dictyostelium discoideum: redistribution of the nuclei, re-arrangement of the actin system and formation of the cleavage furrow. *J Cell Sci*. 110 ( Pt 2):123-37.
Niswonger, M.L., and T.J. O'Halloran. 1997. A novel role for clathrin in cytokinesis. *Proc Natl Acad Sci U S A*. 94:8575-8.
Noegel, A., B.A. Metz, and K.L. Williams. 1985. Developmentally regulated transcription of Dictyostelium discoideum plasmid Ddp1. *Embo J*. 4:3797-3803.
Noegel, A.A., R. Blau-Wasser, H. Sultana, R. Muller, L. Israel, M. Schleicher, H. Patel, and C.J. Weijer. 2004. The cyclase-associated protein CAP as regulator of cell polarity and cAMP signaling in Dictyostelium. *Mol Biol Cell*. 15:934-45.
Noegel, A.A., and M. Schleicher. 2000. The actin cytoskeleton of Dictyostelium: a story told by mutants. *J Cell Sci*. 113 ( Pt 5):759-66.
Ohta, Y., J.H. Hartwig, and T.P. Stossel. 2006. FilGAP, a Rho- and ROCK-regulated GAP for Rac binds filamin A to control actin remodelling. *Nat Cell Biol*. 8:803-14.
Ohta, Y., N. Suzuki, S. Nakamura, J.H. Hartwig, and T.P. Stossel. 1999. The small GTPase RalA targets filamin to induce filopodia. *Proc Natl Acad Sci U S A*. 96:2122-8.

Pagh, K., and G. Gerisch. 1986. Monoclonal antibodies binding to the tail of Dictyostelium discoideum myosin: their effects on antiparallel and parallel assembly and actin-activated ATPase activity. *J Cell Biol*. 103:1527-38.
Pang, K.M., E. Lee, and D.A. Knecht. 1998. Use of a fusion protein between GFP and an actin-binding domain to visualize transient filamentous-actin structures. *Curr Biol*. 8:405-8.
Park, K.C., F. Rivero, R. Meili, S. Lee, F. Apone, and R.A. Firtel. 2004. Rac regulation of chemotaxis and morphogenesis in Dictyostelium. *Embo J*. 23:4177-89.
Parker, P.J. 2004. The ubiquitous phosphoinositides. *Biochem Soc Trans*. 32:893-8.
Piperno, G., and M.T. Fuller. 1985. Monoclonal antibodies specific for an acetylated form of alpha-tubulin recognize the antigen in cilia and flagella from a variety of organisms. *J Cell Biol*. 101:2085-94.
Pollard, T.D., and G.G. Borisy. 2003. Cellular motility driven by assembly and disassembly of actin filaments. *Cell*. 112:453-65.
Popowicz, G.M., M. Schleicher, A.A. Noegel, and T.A. Holak. 2006. Filamins: promiscuous organizers of the cytoskeleton. *Trends Biochem Sci*. 31:411-9.
Prassler, J., S. Stocker, G. Marriott, M. Heidecker, J. Kellermann, and G. Gerisch. 1997. Interaction of a Dictyostelium member of the plastin/fimbrin family with actin filaments and actin-myosin complexes. *Mol Biol Cell*. 8:83-95.
Raisley, B., M. Zhang, D. Hereld, and J.A. Hadwiger. 2004. A cAMP receptor-like G protein-coupled receptor with roles in growth regulation and development. *Dev Biol*. 265:433-45.
Randazzo, P.A., and D.S. Hirsch. 2004. Arf GAPs: multifunctional proteins that regulate membrane traffic and actin remodelling. *Cell Signal*. 16:401-13.
Reymond, C.D., R.H. Gomer, W. Nellen, A. Theibert, P. Devreotes, and R.A. Firtel. 1986. Phenotypic changes induced by a mutated ras gene during the development of Dictyostelium transformants. *Nature*. 323:340-3.
Ridley, A.J. 2001. Rho GTPases and cell migration. *J Cell Sci*. 114:2713-22.
Ridley, A.J., M.A. Schwartz, K. Burridge, R.A. Firtel, M.H. Ginsberg, G. Borisy, J.T. Parsons, and A.R. Horwitz. 2003. Cell migration: integrating signals from front to back. *Science*. 302:1704-9.
Rivero, F., R. Albrecht, H. Dislich, E. Bracco, L. Graciotti, S. Bozzaro, and A.A. Noegel. 1999. RacF1, a novel member of the Rho protein family in Dictyostelium discoideum, associates transiently with cell contact areas, macropinosomes, and phagosomes. *Mol Biol Cell*. 10:1205-19.
Rivero, F., R. Furukawa, A.A. Noegel, and M. Fechheimer. 1996a. Dictyostelium discoideum cells lacking the 34,000-dalton actin-binding protein can grow, locomote, and develop, but exhibit defects in regulation of cell structure and movement: a case of partial redundancy. *J Cell Biol*. 135:965-80.
Rivero, F., B. Koppel, B. Peracino, S. Bozzaro, F. Siegert, C.J. Weijer, M. Schleicher, R. Albrecht, and A.A. Noegel. 1996b. The role of the cortical cytoskeleton: F-actin crosslinking proteins protect against osmotic stress, ensure cell size, cell shape and motility, and contribute to phagocytosis and development. *J Cell Sci*. 109 ( Pt 11):2679-91.
Rivero, F., and M. Maniak. 2006. Quantitative and microscopic methods for studying the endocytic pathway. *Methods Mol Biol*. 346:423-38.
Robinson, D.N., S.S. Ocon, R.S. Rock, and J.A. Spudich. 2002. Dynacortin is a novel actin bundling protein that localizes to dynamic actin structures. *J Biol Chem*. 277:9088-95.
Saran, S., M.E. Meima, E. Alvarez-Curto, K.E. Weening, D.E. Rozen, and P. Schaap. 2002. cAMP signaling in Dictyostelium. Complexity of cAMP synthesis, degradation and detection. *J Muscle Res Cell Motil*. 23:793-802.
Sasaki, A.T., and R.A. Firtel. 2005. Finding the way: directional sensing and cell polarization through Ras signalling. *Novartis Found Symp*. 269:73-87; discussion 87-91, 223-30.
Sasaki, A.T., and R.A. Firtel. 2006. Regulation of chemotaxis by the orchestrated activation of Ras, PI3K, and TOR. *Eur J Cell Biol*. 85:873-95.
Satterwhite, L.L., and T.D. Pollard. 1992. Cytokinesis. *Curr Opin Cell Biol*. 4:43-52.
Scheffzek, K., P. Grunewald, S. Wohlgemuth, W. Kabsch, H. Tu, M. Wigler, A. Wittinghofer, and C. Herrmann. 2001. The Ras-Byr2RBD complex: structural basis for Ras effector recognition in yeast. *Structure*. 9:1043-50.
Schirenbeck, A., T. Bretschneider, R. Arasada, M. Schleicher, and J. Faix. 2005. The Diaphanous-related formin dDia2 is required for the formation and maintenance of filopodia. *Nat Cell Biol*. 7:619-25.
Schleicher, M., B. Andre, C. Andreoli, L. Eichinger, M. Haugwitz, A. Hofmann, J. Karakesisoglou, M. Stockelhuber, and A.A. Noegel. 1995. Structure/function studies on cytoskeletal proteins in Dictyostelium amoebae as a paradigm. *FEBS Lett*. 369:38-42.
Schleicher, M., G. Gerisch, and G. Isenberg. 1984. New actin-binding proteins from Dictyostelium discoideum. *Embo J*. 3:2095-2100.
Seastone, D.J., E. Lee, J. Bush, D. Knecht, and J. Cardelli. 1998. Overexpression of a novel rho family GTPase, RacC, induces unusual actin-based structures and positively affects phagocytosis in Dictyostelium discoideum. *Mol Biol Cell*. 9:2891-904.

Siegert, F., and C.J. Weijer. 1992. Three-dimensional scroll waves organize Dictyostelium slugs. *Proc Natl Acad Sci U S A*. 89:6433-7.
Siegert, F., and C.J. Weijer. 1995. Spiral and concentric waves organize multicellular Dictyostelium mounds. *Curr Biol*. 5:937-43.
Simpson, P.A., J.A. Spudich, and P. Parham. 1984. Monoclonal antibodies prepared against Dictyostelium actin: characterization and interactions with actin. *J Cell Biol*. 99:287-95.
Somesh, B.P., C. Neffgen, M. Iijima, P. Devreotes, and F. Rivero. 2006a. Dictyostelium RacH regulates endocytic vesicular trafficking and is required for localization of vacuolin. *Traffic*. 7:1194-212.
Somesh, B.P., G. Vlahou, M. Iijima, R.H. Insall, P. Devreotes, and F. Rivero. 2006b. RacG regulates morphology, phagocytosis, and chemotaxis. *Eukaryot Cell*. 5:1648-63.
Somlyo, A.P., and A.V. Somlyo. 2000. Signal transduction by G-proteins, rho-kinase and protein phosphatase to smooth muscle and non-muscle myosin II. *J Physiol*. 522 Pt 2:177-85.
Springer, M.L., B. Patterson, and J.A. Spudich. 1994. Stage-specific requirement for myosin II during Dictyostelium development. *Development*. 120:2651-60.
Steimle, P.A., S. Yumura, G.P. Cote, Q.G. Medley, M.V. Polyakov, B. Leppert, and T.T. Egelhoff. 2001. Recruitment of a myosin heavy chain kinase to actin-rich protrusions in Dictyostelium. *Curr Biol*. 11:708-13.
Stites, J., D. Wessels, A. Uhl, T. Egelhoff, D. Shutt, and D.R. Soll. 1998. Phosphorylation of the Dictyostelium myosin II heavy chain is necessary for maintaining cellular polarity and suppressing turning during chemotaxis. *Cell Motil Cytoskeleton*. 39:31-51.
Stock, A., M.O. Steinmetz, P.A. Janmey, U. Aebi, G. Gerisch, R.A. Kammerer, I. Weber, and J. Faix. 1999. Domain analysis of cortexillin I: actin-bundling, PIP(2)-binding and the rescue of cytokinesis. *Embo J*. 18:5274-84.
Stossel, T.P., J. Condeelis, L. Cooley, J.H. Hartwig, A. Noegel, M. Schleicher, and S.S. Shapiro. 2001. Filamins as integrators of cell mechanics and signalling. *Nat Rev Mol Cell Biol*. 2:138-45.
Stradal, T., W. Kranewitter, S.J. Winder, and M. Gimona. 1998. CH domains revisited. *FEBS Lett*. 431:134-7.
Strehle, A., M. Schleicher, and J. Faix. 2006. Trix, a novel Rac guanine-nucleotide exchange factor from Dictyostelium discoideum is an actin-binding protein and accumulates at endosomes. *Eur J Cell Biol*. 85:1035-45.
Sutherland, B.W., G.B. Spiegelman, and G. Weeks. 2001. A Ras subfamily GTPase shows cell cycle-dependent nuclear localization. *EMBO Rep*. 2:1024-8.
Sutoh, K. 1993. A transformation vector for dictyostelium discoideum with a new selectable marker bsr. *Plasmid*. 30:150-4.
Svitkina, T.M., and G.G. Borisy. 1999. Arp2/3 complex and actin depolymerizing factor/cofilin in dendritic organization and treadmilling of actin filament array in lamellipodia. *J Cell Biol*. 145:1009-26.
Tuxworth, R.I., J.L. Cheetham, L.M. Machesky, G.B. Spiegelmann, G. Weeks, and R.H. Insall. 1997. Dictyostelium RasG is required for normal motility and cytokinesis, but not growth. *J Cell Biol*. 138:605-14.
Vadlamudi, R.K., F. Li, L. Adam, D. Nguyen, Y. Ohta, T.P. Stossel, and R. Kumar. 2002. Filamin is essential in actin cytoskeletal assembly mediated by p21-activated kinase 1. *Nat Cell Biol*. 4:681-90.
Vaillancourt, J.P., C. Lyons, and G.P. Cote. 1988. Identification of two phosphorylated threonines in the tail region of Dictyostelium myosin II. *J Biol Chem*. 263:10082-7.
Van Haastert, P.J., and P.N. Devreotes. 2004. Chemotaxis: signalling the way forward. *Nat Rev Mol Cell Biol*. 5:626-34.
Vithalani, K.K., C.A. Parent, E.M. Thorn, M. Penn, D.A. Larochelle, P.N. Devreotes, and A. De Lozanne. 1998. Identification of darlin, a Dictyostelium protein with Armadillo-like repeats that binds to small GTPases and is important for the proper aggregation of developing cells. *Mol Biol Cell*. 9:3095-106.
Vlahou, G., and F. Rivero. 2006. Rho GTPase signaling in Dictyostelium discoideum: insights from the genome. *Eur J Cell Biol*. 85:947-59.
Wallraff, E., and H.G. Wallraff. 1997. Migration and bidirectional phototaxis in Dictyostelium discoideum slugs lacking the actin cross-linking 120 kDa gelation factor. *J Exp Biol*. 200:3213-20.
Weber, I., G. Gerisch, C. Heizer, J. Murphy, K. Badelt, A. Stock, J.M. Schwartz, and J. Faix. 1999. Cytokinesis mediated through the recruitment of cortexillins into the cleavage furrow. *Embo J*. 18:586-94.
Weiner, O.H., J. Murphy, G. Griffiths, M. Schleicher, and A.A. Noegel. 1993. The actin-binding protein comitin (p24) is a component of the Golgi apparatus. *J Cell Biol*. 123:23-34.
Welch, M.D., A.H. DePace, S. Verma, A. Iwamatsu, and T.J. Mitchison. 1997. The human Arp2/3 complex is composed of evolutionarily conserved subunits and is localized to cellular regions of dynamic actin filament assembly. *J Cell Biol*. 138:375-84.
Wessels, D., and D.R. Soll. 1990. Myosin II heavy chain null mutant of Dictyostelium exhibits defective intracellular particle movement. *J Cell Biol*. 111:1137-48.
Wessels, D., D.R. Soll, D. Knecht, W.F. Loomis, A. De Lozanne, and J. Spudich. 1988. Cell motility and chemotaxis in Dictyostelium amebae lacking myosin heavy chain. *Dev Biol*. 128:164-77.

Wessels, D., E. Voss, N. Von Bergen, R. Burns, J. Stites, and D.R. Soll. 1998. A computer-assisted system for reconstructing and interpreting the dynamic three-dimensional relationships of the outer surface, nucleus and pseudopods of crawling cells. *Cell Motil Cytoskeleton*. 41:225-46.

Westphal, M., A. Jungbluth, M. Heidecker, B. Muhlbauer, C. Heizer, J.M. Schwartz, G. Marriott, and G. Gerisch. 1997. Microfilament dynamics during cell movement and chemotaxis monitored using a GFP-actin fusion protein. *Curr Biol*. 7:176-83.

Wilkins, A., M. Khosla, D.J. Fraser, G.B. Spiegelman, P.R. Fisher, G. Weeks, and R.H. Insall. 2000. Dictyostelium RasD is required for normal phototaxis, but not differentiation. *Genes Dev*. 14:1407-13.

Wilkins, A., K. Szafranski, D.J. Fraser, D. Bakthavatsalam, R. Muller, P.R. Fisher, G. Glockner, L. Eichinger, A.A. Noegel, and R.H. Insall. 2005. The Dictyostelium genome encodes numerous RasGEFs with multiple biological roles. *Genome Biol*. 6:R68.

Williams, C.L. 2003. The polybasic region of Ras and Rho family small GTPases: a regulator of protein interactions and membrane association and a site of nuclear localization signal sequences. *Cell Signal*. 15:1071-80.

Witke, W., W. Nellen, and A. Noegel. 1987. Homologous recombination in the Dictyostelium alpha-actinin gene leads to an altered mRNA and lack of the protein. *Embo J*. 6:4143-8.

Worthylake, R.A., and K. Burridge. 2003. RhoA and ROCK promote migration by limiting membrane protrusions. *J Biol Chem*. 278:13578-84.

Yang, F., M. Demma, V. Warren, S. Dharmawardhane, and J. Condeelis. 1990. Identification of an actin-binding protein from Dictyostelium as elongation factor 1a. *Nature*. 347:494-6.

Zhou, K., K. Takegawa, S.D. Emr, and R.A. Firtel. 1995. A phosphatidylinositol (PI) kinase gene family in Dictyostelium discoideum: biological roles of putative mammalian p110 and yeast Vps34p PI 3-kinase homologs during growth and development. *Mol Cell Biol*. 15:5645-56.

**Summary**

The work described here shows the complexity of GTPase signalling in an apparently simple organism *Dictyostelium discoideum*.

Ras Guanine nucleotide exchange factor RasGEF Q is one out of at least 25 RasGEFs in *D. discoideum*. Here we show that it specifically regulates myosin II functions by regulating myosin phosphorylation. RasGEF Q activates the Ras isoform RasB upon stimulation with cAMP. Activated RasB can directly or indirectly activate Myosin Heavy chain kinase A (MHCK A) which then phosphorylates the myosin II heavy chain. Phosphorylated myosin II cannot assemble into filaments and is thus a non-functional form. Furthermore, a DEP domain in RasGEF Q appears to be critical for activating RasGEF Q by release from an autoinhibited state.

Studies on the multidomain Rac Guanine nucleotide exchange factor GxcDD show that it is required for the early phases of development in chemotactic migration and streaming behaviour. The characterization of its single domains revealed that the CH domain (Calponin homology domain) of GxcDD functions as a membrane association domain, the RhoGEF domain can physically interact with a subset of Rac GTPases and the ArfGAP-PH tandem accumulates in cortical regions of the cell and in phagosomes. Our results also suggest that a conformational change is required for activation of GxcDD, which would be important for its downstream signaling.

Studies on the IQGAP related protein GAPA showed that it associates with two actin-corsslinking protein, namely Filamin and Cortexillin I. GAPA is required for cytokinesis and localizes to the cleavage furrow during cytokinesis in a cortexillin I dependent way. We also observed that GAPA is required for proper phototaxis as is its binding partner Filamin.

**Zusammenfassung**

*Dictyostelium discoideum* besitzt mindestens 25 Ras Guaninnukleotid Austauschfaktoren, denen 15 Ras-ähnliche Proteine gegenüber stehen. Wir beschreiben hier die Rolle des RasGEF Q für die Regulation von Myosin II. Auf ein extrazelluläres cAMP Signal hin aktiviert RasGEF Q Ras B, das dann direkt oder indirekt die Myosin-Schwere-Ketten Kinase A (MHCK A) aktiviert, die daraufhin Myosin II phosphoryliert. Phosphorylierung von Myosin II führt zu seiner Inaktivierung und zum Verlust von Myosin II Filamenten aus der kortikalen Region der Zelle mit Konsequenzen für die Zellform. Eine Analyse der funktionellen Domänen von RasGEF Q hat weiterhin Hinweise auf eine kritische Rolle der DEP Domäne für die Aktivierung des Moleküls gegeben.

Der Multidomänen Rac Guaninnukleotid Austauschfaktor GxcDD wird benötigt für die chemotaktische Bewegung und das Strömungsverhalten der Zellen in der frühen Entwicklung von *D. discoideum*. Die Calponin Homologie Domäne ermöglicht eine Assoziation mit der Plasmamembran, die RhoGEF Domäne kann mit mehreren der 18 *D. discoideum* Rac Proteine interagieren und die ArfGAP-PH Tandem Domäne reichert sich in den kortikalen Regionen der Zelle und in den Phagosomen an. Weiterhin erscheint eine Konformationsveränderung als notwendig für die Aktivierung von GxcDD, die dann eine Weiterleitung des Signals erlaubt.

GAPA ist ein IQGAP verwandtes Protein. IQGAPs sind als Aktin-bindende Proteine beschrieben, die für viele Interaktionspartner eine Umgebung formen, damit diese extrazelluläre Signale weitergeben können. GAPA assoziiert mit den zwei F-Aktin quervernetzenden Proteinen Filamin und Cortexillin I. Es wird für die Zytokinese benötigt und verlagert sich dabei in einer Cortexillin-abhängigen Weise an die Einschnürungszone. GAPA besitzt auch eine Rolle in der Entwicklung und wird wie Filamin für eine korrekte Phototaxis benötigt.

## Erklärung

Ich versichere, dass ich die von mir vorgelegte Dissertation selbständig angefertigt, die benutzten Quellen und Hilfsmittel vollständig angegeben und die Stellen der Arbeit, einschließlich Tabellen und Abbildungen, die anderen Werke im Wortlaut oder dem Sinn nach entnommen sind, in jedem Einzelfall als Entlehnung kenntlich gemacht habe; dass diese Dissertation noch keiner anderen Fakultät oder Universität zur Prüfung vorgelegen hat; dass sie, abgesehen von unten angegebenen beantragten Teilpublikationen, noch nicht veröffentlicht ist, sowie dass ich eine Veröffentlichung vor Abschluss des Promotionsverfahrens nicht vornehmen werde. Die Bestimmungen dieser Promotionsordnung sind mir bekannt. Die von mir vorgelegte Dissertation ist von Frau Prof. Dr. Angelika A. Noegel betreut worden.

Cologne
10. November, 2007

Subhanjan Mondal

## Teilpublikationen

- Arasada, R., A. Gloss, B. Tunggal, J.M. Joseph, D. Rieger, **S. Mondal**, J. Faix, M. Schleicher, and A.A. Noegel. 2007. Profilin isoforms in *Dictyostelium discoideum*. *Biochim Biophys Acta*. 1773:631-41.
- **Mondal, S**., D. Neelamegan, F. Rivero, and A.A. Noegel. 2007. GxcDD, a putative RacGEF, is involved in *Dictyostelium* development. *BMC Cell Biol*. 8:23.
- Prabhu, Y., **S. Mondal**, L. Eichinger, and A.A. Noegel. 2007. A GPCR involved in post aggregation events in *Dictyostelium discoideum*. *Dev Biol*.312: 29-43

# Curriculum Vitae


**Name:** Subhanjan Mondal

**Address:** E2-024
Kerpener Str 61-69
Cologne, 50937
Germany


**Date of Birth** 15.04.1981

**Nationality** Indian

## Academic Qualifications

**School Education**

**(1997-1999)** St. Patrick's Higher Secondary School, Asansol, India

**University Education**

**(1999-2002)** Bachelor of Science
Human Biology (major Biophysics)
All India Institute for Medical Sciences, New Delhi, India

**(2002-2004)** Master of Science
Subject: Biotechnology
Madurai Kamaraj University, Madurai, India

**Doctoral Studies**

**(11.2004-11.2007)** Advisor: Prof. Dr. Angelika A Noegel
Institute for Biochemistry I, Medical Faculty
University of Cologne, Cologne, Germany
Title of PhD Thesis: Role of modulators of small GTPases in chemotaxis, Cytokinesis and development in *Dictyostelium discoideum*

# Lebenslauf

| | |
|---|---|
| **Name** | Subhanjan Mondal |
| **Adresse** | E2-024<br>Kerpener Str 61-69<br>Köln, 50937<br>Deutschland |
| **Geburtsdatum** | 15.04.1981 |
| **Staatsangehörigkeit** | Indisch |

**Akademische Qualifikation**

**Schulausbildung**

| | |
|---|---|
| **(1997-1999)** | St. Patrick's Higher Secondary School, Asansol, India |

**Studium**

| | |
|---|---|
| **(1999-2002)** | Bachelor of Science<br>Human Biology (Hauptfach Biophysics)<br>All India Institute for Medical Sciences, New Delhi, India |
| **(2002-2004)** | Master of Science<br>Hauptfach: Biotechnology<br>Madurai Kamaraj University, Madurai, India |

**Promotionsstudium**

| | |
|---|---|
| **(11.2004-11.2007)** | Betreuerin: Prof. Dr. Angelika A Noegel<br>Institut für Biochemie I, Medizinische Fakultät der Universität zu Köln<br>Thema: Role of modulators of small GTPases in chemotaxis, Cytokinesis and development in *Dictyostelium discoideum* |